Theory of Laser-Plasma Axion Production

A thesis submitted for the degree of Doctor of Philosophy

in the Department of Physics

Lancaster University

Author:
Mark Aleksiejuk

Supervised by:
Dr. David Burton

"And here I stand, with all my lore, Poor fool, no wiser than before."
–Johann Wolfgang von Goethe, Faust

Abstract

In this thesis, we investigate the problem of axion production in laser-plasma systems, with the aim of motivating the use of Light-Shining-Through-a-Wall (LSTW) experiments in the search for axions and axion-like particles. We begin with the study of relativistic plasma waves, which culminates in a proposal of a formulation of a $1+1$D scalar field theory for laser wakefield accelerators (LWFA). With this formulation, we derived a condition for the dimensionless laser amplitude required to drive the maximum plasma wakefield only in terms of the wake velocity.

Studying the case of classical axion production in laser-plasma scenarios, we derive a resonance condition for a given axion mass in terms of laser-plasma parameters.

We then move on to studying axion creation in laser-plasma scenarios through the lens of the ponderomotive approximation. We propose a heuristic approach to ponderomotive dynamics and then analyse the laser-plasma-axion dynamics.

Finally, we examine the problem of axion creation with consideration for the quantum nature of the axion. The case of a quantum axion field driven by a classical plasma wave and an external magnetic field is investigated. We calculate the expected axion flux of $N \approx 6.74 \times 10^{18}\text{cm}^{-2}\text{s}^{-1}$ ($N_{m_\psi=0} \approx 1.7 \times 10^{20}\text{cm}^{-2}\text{s}^{-1}$ in the massless case) given the parameters are (axion-photon coupling) $g_\psi = 0.66 \times 10^{-19}\text{eV}$, (magnetic field) $B = 7 \times 10^3\text{eV}^2$ ($B \approx 35\text{T}$), (plasma frequency) $\omega_p = 4.12 \times 10^{-2}\text{eV}$, (plasma wake phase velocity) $v = 0.99995c$ and (axion mass) $m_\psi = 10^{-4}\text{eV}$. This is a promising result. Despite the real flux created being smaller due to multidimensional effects and beam dispersion, it could be potentially feasible to produce a flux that is comparable to the hypothetical solar axion flux in terrestrial laboratories. We also obtain an expression for the axion-photon transition rate given the form of a plasma wave driving the axion field at first order.

Acknowledgments

First and foremost, I would like to express my deepest gratitude to my supervisor, Dr. David Burton, for his steady guidance and unwavering support throughout this PhD. His calm approach to challenges and thoroughness in tackling problems have been invaluable, teaching me how to think critically and truly approach problems like a physicist. I feel incredibly fortunate to have worked with him during this project.

I am also profoundly grateful to my wonderful girlfriend, Heather, for her unwavering support in every aspect of my life during this journey. Her encouragement and understanding have been a cornerstone of my perseverance, and I cannot imagine having navigated this experience without her by my side.

My heartfelt thanks also go to my friends and family back home. My mother and aunt, with their endless encouragement and belief in me, have been a source of constant strength. The support and companionship of my friends, despite the challenges of long-distance, were crucial in helping me maintain perspective and resilience, especially during the difficult pandemic period.

Finally, I want to extend my appreciation to all my office colleagues at Lancaster. Their positivity, camaraderie, and good humour have made my time here not only productive but also memorable and enjoyable.

Declaration

I declare that this thesis is my own work and has not been submitted towards, be it fully or in part, a higher degree or any other form of qualification from any other institution.

List of Publications

- **Chapter 2** : *A scalar field theory of 1+1-dimensional laser wakefield accelerators*
  Mark Aleksiejuk and David Burton
  J. Phys. A: Math. Theor. **57** 355701 (2024)

List of Figures

Contents

Units in This Thesis

Throughout my thesis I have used a set of natural units defined by the condition:

$$c = \hbar = \epsilon_0 = 1. \tag{1}$$

We note that this fixes the value of the magnetic permeability of the vacuum to be $\mu_0 = 1$. This results in conversion factors:

$$\begin{aligned} 1\text{s} &= 1.52 \times 10^{15} \hbar \text{ eV}^{-1} \\ 1\text{m} &= 5.07 \times 10^{6} \hbar c \text{ eV}^{-1} \\ 1\text{kg} &= 5.63 \times 10^{35} c^{-2} \text{ eV} \\ 1\text{C} &= 1.89 \times 10^{18} \epsilon_0^{\frac{1}{2}} \hbar^{\frac{1}{2}} c^{\frac{1}{2}} \\ 1\text{T} &= 1.96 \times 10^{2} \epsilon_0^{-\frac{1}{2}} \hbar^{-\frac{3}{2}} c^{-\frac{5}{2}} \text{ eV}^2, \end{aligned} \tag{2}$$

given to three significant figures.

Chapter 1

Introduction

The problem of *dark matter* is one of central importance to modern theoretical physics. Over the years, many candidate theories have been proposed, ranging from modifying gravity to proposing a new type of fundamental particle. The aim of this thesis is to focus on the latter proposition, more specifically, the axion and the axion-like particle as candidates for dark matter and the search for them using a novel laboratory-based approach based on laser wakefield acceleration. In this chapter, the focus will be placed on a historical review and the motivation for a plasma-based axion search.

1.1 Searching in the Dark

In the landscape of modern physics, dark matter is a hypothetical type of matter which does not interact, or interacts extremely feebly, with the electromagnetic field. The existence of dark matter is inferred solely through its gravitational effects on visible matter. Due to the fact that the overwhelming majority of our experimental observations depend on the electromagnetic field, in one way or another, the direct detection (meaning observation of interactions with regular matter) of dark matter has proven elusive thus far. Furthermore, the actual composition of dark matter is unknown and is one of the biggest open problems in physics today. The purpose of this PhD project is to contribute to the onerous search for dark matter. In the following subsections, I will provide a historical review of the problem of dark matter and how the model was developed.

1.1.1 The Early Years

It could be said that the field of astrophysics was born in 1687 when Isaac Newton published his seminal work Philosophiæ Naturalis Principia Mathematica. Naturally, people studied astronomy before Newton's time, but Newton's introduction of his laws of motion and the universal gravitation law allowed a great deal more predictive power than ever before. More specifically, this allowed for the prediction of celestial objects via inference from their gravitational pull. One of the first examples of such predictions was made by the famous mathematician and astronomer Friedrich

Bessel in 1844 [1], where he inferred the existence of much less luminous partner stars to Sirius and Procyon via the analysis of their motion. Subsequently, the partner star to Sirius (dubbed Sirius B) was first observed in 1862 [2] and the partner to Procyon (similarly dubbed Procyon B) was discovered in 1896 [3]. Inferring the existence of celestial objects via their gravitational effects on other objects is one of the most powerful tools for astrophysicists, which is why dark matter poses such a conundrum. What do you do when you cannot verify your predictions based on gravitational influence with direct observation? Naturally, the two main methods of sidestepping this problem are modifying gravitational models or proposing a new type of matter (dark matter) that cannot be observed conventionally, and then searching for it. In this thesis, we are only concerned with the proposition of dark matter (a candidate for which will be discussed in section 1.2), but for more discussion on modified gravity, see [4].

The concept of "unseen" matter arose out of the study of the distribution of matter in our galaxy in the early twentieth century. One of the first scientists to attempt a quantitative study of our galaxy was Lord Kelvin in 1904 [5], where he used the theory of gases to analyse the Milky Way. In his work, he treated the stars in the Milky Way as particles in a gas. In his treatment, he postulated that there very well may be many stars which are too faint for observation at the time and even estimated the upper limit for the amount of these "dark" stars in relation to the current observations of the time. One of the first recorded uses of the term "dark matter" is attributed to Henri Poincaré [6], [7], written as "matière obscure" in French, which he introduced in a paper discussing Lord Kelvin's approach to the study of the galaxy.

We now fast forward to the year 1922, when a Dutch Astronomer by the name of Jacobus Kapetyn published his magnum opus "First Attempt at a Theory of the Arrangement and Motion of the Sidereal System" [8] (the Sidereal system meaning the Milky Way). In this work, he laid out one of the first quantitative descriptions of the size and shape of our galaxy. More pertinently for our discussion, is that Kapetyn explicitly touched upon the problem of dark matter, and concluded that the amount of dark matter could not be very excessive based on his approach. Over the next decade, several people have improved Kapetyn's work, chief among them being his student, Jan Oort. In a 1932 paper [9] Oort estimated that the density of dark matter near our sun was about half that of the total density of matter, and more interesting still, he referred to this matter as "nebulous" and "meteoric" matter, which gives us a good idea of the hypotheses of what dark matter was comprised of at the time.

1.1.2 The Coma Cluster Conundrum

Just a year after Jan Oort published his work (1933), a Swiss-American astronomer by the name of Fritz Zwicky published his work on galaxy clusters [10]. More specifically, Zwicky was studying the work of Edwin Hubble and Milton Humason [11] on the redshift of different galaxies. Zwicky observed that there was a large scatter (in the statistical sense) in the apparent velocities of

eight different galaxies in the Coma cluster. The resulting dispersion in the data was noticed by Hubble and Humason; however, Zwicky took the analysis further by applying the virial theorem to the system to estimate its mass. Zwicky found that the average velocity dispersion ought to be around 80 km/s, while the observed average velocity dispersion was approximately 1000 km/s. This analysis led him to conclude that the amount of dark matter in the galaxy cluster must have exceeded the amount of "bright" matter by a good margin. Many cite this as the origin of the theory of dark matter, which is not the case. Yet, it remains one of the most pivotal developments in the area.

1.1.3 Galaxy Rotation Curves

Galactic rotation curves result from plotting the circular velocity profile of the stars and gases in a galaxy as a function of their distance from the galactic centre. The study of galactic rotation curves is very commonly attributed as the deciding factor in convincing the larger physics community of the validity of the dark matter model. More precisely, it was the observation of the "flatness" of the rotation curves at large distances from the galactic centre that proved decisive.

In 1939 an American astronomer, Horace Babcock, wrote in his thesis about measurements of the rotation curves of the M31 (or Andromeda) Galaxy [12]. Babcock presented measurements of M31's rotation curve up to 100 arc min, where he found that the angular velocities far from the galactic centre were very high in relation to what was predicted at the time. In his interpretation, he argued that absorption of light might play a role in his observations or that some modified dynamics would be required to explain why the detected mass at the outer edges of the galaxy was much smaller.
In the 1970's, one of the first concrete claims about some galaxies needing to have additional mass was made by Freeman in an appendix of [13]. He argued that if the data he analyzed was correct, then "there must be additional matter which is undetected, either optically or at 21 cm.". In general, the 70's was a time of revolution for the study of what eventually became known as dark matter, as the scientific community was inching towards acknowledging the need for dark matter as a whole [14],[15],[16]. Indeed, in the review article [17], the abstract states that "It is concluded that the case for invisible mass in the universe is very strong and becoming stronger.".

Since then, the study of the problem of dark matter has become a major field of astrophysical and cosmological detail. A full review of the history of dark matter is a grand task, far beyond what can be included in an introduction. For reviews see [7], [18] and [19].

1.1.4 Summary

To conclude this section, it is clear to see that there is a very good reason to study dark matter, as it is a model that matches observation well. There are, of course, alternative theories that can

also match observation, mainly modified gravity (as mentioned in [7]), but the discussion of this topic is beyond the scope of this thesis.

1.2 Washing Away the Strong CP Problem

Having discussed how the theory of dark matter was proposed and the evidence for it, we now ask the question of what it is. Naturally, there are many competing theories about the nature of dark matter. The proposition that we are investigating in this thesis is that of the axion, and in this section we will discuss the origin of the axion theory.

1.2.1 QCD and the Strong CP Problem

To discuss the theory of the axion, we must first discuss Quantum Chromodynamics (QCD) and the strong CP problem.

QCD is a quantum field theory of the strong force (one of the four fundamental forces of nature). One of the most established properties is that it has a Charge-Parity (CP) symmetry. This means that the Lagrangian remains unchanged under transformations which map particles to their anti-particles (charge conjugation) and transformations which send the spatial coordinates $\mathbf{x}$ to their negatives i.e. $\mathbf{x} \to -\mathbf{x}$ (parity transformation). The issue with this is that the theory of QCD initially predicted that there would be a spontaneous breaking of this CP symmetry due to the unique structure of its vacuum [20] [21] [22]. The term in the QCD Lagrangian that is responsible for the CP symmetry breaking is given by:

$$\mathcal{L}_\theta = \theta \frac{g}{32\pi^2} G_{a\mu\nu} \widetilde{G}_a^{\mu\nu}, \tag{1.1}$$

where $G_{a\mu\nu}$ is the gluon field tensor, $\widetilde{G}_{a\mu\nu}$ is the Hodge dual of the gluon field, g is the QCD coupling and θ is a parameter of the theory. The breaking of CP symmetry would induce a non-zero electric dipole moment for the neutron [23] [24] [25], thus one can use its experimental measurement to set a bound on the value of θ. Current experimental measurements set the bound as $\theta < \mathcal{O}(10^{-10})$ [26]. This then poses a question: why should θ have such a small value? In principle, there is no mechanism for it to have a specific value, and the issue worsens once we consider the weak force. The value of θ also gets a contribution from quarks [27]:

$$\theta = \bar{\theta} + \arg\det(M), \tag{1.2}$$

where M is the quark mass matrix (which is in general complex) and $\bar{\theta}$ is the "bare" θ parameter unmodified by the contribution from the weak force. Why is it that these two quantities should almost cancel each other out? Indeed the most straightforward explanation is that they simply do, because if they didn't we wouldn't be able to observe it. This type of argument is known as an anthropic argument and is a topic of much scientific and philosophical debate. Without getting bogged down into too many details, many physicists find it unconvincing (including R.D. Peccei,

whose work proposed a different solution for the strong CP problem) on the basis that a universe is just as likely to have a specific value of θ as it would any other value [27].

1.2.2 Axion as a Solution

Having briefly discussed the strong CP problem, we can now discuss the axion. In 1977, Roberto Peccei and Helen Quinn proposed an elegant solution to this problem [28]. In their approach, they proposed a new chiral $U(1)$ symmetry of the theory, which would necessarily be broken, and the breaking of which would dynamically cancel out the θ term, thus preserving CP symmetry. The breaking of this symmetry would lead to a new pseudo-Nambu-Goldstone boson particle which is called the axion[1] [30], which we will denote as ψ. The standard model Lagrangian is modified by this field as [27]:

$$\mathcal{L} = \mathcal{L}_{\text{SM}} + \theta \frac{g^2}{32\pi^2} G_{a\mu\nu} \widetilde{G}_a^{\mu\nu} + \frac{\psi\xi}{f_a} \frac{g^2}{32\pi^2} G_{a\mu\nu} \widetilde{G}_a^{\mu\nu} - \frac{1}{2} \partial_\mu \psi \partial^\mu \psi + \mathcal{L}_{\text{Int}}, \tag{1.3}$$

where $\mathcal{L}_{\text{SM}}$ is the Lagrangian for the standard model sans the CP-violating term arising from QCD, f_a is an energy scale for the axion (also known as the axion decay constant), ξ is a dimensionless coupling parameter and $\mathcal{L}_{\text{Int}}$ is the term responsible for axions coupling to matter. The term that couples the gluons directly to the axion field can be interpreted as an effective potential, with a minimum occurring at $\langle\psi\rangle = -\theta\frac{f_a}{\xi}$ [27]. This then results in a cancellation of the CP violating term, resolving the strong CP problem. [2]

The axion is not a massless particle. It gains its mass m_ψ via its interactions with matter, which was first calculated by Bardeen and Tye in [31]. Another very important point of note for this thesis is that while axions do not couple directly to the electromagnetic field, they do couple to fermions. Through a fermion loop, they obtain an effective coupling to the electromagnetic field of the form:

$$\mathcal{L}_{\gamma\psi} = -\frac{1}{4} g_{\gamma\psi} \psi F_{\mu\nu} \widetilde{F}^{\mu\nu}, \tag{1.4}$$

where $g_{\gamma\psi}$ is the axion photon coupling, the exact value of which is determined by the axion model used, but it is generally very small in all models due to the inverse dependence with the relatively large axion decay constant $f_a \approx 10^{11}$GeV to 10^{18}GeV [32]. The full effective axion-electromagnetism Lagrangian is then given by:

$$\boxed{\mathcal{L}_{\gamma\psi} = \frac{1}{2} \partial_\mu \psi \partial^\mu \psi - \frac{1}{2} m_\psi^2 \psi^2 - \frac{1}{4} F_{\mu\nu} F^{\mu\nu} - \frac{1}{4} g_\psi \psi F_{\mu\nu} \widetilde{F}^{\mu\nu},} \tag{1.5}$$

where we have dropped the γ subscript in g_ψ, as we are only really concerned with axion couplings to the electromagnetic field in this work.

[1] We note that the name has somewhat of a humorous origin. Frank Wilczek named it after a laundry detergent called Axion, because of how it "cleaned up" the problem and its relation to the axial anomaly [29].

[2] It is common to redefine the axion field, in terms of a "physical" field such that $\psi_{\text{Physical}} = \psi - \langle\psi\rangle$. With this definition, the QCD Lagrangian does not have a CP-violating term, and the minimum of this physical axion field is achieved at $\langle\psi_{\text{Physical}}\rangle = 0$.

1.2.3 Original vs Invisible Axions

An important point of note that we have not addressed is that the original axion model proposed by Peccei and Quinn has long been ruled out. The original mass of the axion was calculated in [30] to be roughly on the order of 100keV, which should have been detected shortly after the development of the theory. Hope for the axion is fortunately not lost, as not too long after the introduction of the Peccei-Quinn theory, two separate models of something known as the "invisible axion" were proposed; firstly, there was the Kim-Shifman-Vainshtein-Zakharov model (KSVZ) [33] [34] and then the Dine-Fischler-Srednicki-Zhitnisky (DFSZ) model [35]. What both of these models had in common is that they predicted an axion mass on the sub-eV order, which would prove much trickier to probe. Indeed, to this day, these invisible axions have not been found, and the search is out for them. [3]

1.2.4 Axions as Dark Matter

Finally, we get to the main reason for our discussion of the axion: they are one of the premier candidate particles for the constituents of cold dark matter. The low mass that the axions would have, combined with their weak coupling and feasibility of early universe production, satisfy observational constraints obtained from cosmology. A comprehensive review of this topic can be found in [36] and [37].

1.2.5 Axion Searches

The axion has proven to be elusive thus far. Many experiments have searched for the axion, with a wide variety of approaches. Some of the high-profile experiments include:

- *ADMX*: The "Axion Dark Matter eXperiment" is perhaps the most well-known of the axion searches. Its approach is based on using microwave cavities in order to detect the dark matter present in our own dark matter galaxy halo. The experiment has been able to rule out several axion models in the μeV range. [38] [37] [39].

- *CAST*: The "Cern Axion Solar Telescope" is an experiment that searches for axions that would be produced in our very own sun. The experiment consists of pointing the telescope at the Sun, inside of which there is a very strong magnetic field which would convert axions into photons. So far it has been able to search the mass range $m_\psi = \mathcal{O}(10^{-1}\text{eV})$ [40]. It was also able to place an upper bound on the axion-photon coupling $g_{\gamma\psi} \leq 0.66\times10^{-10}\text{GeV}^{-1}$[41].

- *PVLAS*: The "Polarizzazione del Vuoto con LASer"[4] experiment sets out to test the predictions of strong field QED, mainly the properties of the QED vacuum. Naturally, as with any big experiment, there are other things that it can look for/rule out, which in this case is also the axion. The core of the experiment was to search for changes in the polarization of

[3] It should also be noted that axions can be introduced as a model that is independent of QCD. It is common to refer to such particles as axion-like particles (ALPs).

[4] *Italian* for "Polarization of the Vacuum with Laser".

light travelling through a magnetic field in a vacuum. If axions exist, they would also affect the polarization of photons, and as such the PVLAS could be used as a vehicle to search for axions. In 2006, a PVLAS result indicated the existence of axions with a mass of the order $m_\psi \approx 1\text{meV}$ and axion-photon coupling of the order $g_{\gamma\psi} \approx 5 \times 10^{-6}\text{GeV}^{-1}$ [42]. This was in contention with the already available CAST results [43], [44]. However, further experiments from PVLAS ruled out this result [45].

1.2.6 Primakoff Effect

The Primakoff effect was introduced in 1951 by American-Russian physicist Henry Primakoff as a way to describe the photoproduction of the π^0 meson in a nuclear electric field [46]. In contrast to the original formulation, in the axion context, the Primakoff effect refers to the production of an axion via an interaction of a photon and a virtual photon provided by a strong external magnetic field (as shown in figure 1.1). The reason for the same name is that the actual structure of the calculation remains similar. The conversion of an axion into photons in an external magnetic field is technically known as the inverse Primakoff effect; however, it is generally also referred to as the Primakoff effect.

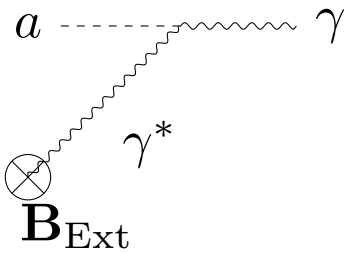

Figure 1.1: A Feynman diagram for the axionic inverse Primakoff effect $a + \gamma^* \to \gamma$ with external magnetic field $\mathbf{B}_{\text{Ext}}$.

For a modern review of the topic of the axionic Primakoff effect in the context of axions scattering off fermions and the case of a strong magnetic field see [47].

1.3 Surfing the Plasma Wave

Plasma is one of the four fundamental states of matter, alongside solids, liquids and gases. It is a quasi-neutral fluid comprised of fully or partially ionised atoms and electrons. The scientific community has been exploring the potential of plasmas for particle acceleration since the late 60's [48], but the concept really took off in the late 70's with Dawson's and Tajima's seminal paper [49]. They proposed what is now known as Laser Wakefield Acceleration (LWFA).

1.3.1 What is Wakefield Acceleration?

Wakefield Acceleration is a method of accelerating charged particles through the use of plasma waves, involving a driving laser pulse (in the case of laser wakefield acceleration) or a particle bunch

(in the case of particle wakefield acceleration). The focus of this thesis is specifically on the case of laser wakefield acceleration (LWFA), and thus we will not be discussing the case of particle wakefield acceleration (PWFA); a great historical overview of PWFA is given in [48]. The main draw of this method is that one can achieve much stronger electric fields than in conventional particle accelerators, which in turn leads to greater acceleration. Conventional particle accelerators use radio-frequency (RF) cavities to accelerate particles via electric fields. The maximum electric field achievable in these standard accelerators is approximately 100MVm^{-1} [50]; beyond this electric field strength, a breakdown in the walls of the accelerator begins. The advantage of plasma accelerators is that plasma is already mostly ionised, and such a breakdown is not an issue. Thus, fields of the order of 100GVm^{-1} are achievable [51]. This results in plasma accelerators being much more compact than conventional accelerators, and thus allows for a broader range of applications.

1.3.2 A Brief Theory Rundown

In this subsection, we will give an overview of some of the most basic concepts of LWFA.

1.3.2.1 Some assumptions

Before we discuss the basic principles of plasmas in the LWFA scheme, we want to introduce some of the assumptions that we will be making.

- *Collisionless*: The first assumption is that any effect that arises from the particles within the plasma colliding is negligible. This assumption is applied to systems in which the average collision time is far greater than the characteristic time scale of the system one is interested in.

- *Static Ions*: Due to the fact that ions have a much higher mass than electrons, they move much less readily than electrons do within the plasma. On short enough time scales, this means that ions can be treated as being essentially static. The time scales during which LWFA happens (i.e. short laser pulses propagating in an underdense plasma) are generally short enough to apply this approximation [52].

- *Cold Plasma*: A regime where thermal effects do not play much of a part in plasma processes is called the cold plasma regime. In this regime, it is reasonable to treat the plasma as if it had zero temperature (and by consequence no pressure effects). LWFA can generally be described within the cold plasma regime.

1.3.2.2 Electron Oscillations

One of the most basic concepts in plasma physics is that of Electron Oscillations (also known as Langmuir Oscillations). It is an oscillation in the electron density that results from the perturbation of the electrons. A mathematical overview of Langmuir Oscillations is given in Chapter 2, so for now we shall make statements without proof. The frequency at which electrons oscillate in a

plasma is given by the plasma frequency, which in turn is given by:

$$\omega_p = \sqrt{\frac{n_e e^2}{m_e}}, \tag{1.6}$$

where n_e is the electron density, e is the elementary charge and m_e is the electron mass.

1.3.2.3 Underdense and Overdense Plasma

Having introduced the notion of plasma frequency, we can now discuss the concept of underdense and overdense plasma. We begin with a discussion of the refractive index; for a cold collisionless plasma, the refractive index η is given as:

$$\eta = \sqrt{1 - \left(\frac{\omega_p}{\omega}\right)^2}, \tag{1.7}$$

where ω_p is the plasma frequency and ω is the laser angular frequency given by $\omega = \frac{2\pi}{\lambda_{\text{Laser}}}$, where λ_{Laser} is the laser wavelength. From equation (1.7) we can see that the scenario of a laser travelling through a plasma has three distinct regimes:

- Firstly, there is the case in which $\omega > \omega_p$, which results in a real refractive index i.e. $\eta \in \mathbb{R}$. This is called the *underdense* regime and is characterised by the laser pulse being able to propagate through the plasma.
- Naturally, we then have the case in which $\omega < \omega_p$ which results in a complex refractive index i.e. $\eta \in \mathbb{C}$. This regime is called *overdense* and is characterised by the laser pulse not being able to penetrate the plasma and thus effectively being reflected.
- Finally, there is the case where $\omega = \omega_p$. The electron density at which this condition occurs is known as the *critical density*. The value for the critical density n_c can be easily found as $n_c = \frac{4\pi^2 m_e}{e^2} \frac{1}{\lambda^2_{\text{Laser}}}$.

From looking at the refractive index, one can easily infer that an underdense plasma should be used for LWFA, as it is the regime in which a laser can propagate through a plasma.

1.3.2.4 Wake Generation and the Ponderomotive Force

The basic mechanism of LWFA is best understood via looking at a concept called the *ponderomotive force*. The ponderomotive force is in no way a fundamental force; rather, it is an effective term that arises from an averaging process. A rigorous derivation of the ponderomotive force is a difficult and contentious topic, and as such we shall accept its validity without proof in this thesis. For further discussion see the references [53], [54], [55] and [56]. The most common form of the (non-relativistic) ponderomotive force is given by the expression:

$$\mathbf{F}_{\text{Pond}} = -\frac{e^2}{2m_e\omega_p^2}\nabla|\mathbf{E}|^2. \tag{1.8}$$

Immediately, from inspection of equation (1.8), we see that the spatial gradient of the electric field is crucial in generating a strong ponderomotive force. As such, a short laser pulse can induce a very strong force which in extreme cases can create areas of little electron density within the plasma. Due to the spatial charge separation, the electric field within those areas of low density is extremely high. In the literature, this is known as the blowout or the bubble regime and is the key mechanism behind LWFA. A final note is that later in this thesis we will take a different (but equivalent) approach to ponderomotive effects, and equation (1.8) is used mostly for illustrative purposes.

1.3.3 Light-Shining-Through-a-Wall Experiment

Having discussed the basic mechanisms of LWFA, we will now discuss its application to the search for axionic dark matter. The method of interest is that of a Light-Shining-Through-a-Wall (LSTW) experiment, the basic principle of which is the utilisation of what makes dark matter so difficult to find: its feeble interaction with the electromagnetic field. The basic principle of the LSTW experiment, which we will consider in this work, is that a non-linear plasma wave is excited via a laser pulse with a static longitudinal magnetic field B_1 externally applied within the plasma channel. Due to the intersection of the magnetic field B_1 and the nonlinear plasma wave, we expect a flux of axions or ALPs to be produced.

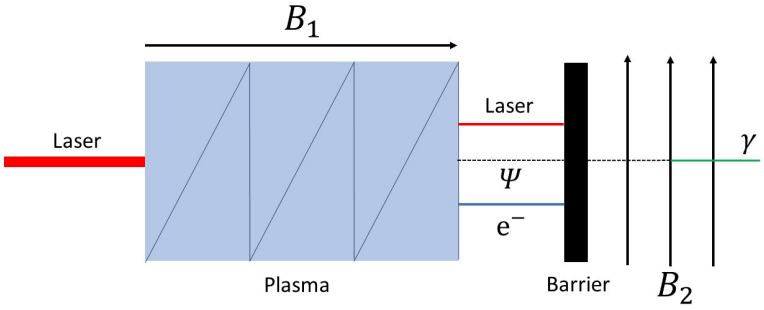

Figure 1.2: A diagram illustrating a LSTW set-up. The blue box containing the sawtooth wave represents the plasma, Ψ is used to label the outgoing axion flux, e^- represents the plasma electrons, and we use γ to label the outgoing photon from the axion-photon conversion process.

Leaving the plasma channel, we expect there to additionally be a strong flux of photons from the laser and high-energy electrons. In order to separate the axions from the photons and the electrons, a barrier is placed, which absorbs the photons and the electrons, but lets axions through due to the weak coupling g_ψ. After the axions leave the barrier, a strong static magnetic field B_2 is applied in the transverse direction and the axions are converted into photons via the Primakoff effect; thus, one could view it as "light, shining through a wall". This procedure is sketched in Figure 1.2. For more references on this topic, see [57],[58] and [59].

1.4 Summary & Thesis Plan

In conclusion, the problem of dark matter is one of the great problems of modern physics. There are a multitude of solutions to it, amongst which the axion is a well-motivated one. As such, searching for axions is an endeavour worth pursuing.

The thesis is structured as follows:

- In the second chapter, we focus on the theory of plasma waves and Laser Wakefield Acceleration. We study some basic results and then expand on the result of a 1D LWFA driven by a tophat laser pulse using a geometric approach [60]. (For a very good review of 1D LWFA theory, see [61].)
- In the third chapter, we introduce the axion field and consider the basic cases of axion production in a laser (see [62] and [63] for some more recent results in this area) and in a plasma (see [64] and [59] for some recent results as well). At the end of the chapter, we derive a resonance condition for the axion within a laser pulse travelling in a plasma, which relates laser plasma parameters to the axion mass.
- In the fourth chapter, we consider the problem of axion creation in a laser plasma, using a ponderomotive formalism (for a recent result which involves the application of a ponderomotive formalism in the context of axions see [65]). We propose an action for the system, derive the equations of motion and analyse a corresponding conservation law.
- In the fifth chapter, we consider the problem of axion production from a quantum perspective. The main result of this chapter is an improvement upon the classical result found in [66].
- In the sixth and final chapter, we briefly discuss the results in the thesis and discuss potential for future work.

Chapter 2

Theory of Relativistic Plasma Waves

In the introduction, we have reviewed the history and basic theory behind laser-plasma wakefield accelerators (LWFA). To adequately capture the key physical aspects of plasma in LWFAs we need to introduce and develop a theory of relativistic plasma waves, and as such, we do so in this chapter. It should be noted that we shall be focusing on analytical methods, and as such the calculations we will be performing will be concerned with simplified low-dimensional models. For a review of low-dimensional analytical methods, see [61], while [67] provides an overview of computation in the broader context of accelerator physics.

2.1 Mathematical Preliminaries

We begin by introducing the mathematical machinery we will be using to study the theory of plasma waves[1]. Space-time is modelled by a 4-dimensional Lorentzian manifold $\mathcal{M}_4$, equipped with a Minkowski metric g. In this thesis, we shall utilise the $(-,+,+,+)$ signature, meaning that in the case of using the Cartesian co-ordinates, the metric can be written as:

$$g = -dt \otimes dt + dx \otimes dx + dy \otimes dy + dz \otimes dz. \tag{2.1}$$

Having specified the metric, we can also introduce the volume form, which specifies the orientation of our space-time manifold. The volume form is given by:

$$\star 1 = dt \wedge dx \wedge dy \wedge dz. \tag{2.2}$$

The $\star$ denotes the Hodge star operator, which defines an operation on p forms on an oriented Riemannian or pseudo-Riemannian manifold that maps them onto $n-p$ forms, where n is the

[1] It should be noted that this geometric approach isn't strictly necessary as it is fully equivalent to conventional methods. However, we chose to use it in order to make some computations simpler and gain geometric insight.

dimension of the manifold. For any two p forms α and β, they satisfy:

$$\alpha \wedge \star\beta = \alpha \cdot \beta \star 1, \tag{2.3}$$

where $\cdot$ denotes the inner product induced by the metric and $\star 1$ is the volume form. The $\wedge$ symbol denotes the wedge product.

2.1.1 Action Principles via Differential Forms

Let us consider a p-form α on the space of differential forms $\alpha \in \Gamma\Lambda^p\mathcal{M}$. We can propose an action of the form:

$$S = \int_{\mathcal{M}} \frac{1}{2} d\alpha \wedge \star d\alpha. \tag{2.4}$$

To obtain equations of motion we naturally apply the principle of stationary action. To vary the action we need to introduce a one-parameter family of p-forms α_ϵ, where the parameter ϵ takes values in the range $\epsilon \in (-1, 1)$. The variation of the action is then given by:

$$\delta S[\alpha] = \frac{d}{d\epsilon} S[\alpha_\epsilon]|_{\epsilon=0}. \tag{2.5}$$

Denoting $\frac{d}{d\epsilon}\alpha_\epsilon|_{\epsilon=0} = \dot{\alpha}$, the first variation of the action given in (2.4) is:

$$\delta S[\alpha] = \int_{\mathcal{M}} \frac{1}{2} \left(d\dot{\alpha} \wedge \star d\alpha + d\alpha \wedge \star d\dot{\alpha} \right). \tag{2.6}$$

Using an identity for forms β and γ of equal degree:

$$\beta \wedge \star\gamma = \gamma \wedge \star\beta, \tag{2.7}$$

we can write $d\alpha \wedge \star d\dot{\alpha}$ as:

$$d\alpha \wedge \star d\dot{\alpha} = d\dot{\alpha} \wedge \star d\alpha, \tag{2.8}$$

thus getting rid of the $\frac{1}{2}$ factor. Furthermore, we can utilise the Leibniz rule for the exterior derivative to express the terms within the integral as follows:

$$d\dot{\alpha} \wedge \star d\alpha = d(\dot{\alpha} \wedge \star d\alpha) - (-1)^p \dot{\alpha} \wedge d \star d\alpha. \tag{2.9}$$

By doing this, we have introduced a total derivative term into our integral, which now allows us to apply Stokes' theorem to our problem, giving us an expression for the variation of the action in the form:

$$\delta S = \int_{\partial\mathcal{M}} \dot{\alpha} \wedge \star d\alpha - (-1)^p \int_{\mathcal{M}} \dot{\alpha} \wedge d \star d\alpha, \tag{2.10}$$

where $\partial\mathcal{M}$ denotes the boundary of the manifold. To proceed further, we shall make the physical assumption that the variations we choose are such that $\dot{\alpha}$ vanishes on the boundary $\partial\mathcal{M}$. With all that in mind, we can apply the principle of least action and assume that the equations of motion

are satisfied when the action is stationary. From this, we see that for

$$(-1)^{p+1}\int_{\mathcal{M}}\dot{\alpha}\wedge d\star d\alpha = 0 \tag{2.11}$$

to be true for all variations, we need

$$d\star d\alpha = 0 \tag{2.12}$$

to also hold true. This is our equation of motion.

2.1.1.1 Example 1 : The Free Electromagnetic Field

Introducing the electromagnetic potential 1-form A, the action for the free electromagnetic field is:

$$S[A] = \int_{\mathcal{M}}\frac{1}{2}dA\wedge\star dA. \tag{2.13}$$

The equation of motion obtained by variation with respect to A is simply

$$d\star dA = 0. \tag{2.14}$$

We can identify dA as the electromagnetic 2-form F. Using this and the nilpotent property of the exterior derivative ($ddA = 0$) we arrive at the coordinate free form of the vacuum Maxwell equations:

$$\begin{aligned} d\star F &= 0, \\ dF &= 0. \end{aligned} \tag{2.15}$$

2.1.1.2 Example 2: The Electromagnetic field with a current.

Introducing a current 3-form $\mathcal{J}$, the action is written as:

$$S[A] = \int_{\mathcal{M}}\frac{1}{2}dA\wedge\star dA - A\wedge\mathcal{J}. \tag{2.16}$$

Varying w.r.t. A, we obtain the sourced Maxwell equation:

$$d\star F = \mathcal{J}, \tag{2.17}$$

whilst the sourceless Maxwell equation follows from $F = dA$ as before:

$$dF = 0. \tag{2.18}$$

2.1.2 Body Manifold Formalism

The formalism that we will utilise here is that by Maugin [68], which we will refer to as the *body manifold formalism*. We are still working with a space-time manifold $\mathcal{M}$ equipped with a

metric (in our case, it is the Minkowski metric, but in general, this can be applied to any Lorentzian metric when considering applications to gravitational systems [69], [70]). We also introduce a body manifold $\mathcal{B}$, which can be interpreted as corresponding to a plasma, i.e. the plasma is modelled by two interpenetrating fluids with corresponding body manifolds (one for the electron fluid and one for the ion fluid). Each infinitesimal point on the body manifold can be referred to as a particle in the context of continuum mechanics. For completeness' sake we mention that in this section $Dim(\mathcal{M}) = 4$ and $Dim(\mathcal{B}) = 3$. Following [71], [70], the information about the dynamics of the electron fluid is contained in a submersion between $\mathcal{M}$ and $\mathcal{B}$ that we shall denote as f, such that:

$$\begin{aligned} f &: \mathcal{M} \to \mathcal{B} \\ x^\mu &\to \xi^A = f^A(x^\mu). \end{aligned} \tag{2.19}$$

Here the index μ runs through $\mu = 0, 1, 2, 3$ and the index A runs through $A = 1, 2, 3$. The mapping f can be interpreted as mapping each world-line onto its corresponding plasma particle. The plasma particles are in one-to-one correspondence with the integral curve of a time-like vector V (see Figure 2.1). V naturally satisfies:

$$\begin{aligned} df^A(V) &= 0, \\ g(V, V) &= -1. \end{aligned} \tag{2.20}$$

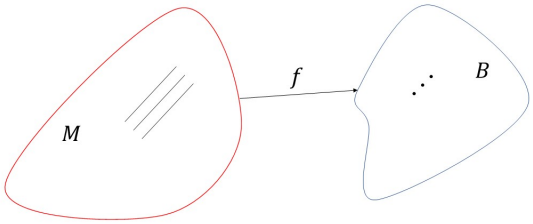

Figure 2.1: A diagram illustrating how the mapping f takes world-lines on $\mathcal{M}$ to points in $\mathcal{B}$. Each world-line is mapped to a unique point in $\mathcal{B}$.

To model the dynamics of the plasma we start by introducing a differential 3-form Ω on the body manifold $\mathcal{B}$. We then define a 3-form on $\mathcal{M}$ as the pull-back of Ω from $\mathcal{B}$ onto $\mathcal{M}$ i.e.:

$$j = f^*\Omega, \tag{2.21}$$

where j is the plasma electron number current 3-form. We will refer to j as the current 3-form. Having defined j, we can write down an action that will generate the equations of motion for the

plasma:

$$\boxed{S[A, f] = \int_{\mathcal{M}} m\, n \star 1 + qA \wedge (j - j_{\text{ion}}) + \frac{1}{2} dA \wedge \star dA,} \tag{2.22}$$

where $n = \sqrt{j \cdot j}$ is the proper number density of the plasma electrons, the parameter m is the electron mass, j_{ion} is the ion current 3-form in the plasma, A is the electro-magnetic potential 1-form and $F = dA$ as previously established. The inner product is, of course, induced by the Minkowski metric for which we are using the $(-,+,+,+)$ convention, and $\star$ is the Hodge map. The application of the inner product to j can be expressed as:

$$j \cdot j = \star^{-1} (j \wedge \star j) \,. \tag{2.23}$$

An additional point of note is that the first term in equation (2.22), $m\, n \star 1$, follows from making the cold plasma approximation, i.e. no pressure effects (note that these would be introduced in the first term of (2.22) by replacing mn with some non-linear function $f(n)$, which corresponds to an equation of state). Finally, we can relate the current 3-form j to the velocity field V via:

$$\widetilde{V} = \frac{1}{n} \star^{-1} j. \tag{2.24}$$

The tilde above a symbol, for example $\widetilde{V}$, denotes the metric dual operation i.e. $\widetilde{V}(X) = g(V, X)$ for all choices of vector X.

2.1.3 Equations of Motion

The variation of equation (2.22) with respect to the electromagnetic potential A leads to the sourced Maxwell equation i.e.

$$d \star F = -q(j - j_{\text{ion}}) \tag{2.25}$$

where we recall that the second, i.e. unsourced, Maxwell equation:

$$dF = 0, \tag{2.26}$$

comes from the nilpotency of the exterior derivative. We obtain the equation of motion for the electron fluid via variation of (2.22) with respect to the map f. This is performed by introducing a 1-parameter family of maps f_ϵ, with the condition that $f_0 = f$. We note that the variation of any field α with respect to f is defined as:

$$\delta_f \alpha = \left. \frac{d\alpha}{d\epsilon} \right|_{\epsilon=0}. \tag{2.27}$$

Varying the proper number density gives:

$$\begin{aligned}\delta_f n &= \delta_f \sqrt{j \cdot j} \\ &= \frac{1}{\sqrt{j \cdot j}} \frac{1}{2} (\delta_f j \cdot j + j \cdot \delta_f j) \\ &= \frac{1}{n} \delta_f j \cdot j \\ &= \frac{1}{n} \star^{-1} (\delta_f j \wedge \star j).\end{aligned} \tag{2.28}$$

The 3-form Ω on $\mathcal{B}$ can be locally given in terms of co-ordinates $\{\xi^1, \xi^2, \xi^3\}$ on $\mathcal{B}$:

$$\Omega = \frac{1}{3!} \Omega_{ABC}(\xi) d\xi^A \wedge d\xi^B \wedge d\xi^C, \tag{2.29}$$

where the Latin indices run through $A, B, C \in \{1, 2, 3\}$. The current 3-form j on $\mathcal{M}$ will then be given by:

$$\begin{aligned}j &= f^* \Omega \\ &= f^* \left(\frac{1}{3!} \Omega_{ABC}(\xi) d\xi^A \wedge d\xi^B \wedge d\xi^C \right) \\ &= \frac{1}{3!} \Omega_{ABC}(f(x)) df^A \wedge df^B \wedge df^C.\end{aligned} \tag{2.30}$$

The variation of j is then given by:

$$\delta_f j = \frac{1}{3!} \left(\frac{\partial \Omega_{ABC}}{\partial \xi^D} \circ f \right) \delta f^D df^A \wedge df^B \wedge df^C + \frac{1}{2!} \left(\Omega_{ABC} \circ f \right) d\delta f^A \wedge df^B \wedge df^C, \tag{2.31}$$

which can then be more simply expressed as:

$$\delta_f j = \mathcal{L}_Y j, \tag{2.32}$$

where $\mathcal{L}$ is the Lie derivative, which is defined by:

$$\mathcal{L}_X T = \frac{d}{d\epsilon}|_{\epsilon=0} (\phi_\epsilon^* T), \tag{2.33}$$

where X is a vector field, ϕ_ϵ is the flow that generates X, ϕ_ϵ^* is the pullback of ϕ_ϵ and T is an arbitrary covariant tensor. The vector field Y is a variation field given by:

$$Y = \delta f^A Y_A, \tag{2.34}$$

where $\{V, Y_1, Y_2, Y_3\}$ is a basis for vector fields on $\mathcal{M}$, such that $df^A(Y_B) = \delta^A_B$ (meaning that df^A and Y_B are orthonormal) and $df^A(V) = 0$ (this stems from V being time-like).

We know that the current 3-form j is a closed form (which is simply a geometrical manifestation of charge conservation), due to Ω being a top form on the body manifold. Thus, the application

of Cartan's identity, $\mathcal{L}_Y j = \iota_Y dj + d\iota_Y j$, leads us to :

$$\mathcal{L}_Y j = d\iota_Y j, \tag{2.35}$$

where ι_Y is the interior operator with respect to the vector field Y. With that in mind, the variation of the electron component of the plasma is given by:

$$\delta_f S = \int_{\mathcal{M}} \frac{m}{n} d\iota_Y j \wedge \star j + qA \wedge d\iota_Y j. \tag{2.36}$$

With the assumption of compact support of δf^A (which means that Y has compact support) on $\mathcal{M}$ we can integrate by parts to get:

$$\delta_f S = -\int_{\mathcal{M}} \iota_Y j \wedge d(\frac{m}{n} \star j - qA). \tag{2.37}$$

Due to the linearity of the interior operator ($\iota_Y = \delta f^A \iota_{Y_A}$) , the condition for stationarity becomes:

$$\iota_{Y_A} j \wedge d(\frac{m}{n} \star j - qA) = 0. \tag{2.38}$$

Finally, we can substitute the expression (2.24) and rearrange the result to obtain:

$$\iota_{Y_A} \iota_V (m d\widetilde{V} - qF) = 0, \tag{2.39}$$

where we used the fact that $\star^{-1} = \star$ on odd degree forms in $3+1D$ spacetime. Since $\{V, Y_1, Y_2, Y_3\}$ is a frame on $\mathcal{M}$, we get:

$$\iota_V d\widetilde{V} = \frac{q}{m} \iota_V F. \tag{2.40}$$

Since $g(V, V)$ is constant, we can write equation (2.40) using the Levi-Civita connection as:

$$\boxed{\nabla_V \widetilde{V} = \frac{q}{m} \iota_V F.} \tag{2.41}$$

Further details on this step are included in Appendix A.1. We note that (2.41) is simply the coordinate-free form of the Lorentz force equation. In the standard index notation, this is written as:

$$\frac{dV^\nu}{d\tau} = \frac{q}{m} V_\mu F^{\mu\nu}, \tag{2.42}$$

where τ denotes the proper time for current with 4-velocity V^ν.

2.1.4 Killing Vector Fields

Let us consider a metric g on a manifold $\mathcal{M}$. A diffeomorphism is an invertible map from one differentiable manifold to another such that the map and its inverse are both continuously differentiable. An isometry is a diffeomorphism that preserves the metric e.g. for a diffeomorphism $f : \mathcal{M}' \to \mathcal{M}$, where the manifolds are equipped with metrics $(\mathcal{M}, g)$ and $(\mathcal{M}', g')$, the pullback

f^* acts on the metric as:

$$f^*(g') = g. \tag{2.43}$$

Suppose we now consider a one-parameter family of isometries $f_\epsilon : \mathcal{M} \to \mathcal{M}$. From the definition of the Lie derivative (2.33) we have:

$$\mathcal{L}_\xi g = \frac{d}{d\epsilon}[f_\epsilon^*(g)]_{\epsilon=0} = \lim_{\epsilon\to 0} \frac{f_\epsilon^*(g) - g}{\epsilon} = 0, \tag{2.44}$$

where ξ is the vector field that generates f_ϵ and is known as a Killing vector field. The importance of Killing vector fields is that they quantify the symmetries of a metric.

2.2 Plasma Waves: Longitudinal Electric Field Case

Having described the equations of motion within our formalism, we can begin to model the waves within the plasma. We begin by studying a simplified case where there is only the longitudinal electric field present. This assumption allows us to capture some essential features of strong longitudinal fields present in LWFA. This requirement will be relaxed in the next section.

2.2.1 2 + 2 Split

The physics of large-amplitude plasma waves is fraught with many issues when it comes to the analytical approach. Dealing with a full 3+1-dimensional treatment analytically can be only done perturbatively or in very specific cases and is otherwise impossible, and thus is usually left to the domain of computational physics. To work on exact analytical solutions to problems, we aim to reduce the dimension of the system via simplifications, such that we can work with an ODE instead of a PDE.

We rewrite the current 3-form given in equation (2.30) as:

$$\begin{aligned} j &= \frac{1}{3!}\Omega_{ABC}(f(\mathbf{x}))df^A \wedge df^B \wedge df^C \\ &= d\hat{\phi} \wedge dx \wedge dy, \end{aligned} \tag{2.45}$$

where $d\hat{\phi} = \Omega_{123}(f(\mathbf{x}))df^1$ (where we change the notation for the co-ordinate argument $\mathbf{x}$ in order to distinguish it from x) and $f^2 = x$, $f^3 = y$. We assume that $\hat{\phi}$ depends only on t and z, and this assumption is what allows us to reduce the dimensionality of our equations. From now on, we will be working on (t, z) slices of $\mathcal{M}$, i.e. we have effectively performed a foliation on $\mathcal{M}$. The Hodge dual of j can then be written as:

$$\star j = \#d\hat{\phi}, \tag{2.46}$$

where $\#1 = dt \wedge dz$ is the Hodge operator on the (t, z) slices, which we shall call the reduced Hodge operator. The reduced metric on the (t, z) slices is given by:

$$g = -dt \otimes dt + dz \otimes dz. \tag{2.47}$$

With that in mind, $j \wedge \star j$ can be expressed as:

$$j \wedge \star j = d\hat{\phi} \cdot d\hat{\phi} \# 1 \wedge dx \wedge dy = d\hat{\phi} \cdot d\hat{\phi} \star 1. \tag{2.48}$$

The same procedure can be applied to the ion current (which is given as data in our setup), and we set:

$$j_{\text{ion}} = d\hat{\phi}_{\text{ion}} \wedge dx \wedge dy \tag{2.49}$$

where $\hat{\phi}_{\text{ion}}$ also depends only on t and z. We also prescribe the form of the electromagnetic potential to be:

$$A = A_0(t, z)dt + A_1(t, z)dz. \tag{2.50}$$

We note that (2.50) leads to an expression for the electromagnetic 2-form of the form:

$$F = E \# 1, \tag{2.51}$$

where $E = \partial_t A_1 - \partial_z A_0$. With these assumptions laid out, we can integrate out the redundant degrees of freedom from the full EM-Plasma action given in (2.22) in order to obtain a reduced action:

$$S[\hat{\phi}, A] = \Lambda \int m\sqrt{d\hat{\phi} \cdot d\hat{\phi}} \# 1 + qA \wedge (d\hat{\phi} - d\hat{\phi}_{\text{ion}}) + \frac{1}{2} F \wedge \# F, \tag{2.52}$$

where Λ is a cross-sectional factor that arose out of integrating out the x and y dependence.

We can now vary (2.52) with respect to $\hat{\phi}$ and A in order to obtain the reduced equations of motion:

$$\delta_{\hat{\phi}} S = 0 \to -d\# \frac{d\hat{\phi}}{\left\| d\hat{\phi} \right\|} + \frac{q}{m} F = 0, \tag{2.53}$$

$$\delta_A S = 0 \to d\# F + q(d\hat{\phi} - d\hat{\phi}_{\text{ion}}) = 0, \tag{2.54}$$

where $\left\| d\hat{\phi} \right\| = \sqrt{d\hat{\phi} \cdot d\hat{\phi}}$ [2].

Inspecting equation (2.54), it is apparent that we can write it as an exterior derivative of a 0-form:

$$d\left(\# F + q(\hat{\phi} - \hat{\phi}_{\text{ion}}) \right) = 0. \tag{2.55}$$

We can immediately integrate equation (2.55):

$$\# F + q(\hat{\phi} - \hat{\phi}_{\text{ion}}) = C, \tag{2.56}$$

where C is a constant of integration that we will set to zero without loss of generality. Noting the identity of the reduced Hodge on forms of even degree $\#\# = -1$, we can obtain an expression for

[2] We define the norm for a p-form α as: $\|\alpha\| = \begin{cases} \sqrt{\alpha \cdot \alpha} & \text{if } \alpha \cdot \alpha > 0 \\ \sqrt{-\alpha \cdot \alpha} & \text{if } \alpha \cdot \alpha < 0 \end{cases}$

F:

$$F = q(\hat{\phi} - \hat{\phi}_{\text{ion}})\#1. \tag{2.57}$$

We can simply then substitute in (2.57) into (2.53) in order to obtain:

$$d\#\frac{d\hat{\phi}}{\left\|d\hat{\phi}\right\|} = \frac{q^2}{m}(\hat{\phi} - \hat{\phi}_{\text{ion}})\#1. \tag{2.58}$$

One further very common approximation that we will apply is that, for now, we will neglect the dynamics of the ions within the plasma, as they typically move on much longer time scales than the electrons. With that in mind, we set $d\hat{\phi}_{\text{ion}} = n_{\text{ion}}dz$, where n_{ion} is a constant ion density. We now re-scale the fields:

$$\begin{aligned} \phi &= \frac{1}{n_{\text{ion}}}\hat{\phi}, \\ \phi_{\text{ion}} &= \frac{1}{n_{\text{ion}}}\hat{\phi}_{\text{ion}}. \end{aligned} \tag{2.59}$$

Equation (2.58) then becomes:

$$\boxed{d\#\frac{d\phi}{\|d\phi\|} = \omega_p^2\left(\phi - \phi_{\text{ion}}\right)\#1,} \tag{2.60}$$

where $\omega_p = \sqrt{\frac{q^2 n_{\text{ion}}}{m}}$ is the plasma frequency. Although it is very succinct, the covariant representation (2.60) of the electron dynamics in terms of the scalar field ϕ (which can be loosely thought of as a potential due to $d\phi$ corresponding to a current) appears to have received little attention in laser-plasma physics.

2.2.2 Langmuir Oscillations

We can illustrate the workings of our formalism by calculating some basic results from the theory of plasmas. The simplest possible example are the cold plasma Langmuir oscillations.

We begin by assuming that the amplitude of the electron wave is small and recalling that we are considering a constant ion background:

$$\phi_{\text{ion}} = z, \tag{2.61}$$

$$\phi = \phi_{\text{ion}} + \epsilon\psi, \tag{2.62}$$

where ψ denotes the electron fluid perturbation and ϵ is a perturbation parameter such that $|\epsilon| \ll 1$. We can apply these assumptions to equation (2.60) to arrive at a linear equation of motion. Firstly,

we expand $d\phi \cdot d\phi$ as:

$$\begin{aligned} d\phi \cdot d\phi &= d\phi_{\text{ion}} \cdot d\phi_{\text{ion}} + 2\epsilon d\phi_{\text{ion}} \cdot d\psi + \mathcal{O}(\epsilon^2) \\ &= 1 + 2\epsilon \partial_z \psi + \mathcal{O}(\epsilon^2), \end{aligned} \tag{2.63}$$

and taking the magnitude:

$$\begin{aligned} \|d\phi\| &= \sqrt{d\phi \cdot d\phi} \\ &= 1 + \epsilon \partial_z \psi + \mathcal{O}(\epsilon^2). \end{aligned} \tag{2.64}$$

We then express $\frac{d\phi}{\|d\phi\|}$ as:

$$\begin{aligned} \frac{d\phi}{\|d\phi\|} &= dz - \epsilon \partial_z \psi dz + \epsilon d\psi + \mathcal{O}(\epsilon^2) \\ &= dz + \epsilon \partial_t \psi dt + \mathcal{O}(\epsilon^2), \end{aligned} \tag{2.65}$$

since $d\psi = \partial_t \psi dt + \partial_z \psi dz$. We can then finally express the kinetic term in the equation of motion (2.60) for ϕ as:

$$d\# \frac{d\phi}{\|d\phi\|} = -\epsilon \partial_t^2 \psi \# 1 + \mathcal{O}(\epsilon^2). \tag{2.66}$$

The other term in the equation is simply given by:

$$\omega_p^2 \left(\phi - \phi_{\text{ion}}\right) \# 1 = \epsilon \omega_p^2 \psi \# 1. \tag{2.67}$$

We now simply drop $\mathcal{O}(\epsilon^2)$ terms to arrive at:

$$\partial_t^2 \psi = -\omega_p^2 \psi, \tag{2.68}$$

whose solutions describe the Langmuir oscillations of a cold plasma.

2.2.3 Cold Plasma Wave Breaking Limit

In this section, we will consider a classic result in the theory of non-linear plasma waves, that being the cold plasma wave breaking limit, as derived by A. I. Akhiezer and R. V. Polovin in [72].
We begin by making a few assumptions; firstly we once again assume a constant ion background:

$$\phi_{\text{ion}} = z. \tag{2.69}$$

Secondly, we assume that the electron fluid has the form:

$$\phi = \phi_{\text{ion}} + \psi, \tag{2.70}$$

where ψ depends only on a coordinate $\zeta = z - vt$, which is adapted to an observer travelling at velocity v in the frame of the ions. Denoting $\psi^{'} = \frac{d\psi}{d\zeta}$, we can write:

$$\|d\phi\| = \sqrt{(1+\psi')^2 - v^2\psi'^2}. \tag{2.71}$$

The kinetic term in (2.60) is then given by:

$$d\#\frac{d\phi}{\|d\phi\|} = \left(\frac{(1+\psi') - v^2\psi'}{\sqrt{(1+\psi')^2 - v^2\psi'^2}}\right)' \#1. \tag{2.72}$$

The right hand side of (2.60) becomes:

$$\omega_p^2(\phi - \phi_{\text{ion}})\#1 = \omega_p^2\psi\#1, \tag{2.73}$$

leading to the full ODE of the form:

$$\left(\frac{(1+\psi') - v^2\psi'}{\sqrt{(1+\psi')^2 - v^2\psi'^2}}\right)' = \omega_p^2\psi. \tag{2.74}$$

We can write down a Lagrangian which generates equation (2.74):

$$L = 1 - \sqrt{(1+\psi')^2 - v^2\psi'^2} - \frac{1}{2}\omega_p^2\psi^2. \tag{2.75}$$

Noting that (2.75) has no explicit ζ dependence, we can immediately write down the first integral of the system:

$$\begin{aligned}\mathcal{E} &= \psi'\frac{\partial L}{\partial \psi'} - L \\ &= \frac{1+\psi'}{\sqrt{(1+\psi')^2 - v^2\psi'^2}} - 1 + \frac{1}{2}\omega_p^2\psi^2,\end{aligned} \tag{2.76}$$

where $\mathcal{E}$ is a constant of motion. The additive constant and signs in (2.75) have been chosen to cast (2.76) in an elegant form.

The extrema of ψ occur whenever $\psi' = 0$, therefore the maximum value of ψ should satisfy:

$$\mathcal{E} = \frac{1}{2}\omega_p^2\psi_{\text{max}}^2. \tag{2.77}$$

We shall insist on the solution being oscillatory, and as such, we know from (2.77) that is bounded between two values $-\psi_{\text{max}} \leq \psi \leq \psi_{\text{max}}$. From this we then know that ψ has to take the value of 0 during an oscillation, meaning that the absolute maximum value of ψ is achieved on the oscillation where $\psi \to 0$ as $\psi' \to \infty$ (a sketch of this solution is given in figure 2.2). We can use this to obtain

an expression for the constant of motion $\mathcal{E}$:

$$\lim_{\psi' \to \infty} \mathcal{E} = \frac{1}{\sqrt{1 - v^2}} - 1 = \gamma - 1, \tag{2.78}$$

where γ is the Lorentz factor of the wave. Combining (2.78) and (2.77) we obtain:

$$\psi_{\max} = \frac{1}{\omega_p} \sqrt{2(\gamma - 1)}. \tag{2.79}$$

We recall the form of equation (2.57), and in this case it becomes:

$$F = q n_{\text{ion}} \psi \# 1 = E \# 1, \tag{2.80}$$

where E denotes the z component of the electric field. Therefore, the absolute maximum electric field amplitude inside a 1D cold plasma wave is given by:

$$E_{\max} = \frac{m \omega_p}{e} \sqrt{2(\gamma - 1)}, \tag{2.81}$$

where $q = -e$ has been used.

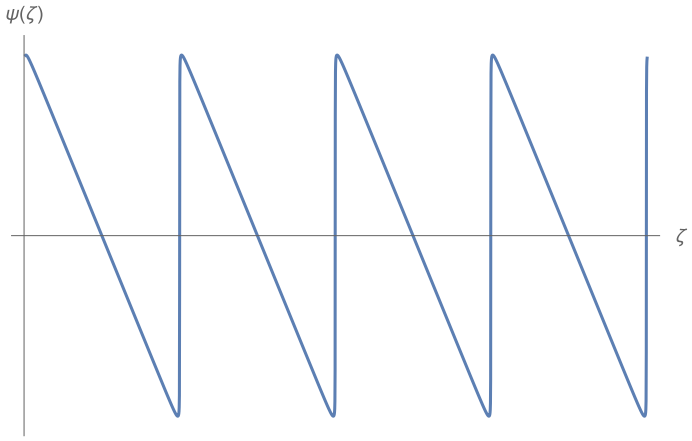

Figure 2.2: An illustration of the maximum amplitude wave solution for ψ.

2.2.4 Ion and Electron Perturbations

Thus far we have only investigated dynamics with a purely static ion background. We will now consider a case where the ion background is also perturbed. We consider the electron and ion fluids of the form:

$$\begin{aligned} \phi^{\epsilon}_{\text{ion}} &= \phi^{(0)}_{\text{ion}} + \epsilon \phi^{(1)}_{\text{ion}} + \mathcal{O}(\epsilon^2), \\ \phi^{\epsilon} &= \phi^{(0)} + \epsilon \phi^{(1)} + \mathcal{O}(\epsilon^2). \end{aligned} \tag{2.82}$$

The zeroth order terms satisfy:

$$\boxed{d\#\frac{d\phi^{(0)}}{\left\|d\phi^{(0)}\right\|}=\omega_p^2(\phi^{(0)}-\phi_{\text{ion}}^{(0)})\#1.} \tag{2.83}$$

At first order, we can write a quantity:

$$\begin{aligned}\frac{d}{d\epsilon}\frac{d\phi^{\epsilon}}{\|d\phi^{\epsilon}\|}|_{\epsilon=0}&=\frac{d\phi^{(1)}}{\left\|d\phi^{(0)}\right\|}-\frac{1}{\left\|d\phi^{(0)}\right\|^3}\left(d\phi^{(1)}\cdot d\phi^{(0)}\right)d\phi^{(0)}\\&=\frac{1}{\left\|d\phi^{(0)}\right\|}\left(\mathbb{1}-\frac{d\phi^{(0)}}{\left\|d\phi^{(0)}\right\|}\otimes\widetilde{\frac{d\phi^{(0)}}{\left\|d\phi^{(0)}\right\|}}\right)(-,d\phi^{(1)}),\end{aligned} \tag{2.84}$$

where $\frac{1}{\left\|d\phi^{(0)}\right\|}\left(\mathbb{1}-\frac{d\phi^{(0)}}{\left\|d\phi^{(0)}\right\|}\otimes\widetilde{\frac{d\phi^{(0)}}{\left\|d\phi^{(0)}\right\|}}\right)$ is a rank (1,1) tensor, which acts on $d\phi^{(1)}$ and $\mathbb{1}=e^0\otimes X_0+e^1\otimes X_1$ is an identity tensor with a basis X_0, X_1 (with e^0, e^1 being a dual basis to it). We can choose our basis to be:

$$\begin{aligned}X_0&=\frac{\widetilde{\#d\phi^{(0)}}}{\left\|\#d\phi^{(0)}\right\|},\\X_1&=\frac{\widetilde{d\phi^{(0)}}}{\left\|d\phi^{(0)}\right\|},\end{aligned} \tag{2.85}$$

with a dual co-basis of:

$$\begin{aligned}e^0&=-\frac{\#d\phi^{(0)}}{\left\|\#d\phi^{(0)}\right\|},\\e^1&=\frac{d\phi^{(0)}}{\left\|d\phi^{(0)}\right\|}.\end{aligned} \tag{2.86}$$

The minus sign in e^0 in (2.86) is required because $d\phi^{(0)}$ is spacelike. We can then write:

$$\mathbb{1}-\frac{d\phi^{(0)}}{\left\|d\phi^{(0)}\right\|}\otimes\widetilde{\frac{d\phi^{(0)}}{\left\|d\phi^{(0)}\right\|}}=\frac{\#d\phi^{(0)}}{\left\|\#d\phi^{(0)}\right\|}\otimes\widetilde{\frac{\#d\phi^{(0)}}{\left\|\#d\phi^{(0)}\right\|}}. \tag{2.87}$$

Noting that[3] $\left\|\#d\phi^{(0)}\right\|=\left\|d\phi^{(0)}\right\|$, we can introduce a vector field U:

$$U=\frac{\widetilde{\#d\phi^{(0)}}}{\|d\phi^0\|} \tag{2.88}$$

which we can use to write the equation of motion for the first-order perturbations $\phi^{(1)}$ and $\phi_{\text{ion}}^{(1)}$:

$$d\#\left(-\frac{1}{\left\|d\phi^{(0)}\right\|}\widetilde{U}\otimes U(-,d\phi^{(1)})\right)=\omega_p^2(\phi^{(1)}-\phi_{\text{ion}}^{(1)})\#1. \tag{2.89}$$

[3]Note $\#d\phi^{(0)}\wedge\#\#d\phi^{(0)}=\#d\phi^{(0)}\wedge d\phi^{(0)}=-d\phi^{(0)}\wedge\#d\phi^{(0)}=-d\phi^{(0)}\cdot d\phi^{(0)}$

Using the property $d\phi^{(1)}(U) = U(\phi^{(1)})$ of the exterior derivative, and the fact that the Lie derivative acting on a 0-form is simply given by $\mathcal{L}_U\phi^{(1)} = U(\phi^{(1)})$ we can write (2.89) as:

$$d\#\left(\frac{1}{\left\|d\phi^{(0)}\right\|}\mathcal{L}_U\phi^{(1)}\widetilde{U}\right) = -\omega_p^2(\phi^{(1)} - \phi_{\text{ion}}^{(1)})\#1. \tag{2.90}$$

Furthermore, we note that for a scalar function f and a vector field U, we have:

$$\begin{aligned} d\#(f\widetilde{U}) &= d\iota_U\#f \\ &= \mathcal{L}_U\#f. \end{aligned} \tag{2.91}$$

This allows us to write (2.90) as:

$$\boxed{\mathcal{L}_U\#\left(\frac{1}{\left\|d\phi^{(0)}\right\|}\mathcal{L}_U\phi^{(1)}\right) = -\omega_p^2(\phi^{(1)} - \phi_{\text{ion}}^{(1)})\#1,} \tag{2.92}$$

which then captures the first-order electron fluid response to first-order ion perturbations.

2.2.4.1 Example 1

We make an assumption that $\phi^{(0)}$ depends on $\zeta = z - vt$ only. The 1-form $\widetilde{U}$ is then written as:

$$\widetilde{U} = \frac{\#d\phi^{(0)}}{\left\|d\phi^{(0)}\right\|} = \frac{-dt + vdz}{\sqrt{1-v^2}}, \tag{2.93}$$

and the metric dual of $\widetilde{U}$ (a vector field) is given by:

$$U = \gamma(\partial_t + v\partial_z). \tag{2.94}$$

Noting that $U(\zeta) = 0$ and $\mathcal{L}_U\#1 = 0$, we can write (2.92) as:

$$\mathcal{L}_U^2\phi^{(1)} = -\left\|d\phi^{(0)}\right\|\omega_p^2(\phi^{(1)} - \phi_{\text{ion}}^{(1)}). \tag{2.95}$$

To continue with the calculation, we need to introduce a new co-ordinate $\xi = t - vz$, which leads us to specify an ortho-normal co-frame $\{\gamma d\zeta\ ,\ \gamma d\xi\}$. The Lie derivative $\mathcal{L}_U$ acting on $\phi^{(1)}$ can thus be written as:

$$\begin{aligned} \mathcal{L}_U\phi^{(1)} &= \frac{\partial\phi^{(1)}}{\partial\xi}U(\xi) + \frac{\partial\phi^{(1)}}{\partial\zeta}U(\zeta) \\ &= \frac{1}{\gamma}\frac{\partial\phi^{(1)}}{\partial\xi}. \end{aligned} \tag{2.96}$$

The expression $\mathcal{L}_U^2\phi^{(1)}$ then becomes:

$$\mathcal{L}_U^2\phi^{(1)} = \frac{1}{\gamma^2}\frac{\partial^2\phi^{(1)}}{\partial\xi^2}. \tag{2.97}$$

We can then write:

$$\frac{1}{\gamma^2}\frac{\partial^2\phi^{(1)}}{\partial\xi^2} = -\left\|d\phi^{(0)}\right\|\omega_p^2(\phi^{(1)} - \phi_{\text{ion}}^{(1)}). \tag{2.98}$$

To proceed, we need to specify the zeroth order dynamics of the system. The simplest prescription that matches the condition $\phi^{(0)} \equiv \phi^{(0)}(\zeta)$ is that $\phi^{(0)} = \zeta$ and $\phi_{\text{ion}}^{(0)} = \zeta$. Equation (2.83) is satisfied trivially with these assumptions.

For example, if the ion dynamics are specified to first order as:

$$\phi_{\text{ion}} = \zeta + \epsilon A e^{-k(|\zeta+\xi|)} + \mathcal{O}(\epsilon^2), \tag{2.99}$$

representing an exponentially decaying perturbation in the ion density. Equation (2.98) is then given by:

$$\frac{\partial^2\phi^{(1)}}{\partial\xi^2} = -\omega_p^2(\phi^{(1)} - Ae^{-k(|\zeta+\xi|)}). \tag{2.100}$$

The solution to (2.100) takes the form $\phi^{(1)} = \chi(\xi)e^{-k\zeta}$, thus we can write:

$$\frac{d^2\chi}{d\xi^2} + \omega_p^2\chi = Ae^{-k|\xi|}. \tag{2.101}$$

The solution of (2.101) is plotted in 2.3, and illustrates the behaviour of the decaying perturbation by showing purely oscillatory behaviour for large ξ.

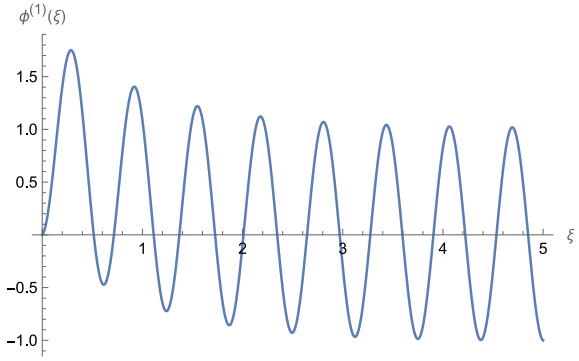

Figure 2.3: The solution to (2.101) in the range $\xi \in [0, 5]$ and with initial conditions $\phi^{(1)}(0) = 0$ and $\phi'^{(1)}(0) = 1$, with parameters $A = 1$, $\omega_p = 1$ and $k = 1$ for illustration.

2.2.4.2 Example 2

We set $\phi_{\text{ion}}^{(1)} = 0$ and $\phi^{(0)} = \phi_{\text{ion}}^{(0)}$ depending only on the coordinate z, with the condition that $\frac{d\phi_{\text{ion}}^{(0)}}{dz} > 0$. Taking $U = \frac{\#\widetilde{d\phi^{(0)}}}{\left\|d\phi^{(0)}\right\|}$, the equation of motion for $\phi^{(1)}$ becomes:

$$\partial_t^2\phi^{(1)} = -\omega(z)^2\phi^{(1)}, \tag{2.102}$$

where $\omega(z) = \frac{d\phi_{\text{ion}}^{(0)}}{dz}\omega_p$. Equation (2.102) is immediately solved by:

$$\phi^{(1)}(t, z) = A(z)\sin(\omega(z)t) + B(z)\cos(\omega(z)t), \tag{2.103}$$

which is plotted in figure 2.4. This shows that for our given conditions, we get a solution that is oscillatory in time with a position-dependent frequency.

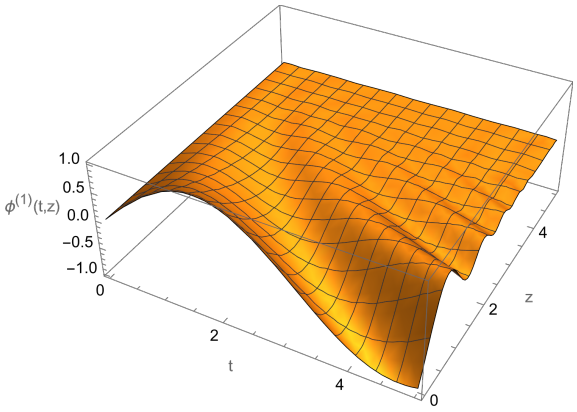

Figure 2.4: An example solution $\phi^{(1)}(t,z)$ with $A(z) = e^{-|z|}$, $B = 0$ and $\omega(z) = e^z$ for illustration.

2.2.5 Killing Vectors

We can use the symmetries of the Minkowski metric (which are described via Killing vectors) to gain insights into some general solutions of (2.60).
Let K be a Killing vector field of the metric g. We will also require that $\mathcal{L}_K\phi = \mathcal{L}_K\phi_{\text{ion}} = \text{constant}$.

2.2.5.1 Example 1: $K = \partial_t + v\partial_z$

Suppose $K = \partial_t + v\partial_z$, which coincides with a vector field corresponding to an observer travelling with a velocity v along the z-axis. Physically, this then represents a current that is constant in the direction of K. It then follows that:

$$\begin{aligned} \mathcal{L}_K(z - vt) &= 0 \\ \mathcal{L}_K(z) &= v. \end{aligned} \tag{2.104}$$

Due to this, we can immediately write down the general solution to $\mathcal{L}_K\phi = \mathcal{L}_K\phi_{\text{ion}} = a$, where a is a constant:

$$\begin{aligned} \phi &= \frac{a}{v}z + \psi(z - vt) \\ \phi &= \frac{a}{v}z + \psi_{\text{ion}}(z - vt), \end{aligned} \tag{2.105}$$

where ψ and ψ_{ion} are arbitrary differentiable functions. This result can be interpreted as a current profile that is transported along z at a constant speed v without dispersing.

2.2.5.2 Example 2: $K = z\partial_t + t\partial_z$

Let us consider a region where $|z| > |t|$ (illustrated in figure 2.5), then the vector field $K = z\partial_t + t\partial_z$, which is a generator of Lorentz boosts in the $t - z$ plane, has a norm $g(K, K) < 0$ i.e. K is time-like. This then physically corresponds to the case of an accelerating current density that remains

unchanged under boosts.

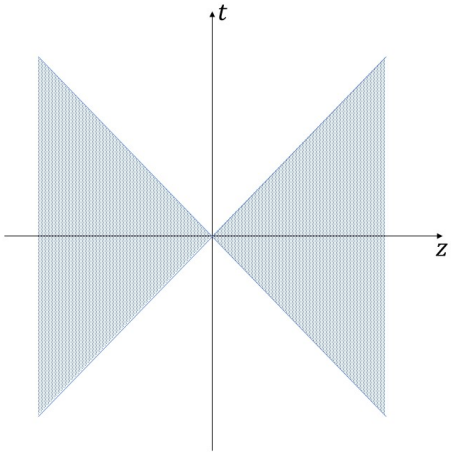

Figure 2.5: A diagram illustrating the region where $|z| > |t|$.

The following holds from direct computation:

$$\mathcal{L}_K(z^2 - t^2) = 0. \tag{2.106}$$

We can introduce a new set of coordinates (which are 2D Rindler co-ordinates):

$$\begin{aligned} z &= \rho\cosh(\chi) \\ t &= \rho\sinh(\chi). \end{aligned} \tag{2.107}$$

We can then express K as :

$$K = \partial_\chi. \tag{2.108}$$

Once again assuming the condition that $\mathcal{L}_K\phi = \mathcal{L}_K\phi_{\text{ion}} = a$, we obtain a general solution of the form:

$$\begin{aligned} \phi &= a\chi + \psi(\rho), \\ \phi_{\text{ion}} &= a\chi + \psi_{\text{ion}}(\rho). \end{aligned} \tag{2.109}$$

Noting that the metric is written:

$$g = d\rho \otimes d\rho - \rho^2 d\chi \otimes d\chi, \tag{2.110}$$

in the new set of coordinates, we can obtain an ODE for $\psi(\rho)$:

$$\frac{1}{\rho}\left(\frac{\rho\psi'}{\sqrt{\psi'^2 - \frac{a^2}{\rho^2}}}\right)' = \omega_p^2(\psi - \psi_{\text{ion}}), \tag{2.111}$$

where $\psi' = \frac{d\psi}{d\rho}$.

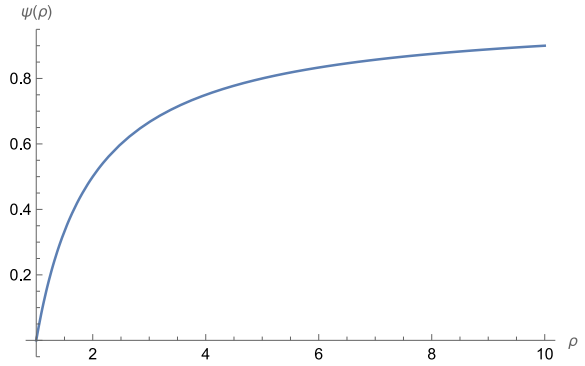

Figure 2.6: A numerical solution to (2.111) with $a = 1$, $\omega_p = 1$ and initial conditions $\psi(1) = 0$ and $\psi'(1) = 1$.

In 2.6, we see an electron density that goes to zero in the Rindler horizon (i.e. light-like observers) and increases towards regions of lower acceleration.

2.3 Plasma Waves: Full Transverse Extended Field

In the previous section, we explored the case of plasma waves where the electromagnetic field was specified to be $F = E\#1$. In this section, we shall relax this condition and consider the transverse components of the electromagnetic field. This will allow us to consider the important case of a plasma driven by a laser pulse.

2.3.1 2+2 Split

Following a similar methodology to the previous section, we want to perform a 2+2 split in order to make our equation tractable.
The electromagnetic 2-form F can be expressed as:

$$F = E\#_{\parallel}1 + dA_j \wedge dx^j - B\#_{\perp}1, \tag{2.112}$$

where $\#_{\parallel}1 = dt \wedge dz$ and $\#_{\perp}1 = dx \wedge dy$. E and B are 0-forms, while $A_j dx^j$ is a 1-form, with $j = 1, 2$ corresponding to the x and y components respectively. The key assumption for this approach is that E, B and the components of dA_j depend only on t and z.
Furthermore, the velocity field V may also be simply decomposed as:

$$V = V_{\parallel} + V_{\perp}, \tag{2.113}$$

where $V_{\parallel} \in span\{\partial_t, \partial_z\}$ and $V_{\perp} \in span\{\partial_x, \partial_y\}$.

2.3.1.1 Maxwell's Equations

Maxwell's equations coupled to a plasma containing both electrons and ions are given by:

$$\begin{aligned} d \star F &= -qn \star \widetilde{V} + qn_{\text{ion}} \star \widetilde{V}_{\text{ion}} \\ dF &= 0, \end{aligned} \tag{2.114}$$

where we assume that $V_{\text{ion}} \in span\{\partial_t, \partial_z\}$. Under all the assumptions mentioned above, we obtain the condition that B is constant and the equations:

$$dE = qn\#_{\|}\widetilde{V}_{\|} - qn_{\text{ion}}\#_{\|}\widetilde{V}_{\text{ion}}, \tag{2.115}$$

$$d\#_{\|}dA_j = qnV_j\#_{\|}1, \tag{2.116}$$

where V_j are the components of $\widetilde{V}_{\perp} = V_j dx^j$.

2.3.1.2 Lorentz Force

Equation (2.40) decomposes into the following equations:

$$\iota_{V_{\|}} d\widetilde{V}_{\|} - V^j dV_j = \frac{q}{m}\left(E\#_{\|}\widetilde{V}_{\|} - V^j dA_j\right), \tag{2.117}$$

$$\left(\iota_{V_{\|}} dV_j\right) dx^j = \frac{q}{m}\left(\iota_{V_{\|}} dA_j\right) dx^j - \frac{q}{m} B\#_{\perp}\widetilde{V}_{\perp}. \tag{2.118}$$

2.3.1.3 Plasma Wave Equations

Considering the constraint that B is a constant, we can consider a choice of $B = 0$, which then allows us to solve equation (2.118):

$$V_j = \frac{q}{m} A_j. \tag{2.119}$$

This then allows equation (2.116) to become:

$$d\#_{\|}dA_j = \frac{q^2 n}{m} A_j\#_{\|}1, \tag{2.120}$$

which is a massive wave equation for A_j and:

$$d\widetilde{V}_{\|} = \frac{q}{m} E\#_{\|}1, \tag{2.121}$$

follows from (2.117). The steps between equation (2.117) and (2.121) are given in appendix A.2. We can conveniently express equation (2.120) in terms of the complex quantity $\mathcal{A} = \frac{q}{m}(A_1 + iA_2)$ as:

$$d\#_{\|}d\mathcal{A} = \frac{q^2 n}{m}\mathcal{A}\#_{\|}1. \tag{2.122}$$

Now noticing that $n\#_{\|}\widetilde{V}_{\|}$ and $n_{\text{ion}}\#_{\|}\widetilde{V}_{\text{ion}}$ are closed forms since both the electron and the ion current are independently conserved, we can write them as exterior derivatives of two 0-forms $\hat{\phi}$

and $\hat{\phi}_{ion}$ i.e.:

$$\begin{aligned} n\#_{\|}\widetilde{V}_{\|} &= d\hat{\phi}, \\ n_{\text{ion}}\#_{\|}\widetilde{V}_{\text{ion}} &= d\hat{\phi}_{\text{ion}}. \end{aligned} \tag{2.123}$$

This, combined with equation (2.115) immediately lets us write:

$$dE = q(d\hat{\phi} - d\hat{\phi}_{\text{ion}}), \tag{2.124}$$

from which :

$$E = q(\hat{\phi} - \hat{\phi}_{\text{ion}}) \tag{2.125}$$

immediately follows up to an integration constant, which we set to zero here. Equation (2.121) hence becomes:

$$d\widetilde{V}_{\|} = \frac{q^2}{m}(\hat{\phi} - \hat{\phi}_{\text{ion}})\#_{\|}1. \tag{2.126}$$

Seeking to eliminate $\widetilde{V}_{\|}$ in favour of $\hat{\phi}$, we note that:

$$\widetilde{V}_{\|} = \left\|\widetilde{V}_{\|}\right\| \frac{\#_{\|}d\hat{\phi}}{\left\|\#_{\|}d\hat{\phi}\right\|}, \tag{2.127}$$

which follows from equation (2.123). The inner product $\#_{\|}d\hat{\phi} \cdot \#_{\|}d\hat{\phi}$ can be shown to be:

$$\#_{\|}d\hat{\phi} \cdot \#_{\|}d\hat{\phi} = -d\hat{\phi} \cdot d\hat{\phi}, \tag{2.128}$$

which implies that $\left\|\#_{\|}d\hat{\phi}\right\| = \left\|d\hat{\phi}\right\|$. We can also use the condition that V is a normalised unit time-like vector field to obtain an expression for $\left\|\widetilde{V}_{\|}\right\|$ i.e.:

$$\begin{aligned} \|V\|^2 &= -\left\|\widetilde{V}_{\|}\right\|^2 + \left\|\widetilde{V}_{\perp}\right\|^2 \\ &= -\left\|\widetilde{V}_{\|}\right\|^2 + |\mathcal{A}|^2 \\ &= -1. \end{aligned} \tag{2.129}$$

Equation (2.119) and $\mathcal{A} = \frac{q}{m}(A_1 + iA_2)$ have been used to substitute $\left\|\widetilde{V}_{\perp}\right\|$ in (2.129). This finally allows us to write the field equation (2.126) for the plasma wave as:

$$d\left(\sqrt{1+|\mathcal{A}|^2}\frac{\#_{\|}d\hat{\phi}}{\left\|d\hat{\phi}\right\|}\right) = \frac{q^2}{m}(\hat{\phi} - \hat{\phi}_{\text{ion}})\#_{\|}1. \tag{2.130}$$

Introducing $\phi = \frac{1}{n_{\text{ion}}}\hat{\phi}$ and $\phi_{\text{ion}} = \frac{1}{n_{\text{ion}}}\hat{\phi}_{\text{ion}}$, where n_{ion} is the ion proper number density, we can write:

$$d\left(\sqrt{1+|\mathcal{A}|^2}\frac{\#_{\|}d\phi}{\|d\phi\|}\right) = \omega_p^2(\phi - \phi_{\text{ion}})\#_{\|}1. \tag{2.131}$$

Equation (2.131) is an equation that now allows us to capture the effects of the transverse components of the electromagnetic field on the motion of the plasma. Using (2.123), the plasma electron proper number density n can be expressed as:

$$n = \frac{\left\|d\hat{\phi}\right\|}{\sqrt{1+|\mathcal{A}|^2}}, \tag{2.132}$$

which immediately allows for equation (2.122) to be written as:

$$d\#_{\|}d\mathcal{A} = \frac{q^2}{m}\frac{\left\|d\hat{\phi}\right\|}{\sqrt{1+|\mathcal{A}|^2}}\mathcal{A}\#_{\|}1. \tag{2.133}$$

This can be rewritten in terms of ϕ as:

$$d\#_{\|}d\mathcal{A} = \omega_p^2\frac{\|d\phi\|}{\sqrt{1+|\mathcal{A}|^2}}\mathcal{A}\#_{\|}1. \tag{2.134}$$

Equation (2.134) captures the evolution of the transverse components of the electromagnetic field. A point of note is that equation (2.134) captures the physics of an effect called relativistic transparency, in which a laser of a sufficient field strength can travel through what would initially be an opaque plasma (for a review of the topic see [73]). This is due to the $\frac{1}{\sqrt{1+|\mathcal{A}|^2}}$ term decreasing the magnitude of the effective coupling of the electromagnetic wave to the plasma.

2.4 Plasma Wave Driven by a Circularly Polarised Pulse

Let us consider the case of a circularly polarised laser pulse. To do this, we express the electromagnetic potential as:

$$\mathcal{A} = ae^{i\Phi}, \tag{2.135}$$

where a is the dimensionless laser amplitude and Φ is the phase of the laser, which in principle depends on z and t; however, due to the structure of (2.131), the exact form of it doesn't matter. With this assumption equation (2.130) becomes:

$$d\left(\sqrt{1+a^2}\frac{\#_{\|}d\phi}{\|d\phi\|}\right) = \omega_p^2(\phi-\phi_{\text{ion}})\#_{\|}1, \tag{2.136}$$

where $\hat{\phi} = n_{\text{ion}}\phi$, $\hat{\phi}_{\text{ion}} = n_{\text{ion}}\phi_{\text{ion}}$ and $\omega_p = \frac{q^2 n_{\text{ion}}}{m}$. For the purposes of this calculation, we adopt an orthonormal co-frame $\{\gamma d\zeta, \gamma d\xi, dx, dy\}$, where $\zeta = z - vt$ and $\xi = vz - t$. This co-frame is adapted to a plasma wave with phase velocity v (note that $0 < v < 1$) moving along the z axis. We then prescribe the function a such that it only depends on ζ, i.e. $a \equiv a(\zeta)$, thereby discarding equation (2.133). This is a strong assumption as we both neglect, the reaction of the laser pulse to the plasma, while still prescribing the pulse's dispersive properties; nevertheless, this approximation is very common in the wider literature surrounding theoretical studies of LWFAs, a good example of which is given in [74].

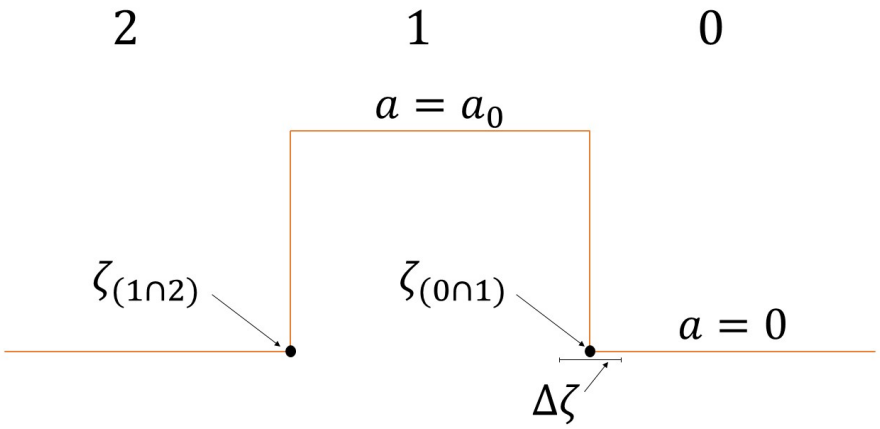

Figure 2.7: A figure illustrating the shape of the prescribed pulse. We separate the domain into three regions 0,1 and 2 which correspond to the region in front of the travelling pulse, the region within the pulse and the plasma wake region respectively.

Additionally we also assume that ϕ_{ion} has the form $\phi_{\text{ion}} = z$. We seek a solution to the motion of the electron fluid of the form $\phi = \phi_{\text{ion}} + \psi$ (a current of the form $j = dN = n\#_{\parallel}\widetilde{V} = n_{\text{ion}}dz + n_{\text{ion}}d\psi$), where ψ also depends only on ζ, so $d\psi = \psi^{'}d\zeta$. We note that the requirement that all dynamical variables depend on ζ is commonly known as the "quasi-static" approximation in the literature. The reason for this nomenclature is that in this situation we can choose a frame in which the electron fluid is static. This reduces the analysis of the plasma wave equation (2.136) to that of solving an O.D.E. of the form:

$$\left(\sqrt{1+a^2}\frac{1+\psi^{'}-v^2\psi^{'}}{\sqrt{(1+\psi^{'})^2-v^2\psi^{'2}}}\right)^{'} = \omega_p^2\psi. \tag{2.137}$$

We now assume that the dimensionless amplitude of the electro-magnetic potential of the laser pulse has the form of a top-hat function, as illustrated in Figure 2.7.

To motivate our approach to this problem, we can solve an approximate problem numerically. Beginning the numerical analysis, we prescribe the shape of the dimensionless laser potential $a(\zeta)$ such that it can mimic the top hat function we are going to use for the analytical results. We define $a(\zeta)$ as:

$$a(\zeta) = a_0\frac{1}{4}\left[1+\tanh\left(\frac{\zeta-\sigma+w}{s}\right)\right]\left[1+\tanh\left(\frac{-\zeta+\sigma+w}{s}\right)\right], \tag{2.138}$$

where the parameters σ, w and s control where the pulse is centred, the width of the pulse and the "steepness" of the edges of the pulse. We solve the electron fluid equation for the case of the pulse centred at $\zeta = 5$, a "steepness" factor of $s = 0.05$ and a range of pulse widths. The numerical solutions are graphed in Figure 2.8.

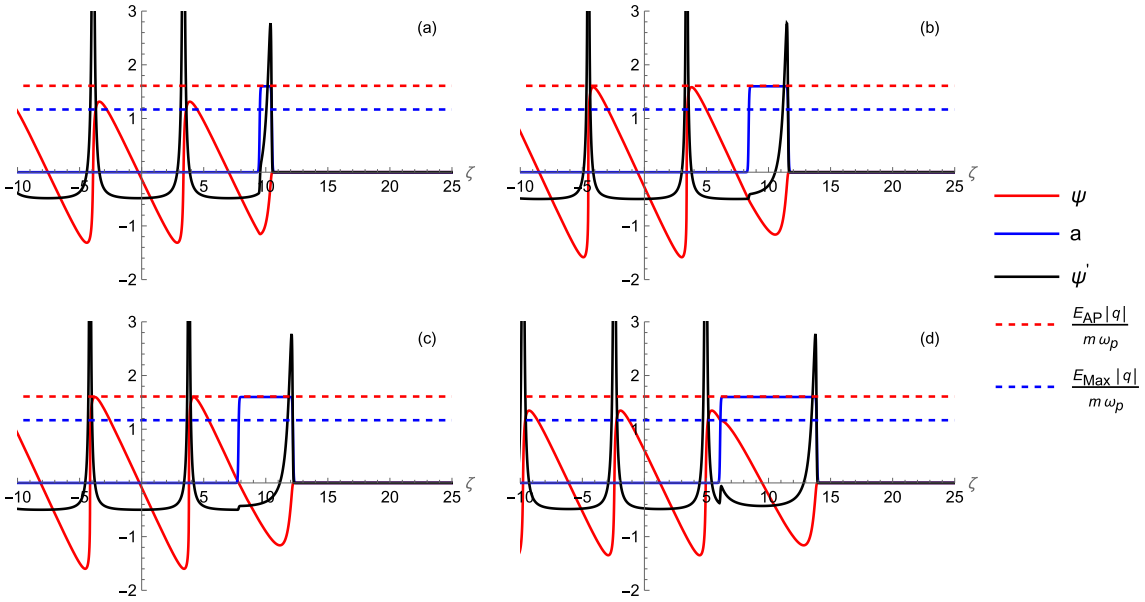

Figure 2.8: The graphs of solutions a, b, c and d correspond to laser pulse widths of 0.5, 1.6, 2.2 and 3.9. The physical parameters chosen for the simulation are $v = 0.9$ and $a_0 = 1.6$. The red dotted line corresponds to the Akhiezer-Polovin cold plasma wave breaking limit from equation (2.154) and the blue dotted line corresponds to the absolute maximum value of the wake within the pulse from equation (2.152).

We now turn to the analysis of the plasma pulse within a prescribed top-hat laser pulse. More specifically we want to consider the case in which the top-hat function wave is "matched" to the plasma wave, meaning that the laser pulse occupies one-half of the first oscillation of the electric field. We will investigate the region around the front of the pulse with length $\Delta\zeta$, more accurately, we are considering the limiting case in which $\Delta\zeta \to 0$. We integrate equation (2.136) with respect to ζ across the interval $\Delta\zeta$, which yields:

$$\left[\sqrt{1+|a|^2}\frac{1+\psi'-v^2\psi'}{\sqrt{(1+\psi')^2-v^2\psi'^2}}\right]_{\zeta^-_{(0\cap1)}}^{\zeta^+_{(0\cap1)}} = \omega_p^2\psi\Delta\zeta + \mathcal{O}(\Delta\zeta^2) \to 0, \tag{2.139}$$

where $\zeta^+_{(0\cap1)} = \zeta_{(0\cap1)} + \frac{\Delta\zeta}{2}$ and $\zeta^-_{(0\cap1)} = \zeta_{(0\cap1)} - \frac{\Delta\zeta}{2}$. The $\pm$ superscript will now denote the limit of a function at a boundary that is approaching from the positive/negative direction respectively e.g. $f^{\pm}_{(0\cap1)} = \lim_{\Delta\zeta\to0} f(\zeta_{(0\cap1)} \pm \frac{\Delta\zeta}{2})$. From the construction of the prescribed form of the laser pulse potential, we know that $a = 0$ outside the pulse and $a = a_0$ inside of the pulse. We then assume that $\psi'^{+}_{(0\cap1)} = 0$ in front of the pulse, which can be justified by the assumption that the plasma is in equilibrium ahead of the pulse. Equation (2.139) then becomes:

$$1 - \sqrt{1+a_0^2}\frac{1+\psi'^{-}_{(0\cap1)} - v^2\psi'^{-}_{(0\cap1)}}{\sqrt{(1+\psi'^{-}_{(0\cap1)})^2 - v^2\psi'^{2-}_{(0\cap1)}}} = 0, \tag{2.140}$$

where the $(0\cap1)$ subscript denotes that the quantity is evaluated at the interface of regions 0 and 1.

2.4.1 Maximum Wave Amplitude Inside The Laser Pulse

The case of a maximum amplitude electric field $E_{\max}$ within the laser pulse occurs for the solution in which $\psi^{'}_{(0\cap1)} \to \infty$. In this limit equation (2.140) becomes:

$$1 - \sqrt{1+a_0^2}\sqrt{1-v^2} = 0. \tag{2.141}$$

This yields the condition for the amplitude a_0:

$$a_0 = \gamma v. \tag{2.142}$$

We now turn to a Lagrangian-based approach to derive the value for the maximum electric field. A Lagrangian that generates equation (2.137) inside the pulse has the form:

$$L = -\sqrt{1+a_0^2}\sqrt{(1+\psi^{'}_{(1)})^2 - v^2\psi^{'2}_{(1)}} + \sqrt{1+a_0^2} - \frac{1}{2}\omega_p^2\psi^2_{(1)}. \tag{2.143}$$

The restriction of ψ to region (1) is denoted as $\psi_{(1)}$. Due to no explicit ζ dependence, we can immediately identify a constant of integration $\mathcal{E}_{(1)}$:

$$\begin{aligned}\mathcal{E}_{(1)} &= \psi^{'}_{(1)}\frac{\partial L}{\partial \psi^{'}_{(1)}} - L \\ &= \frac{\sqrt{1+a_0^2}(1+\psi^{'}_{(1)})}{\sqrt{(1+\psi^{'}_{(1)})^2 - v^2\psi^{'2}_{(1)}}} - \sqrt{1+a_0^2} + \frac{1}{2}\omega_p^2\psi^2_{(1)}.\end{aligned} \tag{2.144}$$

By assumption, $\psi_{(1)}$ is a continuous function; therefore in the limit $\Delta\zeta \to 0$ the condition $\psi^{+}_{(0\cap1)} = 0$ ensures that $\psi^{-}_{(0\cap1)} = 0$ holds. Then, the constant of integration in region 1, $\mathcal{E}_{(1)}$, is:

$$\mathcal{E}_{(1)} = \frac{\sqrt{1+a_0^2}(1+\psi^{'-}_{(0\cap1)})}{\sqrt{(1+\psi^{'-}_{(0\cap1)})^2 - v^2\psi^{'-2}_{(0\cap1)}}} - \sqrt{1+a_0^2}. \tag{2.145}$$

As noted before, the maximum value of the electric field will occur in the case of $\psi^{'-}_{(0\cap1)} \to \infty$. $\mathcal{E}_{(1)}$ in this limit can be expressed as:

$$\begin{aligned}\mathcal{E}_{(1)} &= \sqrt{1+a_0^2}(\frac{1}{\sqrt{1-v^2}} - 1) \\ &= \sqrt{1+a_0^2}(\gamma - 1) \\ &= \sqrt{1+a_0^2}(\sqrt{1+a_0^2} - 1),\end{aligned} \tag{2.146}$$

where the condition from equation (2.141) was used.

In order to get an explicit expression for $\psi^{'-}_{(0\cap1)}$, in the case of $a_0 < \gamma v$, we solve the jump

condition (2.140) at the front of the pulse:

$$\psi'^{-}_{(0\cap1)} = \gamma^2(-1 \pm \frac{\gamma v}{\sqrt{\gamma^2 - 1 - a_0^2}}). \tag{2.147}$$

We now require, that in the case of $a_0 = 0$ (i.e. no laser pulse) $\psi'_{(0\cap1)} = 0$. This restricts the choice of root:

$$\psi'^{-}_{(0\cap1)} = \gamma^2(-1 + \frac{\gamma v}{\sqrt{\gamma^2 - 1 - a_0^2}}). \tag{2.148}$$

Using (2.145), we can now express the constant of motion $\mathcal{E}_{(1)}$ as:

$$\mathcal{E}_{(1)} = -\gamma v\sqrt{\gamma^2 - 1 - a_0^2} + \gamma^2 - \sqrt{1 + a_0^2}. \tag{2.149}$$

Evaluating (2.144) at a maximum of the wave amplitude gives the constant of motion:

$$\mathcal{E}_{(1)} = \frac{1}{2}\omega_p^2\psi_{\max}^2, \tag{2.150}$$

since $\psi'_{(1)} = 0$ where $\psi_{(1)} = \psi_{\max}$. Recalling that E can be expressed by:

$$\begin{aligned} E &= q(\hat{\phi} - \hat{\phi}_{\text{ion}}) \\ &= qn_{\text{ion}}(\phi - \phi_{\text{ion}}) \\ &= qn_{\text{ion}}\psi \end{aligned} \tag{2.151}$$

we can finally find the expression for the maximum electric field amplitude:

$$E_{\max} = \frac{m\omega_p}{|q|}\left[2\left(\gamma^2 - \gamma v\sqrt{\gamma^2 - 1 - a_0^2} - \sqrt{1 + a_0^2}\right)\right]^{\frac{1}{2}}. \tag{2.152}$$

The same expression as (2.152) is derived in [74] using a different approach (with a factor of $\sqrt{2}$ difference likely due to a typo). The absolute maximum value of $E_{\max}$ occurs at $a_0 = \sqrt{\gamma^2 - 1}$ (see equation (2.139)) i.e.:

$$E_{\text{AM}} = \frac{m\omega_p}{|q|}[2(\gamma^2 - \gamma)]^{\frac{1}{2}}. \tag{2.153}$$

We note that this is a factor of $\sqrt{\gamma}$ larger than the cold plasma wave breaking limit due to Akhiezer and Polovin [72] :

$$E_{AP} = \frac{m\omega_p}{|q|}\sqrt{2(\gamma - 1)}. \tag{2.154}$$

We illustrate this in figure 2.9.

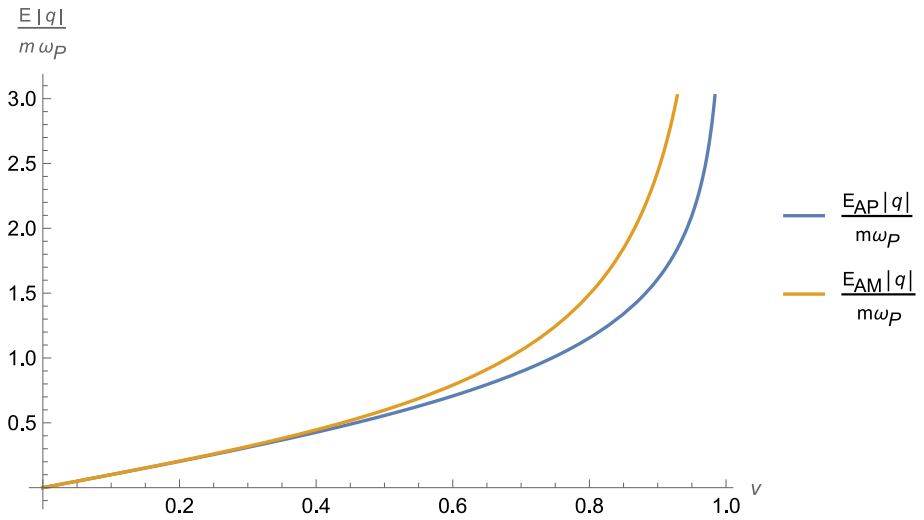

Figure 2.9: A graph illustrating the different maximum electric field values related to the phase velocity of the plasma wake.

2.4.2 Relating the Dimensionless Laser Amplitude to the Phase Velocity of the Maximum Amplitude Plasma Wave

We now turn our attention to the behaviour at the back of the laser pulse. Integrating equation (2.137) across the back of the pulse yields:

$$\frac{1+\psi'^{-}_{(1\cap 2)}-v^2\psi'^{-}_{(1\cap 2)}}{\sqrt{(1+\psi'^{-}_{(1\cap 2)})^2-v^2\psi'^{-2}_{(1\cap 2)}}}-\sqrt{1+a_0^2}\,\frac{1+\psi'^{+}_{(1\cap 2)}-v^2\psi'^{+}_{(1\cap 2)}}{\sqrt{(1+\psi'^{+}_{(1\cap 2)})^2-v^2\psi'^{+2}_{(1\cap 2)}}}=0. \tag{2.155}$$

We introduce a new constant of motion for the boundary of regions 1 and 2 using equation (2.144), which we will call $\mathcal{E}_{(2)}$. It can be expressed in terms of $\psi_{(2)}$ as :

$$\mathcal{E}_{(2)}=\frac{1+\psi'_{(2)}}{\sqrt{(1+\psi'_{(2)})^2-v^2\psi'^{2}_{(2)}}}-1+\frac{1}{2}\omega_p^2\psi^2_{(2)}, \tag{2.156}$$

which holds at all points behind the pulse. For the case of the maximum amplitude plasma wake behind the pulse, we recall from section 2.2.3 that there exists a point at which $\psi'_{(2)}\to\infty$ as $\psi_{(2)}\to 0$. Equation (2.156) then allows us to express the constant of integration $\mathcal{E}_{(2)}$ as:

$$\mathcal{E}_{(2)}=\gamma-1. \tag{2.157}$$

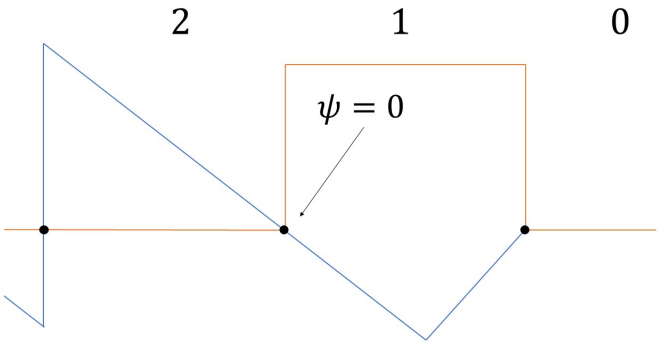

Figure 2.10: An illustration of the case for which the plasma pulse satisfies $\psi = 0$ and has a finite ψ' value at $\zeta = \zeta_{(1\cap 2)}$

Now, let us consider a situation in which $\psi^{-}_{(1\cap 2)} = 0$ and $\psi'^{-}_{(1\cap 2)}$ is finite. In that case the expressions from equations (2.157) and (2.156) become:

$$\gamma - 1 = \frac{1 + \psi'^{-}_{(1\cap 2)}}{\sqrt{(1 + \psi'^{-}_{(1\cap 2)})^2 - v^2 \psi'^{-2}_{(1\cap 2)}}} - 1, \tag{2.158}$$

which yields:

$$\psi'^{-}_{(1\cap 2)} = -\frac{1}{2}. \tag{2.159}$$

The continuity condition (2.155) becomes:

$$\frac{1+v^2}{\sqrt{1-v^2}} - \sqrt{1+a_0^2}\frac{1 + \frac{1}{\gamma^2}\psi'^{+}_{(1\cap 2)}}{\sqrt{(1 + \psi'^{+}_{(1\cap 2)})^2 - v^2 \psi'^{+2}_{(1\cap 2)}}} = 0. \tag{2.160}$$

At the back of (but still inside) the laser pulse, the constant of motion $\mathcal{E}_{(1)}$, using equation (2.144) with $\psi^{+}_{(1\cap 2)} = 0$, is expressed as:

$$\mathcal{E}_{(1)} = \sqrt{1+a_0^2}\frac{1 + \psi'^{+}_{(1\cap 2)}}{\sqrt{(1 + \psi'^{+}_{(1\cap 2)})^2 - v^2 \psi'^{+2}_{(1\cap 2)}}} - \sqrt{1+a_0^2}. \tag{2.161}$$

Using equations (2.149) and (2.161) we arrive at the expression for $\psi'^{+}_{(1\cap 2)}$:

$$\psi'^{+}_{(1\cap 2)} = -\frac{1}{1 \pm \frac{v\eta}{\sqrt{\gamma^2 - 1 - a_0^2}}}, \tag{2.162}$$

where $\eta = \gamma^2 - \gamma v\sqrt{\gamma^2 - 1 - a_0^2}$. With a choice of the root, which we will justify numerically in the next section, we find the expression:

$$a_0^2 = \frac{1}{4v^2}\frac{(\gamma - 1)}{\gamma^3}(\gamma^3(v^4 + 6v^2 + 1) - 1), \tag{2.163}$$

for the dimensionless laser amplitude required to drive the maximum plasma wakefield, which is

plotted in figure 2.11.

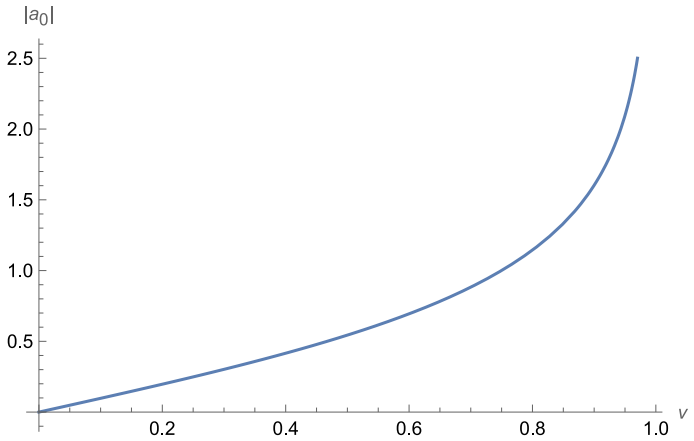

Figure 2.11: A plot illustrating the dependence of the magnitude of the dimensionless laser amplitude required for a maximum amplitude wake on the phase velocity of the wake.

2.4.3 Numerical Analysis

An issue that arose in subsection 2.4.2 was that of the ambiguity of the choice of root in equation (2.162). It was mentioned that it is going to be justified numerically, and we shall endeavour to do so now (for an analytical approach to this, see the appendix of [60]). This shall be done by numerically analysing the equations arising from the constants of integration and jump conditions. Firstly, we obtain another equation for $\psi'^{+}_{(1\cap 2)}$ by using equations (2.149) and (2.161) for the integral constant $\mathcal{E}_{(1)}$ to obtain:

$$\gamma^2 - \gamma v\sqrt{\gamma^2 - a_0^2 - 1} - \frac{\sqrt{1+a_0^2}(1+\psi'^{+}_{(1\cap 2)})}{\sqrt{(1+\psi'^{+}_{(1\cap 2)})^2 - v^2\psi'^{+2}_{(1\cap 2)}}} = 0. \tag{2.164}$$

Equation (2.164) combined with equation (2.160) will form the basis of our numerical justification of the choice of roots in equation (2.162).

For a given choice of v and a_0 we can numerically solve equations (2.164) and (2.160) for $\psi'^{-}_{(1\cap 2)}$. Solving (2.160) numerically in a physically relevant range of the variables v and a_0, we find that the solutions of $\psi'^{-}_{(1\cap 2)}$ are purely negative, while for equation (2.164), we get positive and negative branches. One of the solutions of equation (2.160) agrees with one of the solutions of equation (2.164), but the other two solutions disagree. This, of course, motivates us to only choose the negative branch solutions of (2.164). With that in mind, we can compare the numerical values we obtain from the jump condition and the condition derived from the constant of integration. The values of the parameters v and a_0 for which the solutions $\psi'^{-}_{(1\cap 2)}$ coincide will give us the relationship between the dimensionless laser amplitude and the phase velocity of the plasma wave. This relation is illustrated in Figures 2.12 and 2.13. If we approach solving this relation algebraically, we obtain

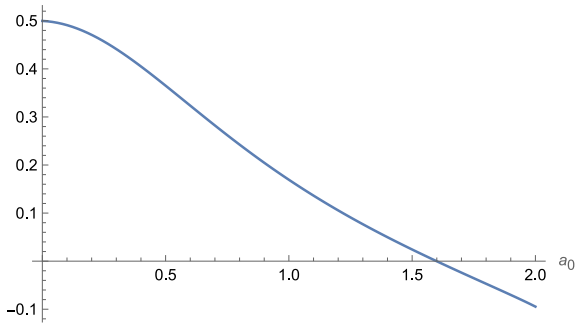

Figure 2.12: A graph plotting the difference in the numerical solutions for $\psi'_{(1\cap 2)}$ obtained from equations (2.164) and (2.160) against the dimensionless laser amplitude a_0. The value of the wake phase velocity is fixed at $v = 0.9$.

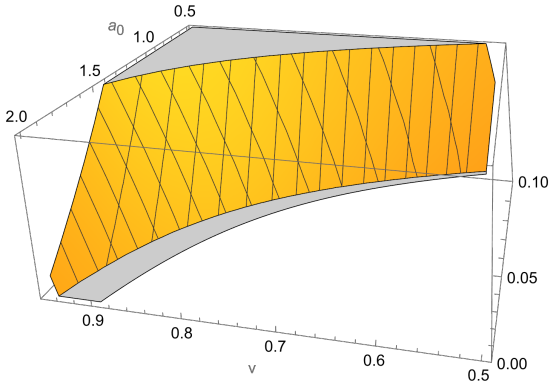

Figure 2.13: A two-dimensional plot plotting the difference in $\psi'_{(1\cap 2)}$ against both the dimensionless laser amplitude a_0 and the wake phase velocity.

four solutions.

$$a_0 = \pm\frac{1}{2v}\sqrt{\frac{-v^6 - 4v^4 + 3v^2 \pm 2\sqrt{-v^{10} - 3v^8 - 2v^6 + 2v^4 + 3v^2 + 1} + 2}{v^2 - 1}}.$$

Numerical verification allows us to pick the relevant branch:

$$a_0 = \frac{1}{2v}\sqrt{\frac{-v^6 - 4v^4 + 3v^2 - 2\sqrt{-v^{10} - 3v^8 - 2v^6 + 2v^4 + 3v^2 + 1} + 2}{v^2 - 1}},$$

which coincides with the analytical result from equation (2.163).

One final observation about this calculation is that the numerical value of the dimensionless laser amplitude a_0 that drives the maximum amplitude wake is almost equal to the maximum of the (non-dimensionalised) electric field of the wake $\epsilon = \frac{E_{\mathrm{AP}}|q|}{m\omega_p}$, regardless of the phase speed of the wave. This is illustrated in Figure 2.14.

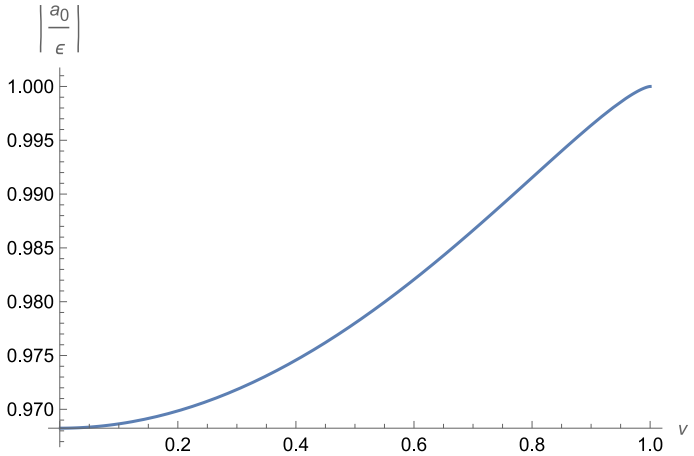

Figure 2.14: A plot of the absolute value of the ratio of the dimensionless laser amplitude a_0 and the dimensionless electric field if the wake ϵ plotted against the phase velocity of the wake v.

Chapter 3

Classical Axion Production

In this chapter, we shall discuss the classical treatment of axion production[1]. Although axions arose out of a fundamentally quantum theory, within the context of axion searches, classical approaches are a good approximation due to the relative strengths of the electromagnetic fields used. As such, in this Chapter, we provide an overview of some basics of axion production in a laser and also consider the case of axions in a plasma.

3.1 Classical Axion-Electrodynamics

As mentioned in the introductory chapter, the Lagrangian for axion-electrodynamics is given by:

$$\boxed{\mathcal{L} = -\frac{1}{4}F^{\mu\nu}F_{\mu\nu} + \frac{1}{2}\partial^{\mu}\psi\partial_{\mu}\psi - \frac{1}{2}m_{\psi}\psi^2 - \frac{1}{4}g_{\psi}\psi F_{\mu\nu}\widetilde{F}^{\mu\nu}.} \tag{3.1}$$

To coincide with the formalism we laid out in Chapter 2, we will write the action for axion-electrodynamics in terms of differential forms:

$$\boxed{S[A,\psi] = \int \frac{1}{2}(F\wedge\star F + d\psi\wedge\star d\psi + m_{\psi}^2\psi^2\star 1 - g_{\psi}\psi F\wedge F).} \tag{3.2}$$

The corresponding equations of motion are thus given by:

$$\begin{aligned} dF &= 0, \\ d\star dA &= g_{\psi}d\psi\wedge F, \\ -d\star d\psi + m_{\psi}^2\psi\star 1 &= g_{\psi}\frac{1}{2}F\wedge F. \end{aligned} \tag{3.3}$$

[1]The concept of classical particle production can be a somewhat nebulous one. Strictly speaking, particle production is not something that can be accounted for classically. The term "Classical Axion Production" is used here heuristically, where it refers to calculating the amplitude of the classical axion field equation solution.

3.1.1 2+2 Split

Following the method from Chapter 2, we perform a decomposition of the electromagnetic 2-form as:

$$F = E\#_{\parallel}1 + dA_j \wedge dx^j - B\#_{\perp}1 \tag{3.4}$$

where $j = 1, 2$. The indexed coordinates can be written as:

$$\begin{aligned} x^0 &= t \\ x^1 &= x \\ x^2 &= y \\ x^3 &= z \end{aligned} \tag{3.5}$$

and the reduced Hodge operators are once again given by:

$$\begin{aligned} \#_{\parallel}1 &= dt \wedge dz, \\ \#_{\perp}1 &= dx \wedge dy, \end{aligned} \tag{3.6}$$

where we also note that E,B and the components of A_j all only depend on t and z. With that in mind, we can express $F \wedge F$ as:

$$\begin{aligned} F \wedge F &= -2EB \star 1 + dA_j \wedge dx^j \wedge dA_k \wedge dx^k \\ &= -2EB \star 1 + id\overline{\mathcal{A}} \wedge d\mathcal{A} \wedge \#_{\perp}1. \end{aligned} \tag{3.7}$$

We have defined $\mathcal{A}$ as:

$$\mathcal{A} = A_x + iA_y. \tag{3.8}$$

We now set $B = 0$, and with that assumption, the 2D axion electrodynamics equations become:

$$\boxed{d\#_{\parallel}d\psi - m_{\psi}^2\psi\#_{\parallel}1 = i\frac{g_{\psi}}{2}d\mathcal{A} \wedge d\overline{\mathcal{A}}} \tag{3.9}$$

$$\boxed{d\#_{\parallel}d\mathcal{A} = ig_{\psi}d\psi \wedge d\mathcal{A}.} \tag{3.10}$$

3.2 Axion Production in a Laser

3.2.1 Linear Polarisation and the two-level system

We begin the analysis with perturbation theory, expanding around a background solution $\mathcal{A}_0$:

$$\begin{aligned} \mathcal{A} &= \mathcal{A}_0 + \mathcal{A}_1 \\ \psi &= \psi_0 + \psi_1. \end{aligned} \tag{3.11}$$

We assume no initial axion density, so $\psi_0 = 0$. Furthermore, we change to a null coordinate system:

$$\begin{aligned} x^+ &= t + z \\ x^- &= t - z, \end{aligned} \tag{3.12}$$

and impose the condition that the background laser pulse only depends on x^-. The equations of motion, to first order, become:

$$\begin{aligned} d\#_\parallel d\psi_1 - m^2\psi_1\#_\parallel 1 &= i\frac{g_\psi}{2}(d\mathcal{A}_0 \wedge d\bar{\mathcal{A}}_1 + d\mathcal{A}_1 \wedge d\bar{\mathcal{A}}_0) \\ d\#_\parallel d\mathcal{A}_1 &= ig_\psi d\psi_1 \wedge d\mathcal{A}_0 \\ d\#_\parallel dA_0 &= 0. \end{aligned} \tag{3.13}$$

Additionally, we assume that the background field, $\mathcal{A}_0$, is purely real (meaning that it is linearly polarised). We also express ψ_1 and $\mathcal{A}_1$ as:

$$\begin{aligned} \psi_1 &= \Psi e^{-i\omega x^+} + \overline{\Psi} e^{i\omega x^+} \\ i\mathcal{A}_1 &= a e^{-i\omega x^+} + \overline{a} e^{i\omega x^+}, \end{aligned} \tag{3.14}$$

where $\Psi \equiv \Psi(x^-)$ and $a \equiv a(x^-)$. The equations of motion for the coefficients in (3.14) are:

$$\begin{aligned} 2i\omega\frac{d\Psi}{dx^-} &= \frac{1}{2}m_\psi^2\Psi + i\omega g_\psi \frac{d\mathcal{A}_0}{dx^-}a, \\ 2i\omega\frac{da}{dx^-} &= -i\omega g_\psi \frac{d\mathcal{A}_0}{dx^-}\Psi, \end{aligned} \tag{3.15}$$

where we note that the equation of motion for $\mathcal{A}_0$ is satisfied automatically due to the fact it only depends on x^-. We can re-scale Ψ and a in order to simplify our equations:

$$\begin{aligned} \Psi &= e^{-i\frac{m_\psi^2}{8\omega}x^-}\phi, \\ a &= e^{-i\frac{m_\psi^2}{8\omega}x^-}b. \end{aligned} \tag{3.16}$$

This choice of scaling allows us to write the equations of motion in terms of a Schrödinger-like equation for a two-level system, where the "state vector" is given by :

$$\Phi = \begin{bmatrix} b \\ \phi \end{bmatrix}, \tag{3.17}$$

and the Schrödinger-like equation becomes:

$$i\frac{d\Phi}{dx^-} = \left(-\frac{m_\psi^2}{8\omega}\sigma_3 + \frac{g_\psi}{2}\frac{d\mathcal{A}_0}{dx^-}\sigma_2\right)\Phi. \tag{3.18}$$

We note that σ_1, σ_2 and σ_3 denote the usual Pauli matrices:

$$\begin{aligned}\sigma_1 &= \begin{bmatrix} 0 & 1 \\ 1 & 0 \end{bmatrix} \\ \sigma_2 &= \begin{bmatrix} 0 & -i \\ i & 0 \end{bmatrix} \\ \sigma_3 &= \begin{bmatrix} 1 & 0 \\ 0 & -1 \end{bmatrix}.\end{aligned} \tag{3.19}$$

To continue with the analysis, we will need to set a value for the driving field $\mathcal{A}_0$. For simplicity, we will assume a sine wave of the form:

$$\mathcal{A}_0 = \frac{\beta_0}{\omega_0} \sin\big(\omega_0 x^-\big). \tag{3.20}$$

The Hamiltonian for the two-level system can then be explicitly written in matrix form as:

$$\hat{H} = \begin{bmatrix} -\frac{m_\psi^2}{8\omega} & -i\frac{g_\psi \beta_0}{2}\cos(\omega_0 x^-) \\ i\frac{g_\psi \beta_0}{2}\cos(\omega_0 x^-) & \frac{m_\psi^2}{8\omega} \end{bmatrix}. \tag{3.21}$$

3.2.1.1 Rotating Wave approximation and Rabi-Like Frequency

Having obtained an explicit form for the Hamiltonian for the Schrödinger-like equation we can start to apply all the standard techniques from the theory of quantum mechanics. A very common method that we can borrow from the field of quantum optics is known as the *rotating wave approximation* (for further reference, one could read any introductory quantum optics text such as [75]). The core principle of it is that, when the system is at or near resonance, rapidly oscillating off resonant terms can be neglected. To obtain the form of the Hamiltonian in the rotating wave approximation we express it in terms of the interaction picture:

$$\hat{H}_I = \begin{bmatrix} 0 & -\frac{ig_\psi\beta_0}{4}\big(e^{i(\omega_0 - \frac{m_\psi^2}{4\omega})x^-} + e^{-i(\omega_0 + \frac{m_\psi^2}{4\omega})x^-}\big) \\ \frac{ig_\psi\beta_0}{4}\big(e^{i(\omega_0 + \frac{m_\psi^2}{4\omega})x^-} + e^{-i(\omega_0 - \frac{m_\psi^2}{4\omega})x^-}\big) & 0 \end{bmatrix}. \tag{3.22}$$

In the rotating wave approximation, this Hamiltonian becomes:

$$\hat{H}_I^{\text{RWA}} = \begin{bmatrix} 0 & -\frac{ig_\psi\beta_0}{4}e^{i(\omega_0 - \frac{m_\psi^2}{4\omega})} \\ \frac{ig_\psi\beta_0}{4}e^{-i(\omega_0 - \frac{m_\psi^2}{4\omega})x^-} & 0 \end{bmatrix}. \tag{3.23}$$

Following a method outlined in appendix B.1, we can solve explicitly for Φ. More particularly, we are interested in ϕ whose magnitude squared is given by:

$$\boxed{|\phi|^2 = \frac{1}{\Omega^2}\left(\frac{g_\psi\beta_0}{4}\right)^2 \sin^2\left(\Omega x^-\right)|b|^2,} \tag{3.24}$$

where $\Omega = \sqrt{\left(\frac{\omega_0}{2} - \frac{m_\psi^2}{8\omega}\right)^2 + \left(\frac{g_\psi \beta_0}{4}\right)^2}$. The result from (3.24) is plotted alongside the exact solution in figure 3.1, showing the correspondence between the exact and approximate solution in the near resonant case. We observe that a resonance occurs at $4\omega\omega_0 = m_\psi^2$.

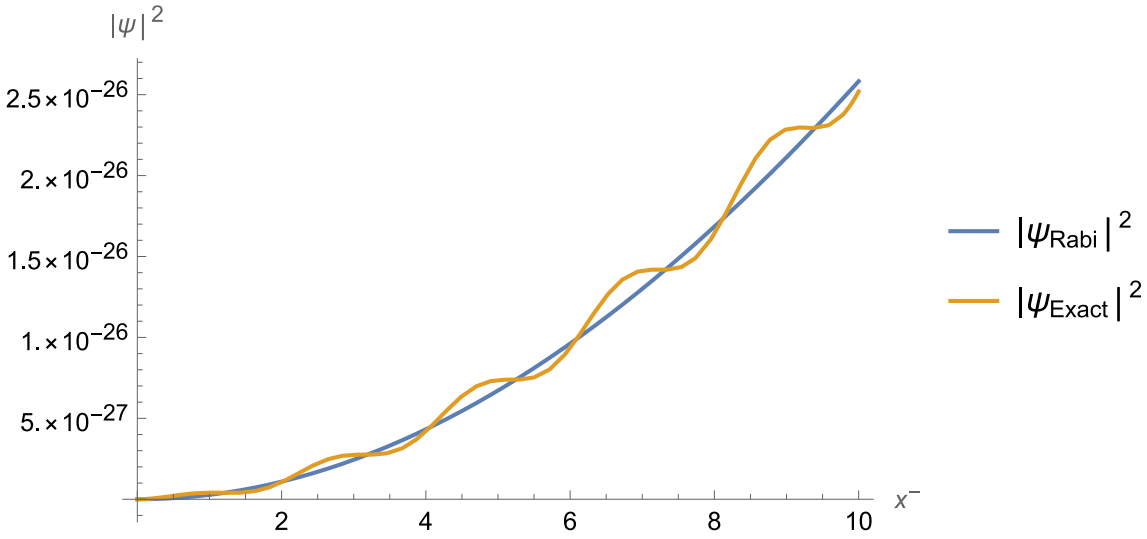

Figure 3.1: A graph showing the comparison of the exact numerical solution vs the solution obtained via the rotating wave approximation. The values for the parameters are $g_\psi = 0.66 \times 10^{-19}$ eV^{-1}, $m_\psi = 10^{-4}$ eV, $\omega_0 \approx 1.51$ eV, $\omega \approx 10^{-9}$ eV and $\beta_0 = 10^3$ eV^2.

This resonance condition can be easily understood by thinking about axion creation via a scattering process. We can consider the case of two counter-propagating photons colliding and creating an axion particle (illustrated in Figure 3.2).

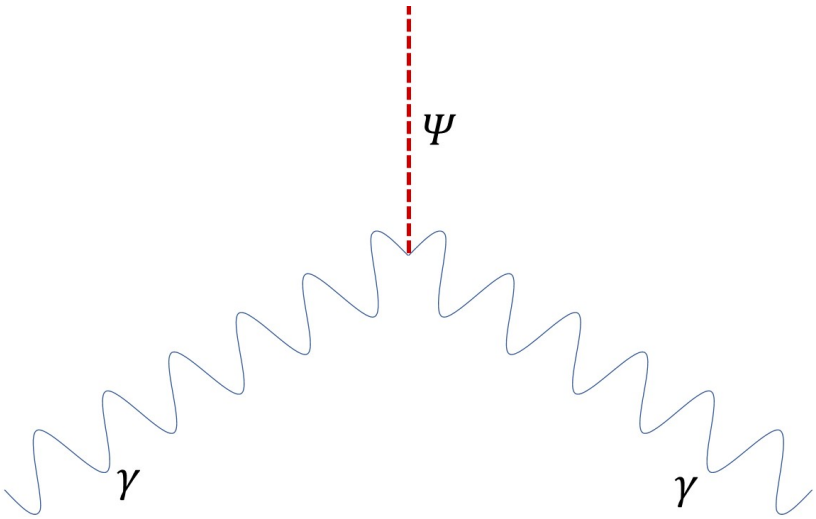

Figure 3.2: A diagram illustrating the $\gamma + \gamma \to \psi$ scattering process.

Let us denote two photons as Photon I and II. Their momentum 4-vectors are given by:

$$P_I = (\omega_0, 0, 0, \omega_0)\,, \tag{3.25}$$

$$P_{II} = (\omega, 0, 0, -\omega)\,. \tag{3.26}$$

The 4-vector for the axion in the rest frame is simply:

$$P_\psi = (m_\psi, 0, 0, 0). \tag{3.27}$$

Through the conservation of momentum, we have:

$$P_I + P_{II} = P_\psi. \tag{3.28}$$

We can use the fact that P_I and P_{II} are null vectors and we can write:

$$2P_I \cdot P_{II} = P_\psi^2, \tag{3.29}$$

which gives us the resonance condition:

$$\boxed{4\omega\omega_0 = m_\psi^2.} \tag{3.30}$$

3.2.2 Circular Polarisation and the Three Level System

The analysis of the system in the case of circular polarization begins in a similar manner to the linearly polarized case. The main difference is the form of the perturbations to the electro-magnetic potential and the axion field:

$$\begin{aligned} \Psi_1 &= \psi' e^{-i\omega x^+} + \bar{\psi}' e^{i\omega x^+} \\ i\mathcal{A}_1 &= a' e^{-i\omega x^+} + \bar{b}' e^{i\omega x^+}. \end{aligned} \tag{3.31}$$

This leads to equations of motion for the perturbations of the form:

$$i\frac{da'}{dx^-} = -i\frac{g_\psi}{2}\frac{d\mathcal{A}_0}{dx^-}\psi', \tag{3.32}$$

$$i\frac{db'}{dx^-} = -i\frac{g_\psi}{2}\frac{d\bar{\mathcal{A}}_0}{dx^-}\psi', \tag{3.33}$$

$$i\frac{d\psi'}{dx^-} = \frac{m_\psi^2}{4\omega}\psi' + i\frac{g_\psi}{4}\left(\frac{d\mathcal{A}_0}{dx^-}b' + \frac{d\bar{\mathcal{A}}_0}{dx^-}a'\right). \tag{3.34}$$

We now prescribe the form of $\mathcal{A}_0$ and re-scale ψ, a and b such that

$$\begin{aligned} \frac{d\mathcal{A}_0}{dx^-} &= \beta e^{-i\omega_0 x^-}, \\ b' &= e^{i\omega_0 x^-} b, \\ a' &= e^{-i\omega_0 x^-} a, \\ \psi' &= \psi. \end{aligned} \tag{3.35}$$

This then allows us to write:

$$\begin{aligned} i\frac{da}{dx^-} &= -\omega_0 a - i\frac{g_\psi \beta}{2}\psi, \\ i\frac{db}{dx^-} &= \omega_0 b - i\frac{g_\psi \beta}{2}\psi, \\ i\frac{d\psi}{dx^-} &= \frac{m_\psi^2}{4\omega}\psi + i\frac{g_\psi \beta}{4}(a+b). \end{aligned} \tag{3.36}$$

We note that a similar analysis can be performed to the one carried out in the case of a linearly polarised pulse, with the use of Gell-Mann Matrices, however, the usefulness of such an approach is more limited as the rotating wave approximation starts to lose meaning in relation to the laser-axion system. Nevertheless, the system of equations given in (3.36) can be solved analytically, although the exact form of the solution is not given as it is an incredibly cumbersome expression. The solutions for ψ are plotted in Figure 3.3.

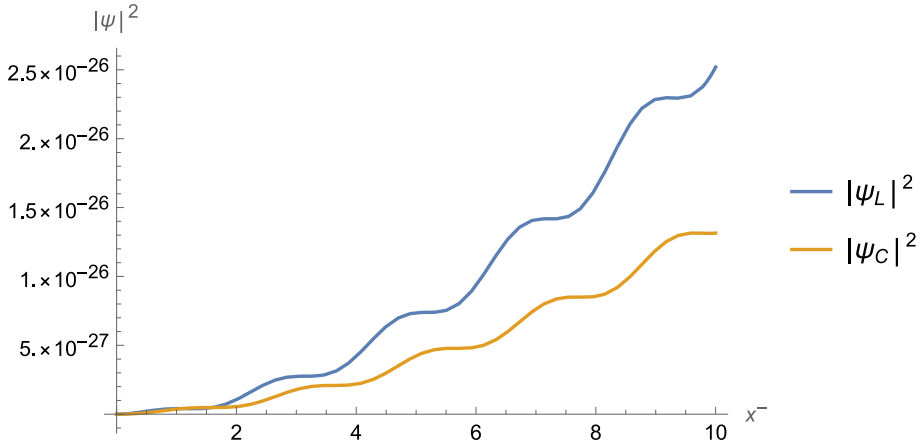

Figure 3.3: A graph comparing the numerical solutions of the axion field given a circularly polarised laser and a linearly polarised one. The values for the parameters are $g_\psi = 0.66 \times 10^{-19}$ eV^{-1}, $m_\psi = 10^{-4}$ eV, $\omega_0 \approx 1.51$ eV, $\omega \approx 10^{-9}$ eV and $\beta_0 = 10^3$ eV^2.

We observe in figures 3.3 and 3.4 that the axion field is stronger in the case of linear polarisation than in the case of a circularly polarized pulse. This can be interpreted intuitively as the energy in a system being distributed between two degrees of freedom i.e. the two levels corresponding to the two laser polarisations.

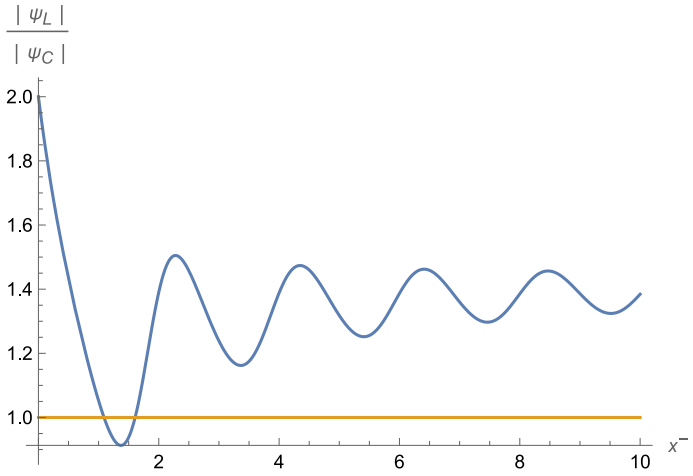

Figure 3.4: A plot of the ratio of the magnitude of the axion field produced in a linearly polarised laser pulse ψ_L and a circularly polarised laser pulse ψ_C.

3.3 Axions in a Plasma

In this section, we will now move on to the case of a classical axion field inside of a plasma. The action for the system is given by:

$$\boxed{\begin{aligned} S[f,A,\psi] = \int\, & mn \star 1 + qA \wedge (j - j_{\text{ion}}) + \frac{1}{2} F \wedge \star F \\ & + \frac{1}{2} d\psi \wedge \star d\psi + \frac{1}{2} m_\psi \psi^2 \star 1 - \frac{1}{2} g_\psi \psi F \wedge F. \end{aligned}} \tag{3.37}$$

Variation with respect to the axion field ψ leads to the equation of motion for the axions:

$$\delta_\psi S = 0 \rightarrow -d \star d\psi + m_\psi^2 \psi \star 1 = \frac{1}{2} g_\psi F \wedge F. \tag{3.38}$$

Assuming that $\psi \equiv \psi(t,z)$, we can use the decomposition of the electromagnetic 2-form we used in the previous section in order to obtain a reduced equation:

$$\boxed{d\#d\psi - m_\psi^2 \psi \# 1 = g_\psi EB\#1 - \frac{1}{2} i g_\psi d\bar{\mathcal{A}} \wedge d\mathcal{A}.} \tag{3.39}$$

Variation with respect to A gives:

$$\delta_A S = 0 \rightarrow d \star F - g_\psi d\psi \wedge F = -qn \star \widetilde{V} + q n_{\text{ion}} \star \widetilde{V}_{\text{ion}}. \tag{3.40}$$

We assume that $\widetilde{V}_{\text{ion}} \equiv \widetilde{V}_{\text{ion}}(t,z)$ and $\widetilde{V} \equiv \widetilde{V}(t,z)$. Additionally, we also write $\widetilde{V}$ as

$$\widetilde{V} = \widetilde{V}_{\parallel} + \widetilde{V}_{\perp}, \tag{3.41}$$

where $\widetilde{V}_\perp = V_j dx^j$. We can use these assumptions to write:

$$dE - g_\psi B d\psi = qn\#_\parallel \widetilde{V}_\parallel - qn_{\text{ion}}\#_\parallel \widetilde{V}_{\text{ion}} \tag{3.42}$$

and:

$$d\#_\parallel dA_j + g_\psi d\psi \wedge \epsilon_j{}^k dA_k = qnV_j\#_\parallel 1, \tag{3.43}$$

where $\epsilon_j{}^k$ is the Levi-Civita symbol. Since, in the standard formulation of axion-electrodynamics, the couplings to matter (i.e. fermions) are usually ignored due to the dominance of the coupling to photons, the plasma equations remain unchanged from the form they took in the previous chapter. We state them here for completeness:

$$\begin{aligned} \delta_f S = 0 \rightarrow & \nabla_V \widetilde{V} = \frac{q}{m}\iota_V F, \\ & V \cdot V = -1. \end{aligned} \tag{3.44}$$

The form structure of (3.44) allows it to be split (like in equations (2.117) and (2.118)):

$$\iota_{V_\parallel} d\widetilde{V}_\parallel - V^j dV_j = \frac{q}{m}\left(E\#_\parallel \widetilde{V}_\parallel - V^j dA_j\right), \tag{3.45}$$

and

$$(\iota_{V_\parallel} dV_j)dx^j = \frac{q}{m}(\iota_{V_\parallel} dA_j)dx^j - \frac{q}{m}B\#_\perp \widetilde{V}_\perp. \tag{3.46}$$

Similar to what was done in the previous chapter, we set $B = 0$, which allows us to write:

$$V_j = \frac{q}{m}A_j. \tag{3.47}$$

This leads to a massive wave equation for A_j:

$$d\#_\parallel dA_j + g_\psi d\psi \wedge \epsilon_j{}^k dA_k = \frac{q^2 n}{m}A_j\#_\parallel 1. \tag{3.48}$$

We can once again write down the EM potential in the form $\mathcal{A} = A_1 + iA_2$, in order to arrive at:

$$d\#_\parallel d\mathcal{A} - ig_\psi d\psi \wedge d\mathcal{A} = \frac{q^2 n}{m}\mathcal{A}\#_\parallel 1. \tag{3.49}$$

Using equation (2.132), we have:

$$n = n_{\text{ion}}\frac{\|d\phi\|}{\sqrt{1 + |\mathcal{A}|^2}}, \tag{3.50}$$

we then have:

$$d\#_\parallel d\mathcal{A} - ig_\psi d\psi \wedge d\mathcal{A} = \omega_p^2 \frac{\|d\phi\|}{\sqrt{1 + |\mathcal{A}|^2}}\mathcal{A}\#_\parallel 1. \tag{3.51}$$

The equation for ϕ is the same as (2.131):

$$d\left(\sqrt{1+|\mathcal{A}|^2}\frac{\#_\parallel d\phi}{\|d\phi\|}\right) = \omega_p^2(\phi - \phi_{\text{ion}}). \tag{3.52}$$

3.3.1 Electromagnetic Wave in a Plasma

In order to describe the process of axion creation in a laser plasma system, we now seek to describe the behaviour of the electromagnetic wave in the plasma. Dropping the influence of the axion field on the electromagnetic field (as it is negligible compared to the effect of the plasma), equation (3.51) becomes:

$$d\#_\parallel d\mathcal{A} = \omega_p^2 \frac{\|d\phi\|}{\sqrt{1+|\mathcal{A}|^2}}\mathcal{A}\#_\parallel 1. \tag{3.53}$$

We write down the form of the electromagnetic potential as a circularly polarized pulse:

$$\mathcal{A} = ae^{i\theta}, \tag{3.54}$$

where a and θ are real 0-forms. Equation (3.53) results in two equations corresponding to its real and imaginary parts:

$$\begin{aligned} -ad\theta \wedge \#_\parallel d\theta + d\#_\parallel da &= \omega_p^2 \frac{\|d\phi\|}{\sqrt{1+a^2}} a\#_\parallel 1, \\ d(a^2\#_\parallel d\theta) &= 0, \end{aligned} \tag{3.55}$$

respectively. We now make the assumption that a depends only on one variable $\zeta = z - vt$ i.e. $a \equiv a(\zeta)$ and that $\theta = \omega_0\xi$, where $\xi = vz - t$. Furthermore, we also prescribe the form of $\phi = z + \psi$, where ψ depends only on the coordinate $\zeta = z - vt$. This results in (3.55) reducing to the form:

$$a'' + \omega_0^2 a = \gamma^2\omega_p^2 \frac{\sqrt{(1+\psi')^2 - v^2\psi'^2}}{\sqrt{1+a^2}} a, \tag{3.56}$$

where $a'' = \frac{d^2a}{d\zeta^2}$ and $d(a^2\#_\parallel d\theta) = 0$ is trivially satisfied.

We now make the assumption that $\psi' \approx -\frac{1}{2}$ in a regime where $\gamma >> 1$ and $\omega_0 >> \omega_p$. This can be justified numerically and will be included in Appendix B.2. Equation (3.56) in this regime can be written down as:

$$\boxed{a'' + \omega_0^2 a = \frac{\gamma\omega_p^2}{2}\frac{a}{\sqrt{1+a^2}}.} \tag{3.57}$$

Provided that the condition $\frac{\omega_p}{\omega_0}\sqrt{\frac{\gamma}{2}} << 1$ is satisfied, we can utilise the *Krylov-Boguliobov* averaging method [76].

3.3.1.1 Krylov-Bogoliubov Method

The general form of an ODE that can be treated with the Krylov-Bogoliubov method is:

$$a'' + \omega_0^2 a = f(a, a'), \tag{3.58}$$

where $|f(a,a')| << \left|a'' + \omega_0^2 a\right|$. Assuming the form of $a = \alpha\cos(\omega_0\zeta + \varphi)$, the first derivative is:

$$a' = \alpha'\cos(\omega_0\zeta + \varphi) - \alpha(\omega_0 + \varphi')\sin(\omega_0\zeta + \varphi), \tag{3.59}$$

and the second derivative is given by:

$$\begin{aligned} a'' = &-2\alpha'\omega_0\sin(\omega_0\zeta + \varphi) - 2\omega_0\varphi'\alpha\cos(\omega_0\zeta + \varphi) \\ &- \omega_0^2\alpha\cos(\omega_0\zeta + \varphi) + \mathcal{O}(\alpha'', \varphi'', \alpha'\varphi', \varphi'^2). \end{aligned} \tag{3.60}$$

At first order (3.58) is given by:

$$-2\omega_0(\alpha'\sin(\psi) + \alpha\varphi'\cos(\psi)) = f(\alpha\cos(\psi), -\alpha\omega_0\sin(\psi)), \tag{3.61}$$

where $\psi = \omega_0\zeta + \varphi$.

To proceed further with this method, we assume that α and φ are slowly varying, and as such we hold them constant in the terms on the right hand side of (3.61). We then introduce an averaging operator $\langle\cdot\rangle$, which is given by:

$$\langle h(\psi)\rangle = \frac{1}{2\pi}\int_0^{2\pi} h d\psi. \tag{3.62}$$

Similarly to what is done in the theory of Fourier series, we use the orthogonality of the function space $\{\sin(nx), \cos(mx)\}$ in order to arrive at:

$$\begin{aligned} -\alpha'\omega_0 &= \langle\sin(\psi)f(a,a')\rangle, \\ -\alpha\omega_0\varphi' &= \langle\cos(\psi)f(a,a')\rangle, \end{aligned} \tag{3.63}$$

where α and φ are regarded as constants in the integrand. We can identify $f(a,a')$ using (3.57) as:

$$f(a,a') \equiv f(a) = \frac{\gamma\omega_p^2}{2}\frac{a}{\sqrt{1+a^2}}. \tag{3.64}$$

Equations (3.63) are then:

$$\alpha'\omega_0 = -\frac{\gamma\omega_p^2}{2}\langle\frac{a\sin(\psi)}{\sqrt{1+a^2}}\rangle, \tag{3.65}$$

and

$$\alpha\omega_0\varphi' = -\frac{\gamma\omega_p^2}{2}\langle\frac{a\cos(\psi)}{\sqrt{1+a^2}}\rangle. \tag{3.66}$$

Firstly, equation (3.65) evaluates to:

$$\alpha' = 0, \tag{3.67}$$

because $a = \alpha\cos(\psi)$ and $\langle\cos^n(\psi)\sin(\psi)\rangle = 0$ for $n \geq 1$. This result means that α is equal to a constant (this is self-consistent with the previous assumptions), which we will set to the dimensionless laser amplitude a_0. Equation (3.66) is then given by:

$$\varphi' = -\frac{\gamma\omega_p^2}{2\pi\omega_0}F(a_0), \tag{3.68}$$

where $F(a)$ is given in terms of complete elliptic integrals K and E of the first and second kind [2]:

$$F(a_0) = \frac{2}{a_0^2}\left(E(ia_0) - K(ia_0)\right), \tag{3.69}$$

where:

$$K(x) = \int_0^{\frac{\pi}{2}} \frac{d\theta}{\sqrt{1 - x^2\sin^2(\theta)}}, \tag{3.70}$$

and

$$E(x) = \int_0^{\frac{\pi}{2}} \sqrt{1 - x^2\sin^2(\theta)}\, d\theta. \tag{3.71}$$

We can immediately integrate (3.68) to obtain:

$$\varphi = -\frac{\gamma\omega_p^2}{2\pi\omega_0}F(a_0)\zeta + \varphi_{0.}, \tag{3.72}$$

where φ_0 is given by some initial condition. The exact value of φ_0 does not matter as it amounts to a phase shift in the laser pulse.

Returning to our expression for the electromagnetic field potential $\mathcal{A}$ we have:

$$\mathcal{A} = ae^{i\theta} = a_0\cos(\Omega_0\zeta + \varphi_0)e^{i\omega_0\xi}, \tag{3.73}$$

where $\Omega_0 = \omega_0 - \frac{\gamma\omega_p^2}{2\pi\omega_0}F(a_0)$. For illustrative purposes, we rewrite (3.73) as:

$$\mathcal{A} = a_0\frac{1}{2}(e^{i(\omega_0\xi + \Omega_0\zeta + \varphi_0)} + e^{i(\omega_0\xi - \Omega_0\zeta - \varphi_0)}). \tag{3.74}$$

(3.74) illustrates that our solution can be thought of as a sum of two counter-propagating wave components.

3.3.2 Axion Resonance Condition

We are interested in deriving a condition for axion resonance that ties together the axion mass and the laser-plasma parameters. To do this, we shall now restrict our scope of consideration to a particular physical example. We consider the physical setup of an experiment where a laser pulse is travelling through a plasma, with an external magnetic field applied. For this calculation, we will neglect the effect of the magnetic field on the plasma, assuming that its magnitude is such that

[2] Using a standard relation for the derivative of the complete elliptic integral of the second kind, we can write $F(a_0)$ even more concisely as $F(a_0) = \frac{2}{a_0}\frac{dE(ia_0)}{da_0}$

it doesn't significantly alter the dynamics of the plasma, yet is sufficient to mediate the process of axion production.

The complex electromagnetic potential $\mathcal{A}$ is given by:

$$\mathcal{A} = \mathcal{A}_{\text{laser}} + \mathcal{B}z, \tag{3.75}$$

where $\mathcal{B} = -iB_x + B_y$ and is a constant corresponding to the magnetic field strength in the $x-y$ plane. For convenience we set $B_x = 0$ and $B_y = B$. We will additionally assume that the form of $\mathcal{A}_{\text{laser}}$ will take the form given in equation (3.73). Looking at the source term in equation (3.39), we are interested in the quantity:

$$\begin{aligned}\frac{1}{2}ig_\psi d\mathcal{A}\wedge d\bar{\mathcal{A}} =& \frac{1}{2}ig_\psi\Big(i\frac{a_0^2\omega_0\Omega_0}{\gamma^2}\sin(2(\Omega_0\zeta+\phi_0))\\ &- ia_0\omega_0 B(\cos(\chi_+)+\cos(\chi_-))\\ &- ia_0\omega_0 B(\cos(\chi_+)-\cos(\chi_-))\Big)\#1,\end{aligned} \tag{3.76}$$

where we introduced new co-ordinates $\chi_\pm = \omega_0\xi \pm (\Omega_0\zeta + \varphi_0)$. We now focus on the creation of axions due to the terms in (3.76) proportional to B. With that in mind, we can obtain a resonance condition:

$$d\chi_\pm \cdot d\chi_\pm = -\frac{1}{\gamma^2}(\omega_0^2 - \Omega_0^2) = -m_\psi^2. \tag{3.77}$$

This in turn leads to a relationship between the axion mass and the laser plasma parameters in the resonant regime:

$$\boxed{m_\psi^2 = \frac{\omega_p^2}{\pi}F(a_0)\left(\frac{1}{\gamma} - \frac{\omega_p^2}{4\pi\omega_0^2}F(a_0)\right).} \tag{3.78}$$

The utility of equation (3.78) is that it allows for an experiment to probe the axion mass range by tuning the laser-plasma parameters, and searching for resonant axion production. Figure 3.5 illustrates how equation (3.78) can be used to scan the axion mass parameter space.

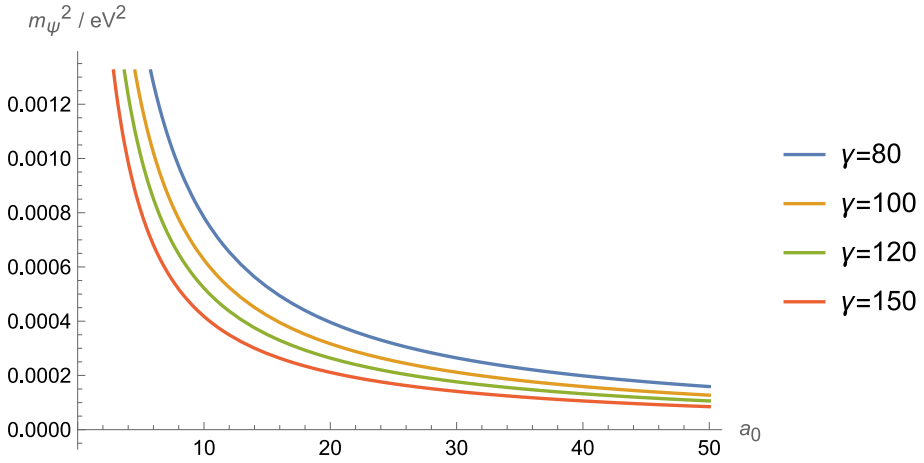

Figure 3.5: A graph showing the axion mass range that can be explored using the resonance condition (3.78). The plasma frequency is set as $\omega_p = 1\text{eV}$, the laser frequency is set such that $\omega_0^2 = 0.8\frac{\omega_p^2\gamma^2}{\sqrt{1+a_0^2}}$, where a_0 is the dimensionless laser amplitude at the front of the pulse.

Chapter 4

Ponderomotive Axion Production

4.1 Introduction

One of the biggest challenges within the field of laser-plasma physics is dealing with the inherent separation of time frames within the system. The time scale of the laser oscillations within its pulse envelope can be much shorter than the timescale of the plasma dynamics. This makes simulations of the full laser-plasma system incredibly computationally expensive. One way to overcome this hurdle is via the ponderomotive approximation. The ponderomotive approximation is a ubiquitous technique in the field of laser-plasma physics. Generally, it involves averaging out the "fast scale" dynamics (e.g. the short time scale dynamics associated with laser oscillations) of a system, in order to obtain an effective force. This, in turn, allows for the inclusion of the effects of the laser oscillations within the laser pulse, without having to do extremely computationally demanding simulations. In this Chapter, we introduce a heuristic approach to ponderomotive dynamics and apply it to the problem of axion creation.

4.2 The Ponderomotive Formalism

The ponderomotive approximation formalism is often introduced via heuristic arguments within the laser-plasma literature. For a more rigorous approach to the relativistic ponderomotive approximation one may read [77]. In this section, we present our approach to the ponderomotive formalism.

The key ingredient in the formalism is the introduction of an "averaging map" $\langle - \rangle$, for which we will not give an explicit expression, but rather introduce it in relation to how it acts upon tensors. This averaging map is a linear, tensor order-preserving mapping on the space of tensors. The averaging map satisfies:

$$\begin{aligned} \langle R + T \rangle &= \langle R \rangle + \langle T \rangle, \\ \langle \langle T \rangle \rangle &= \langle T \rangle, \end{aligned} \tag{4.1}$$

where T and R are arbitrary rank tensors. For the case of anti-symmetric rank $(0, n)$ tensors i.e. differential forms, the map satisfies:

$$\begin{aligned} \langle\langle\alpha\rangle \wedge \beta\rangle &= \langle\alpha\rangle \wedge \langle\beta\rangle, \\ \langle\iota_U\langle\alpha\rangle\rangle &= \iota_{\langle U\rangle}\langle\alpha\rangle, \\ \langle d\langle\alpha\rangle\rangle &= d\langle\alpha\rangle, \end{aligned} \tag{4.2}$$

where α and β are arbitrary n-forms, U is an arbitrary vector field and ι_U is the interior operator on forms with respect to U. Finally, since we will only be working with the Minkowski metric, the metric is equal to its average:

$$\langle g\rangle = g, \tag{4.3}$$

which leads directly to the condition that the averaging map and the Hodge star operator commute:

$$\langle\star\alpha\rangle = \star\langle\alpha\rangle. \tag{4.4}$$

For example, suppose we have a tensor T that can be written as: $T = T_0 + T_1\cos(\tau)$, where $\cos(\tau)$ oscillates rapidly from point to point in space-time in comparison to T_0 and T_1. The averaging map acting on T will result in $\langle T\rangle = T_0$.

Now let us move on to seeing how one might use this formalism in a calculation. Let $C : s \to x^\mu = C^\mu(s)$ be the worldline of a point particle with charge q and a rest mass m. The particle worldline naturally satisfies the covariant Lorentz force equation:

$$\nabla_{\dot{C}}\dot{C} = \frac{q}{m}\widetilde{\iota_{\dot{C}}F}, \tag{4.5}$$

where F is the electro-magnetic 2-form, the tilde (i.e. $\widetilde{\ }$) denotes the metric dual, ∇ is the Levi-Civita connection and $\dot{C}$ is given by:

$$\dot{C} = \frac{dC^\mu}{ds}\frac{\partial}{\partial x^\mu}, \tag{4.6}$$

where s is the particle's proper time. It follows that $\dot{C}\cdot\dot{C} = -1$, where the dot denotes the metric-induced inner product, i.e. $X \cdot Y = g(X, Y)$, where X and Y are vectors.

The principle behind the ponderomotive approximation formalism is to replace the worldline C with an effective "averaged" worldline $\mathcal{C}$. In our approach, we begin by replacing equation (4.5) with a field system:

$$\nabla_U\widetilde{U} = \frac{q}{m}\iota_U F, \tag{4.7}$$

$$U \cdot U = -1, \tag{4.8}$$

where U is a vector field for which C is an integral curve. Here we note that for the Levi-Civita connection, the following holds true:

$$\nabla_U \widetilde{U} = \iota_U d\widetilde{U}, \tag{4.9}$$

which directly leads us to express equation (4.7) as:

$$\iota_U (d\widetilde{U} - \frac{q}{m} F) = 0. \tag{4.10}$$

It follows that we can now write:

$$d\widetilde{U} = \frac{q}{m} F + \Lambda, \tag{4.11}$$

where Λ is a 2-form satisfying $\iota_U \Lambda = 0$ (due to equation (4.10)) and $d\Lambda = 0$ (due to the Gauss-Faraday Law $dF = 0$). Λ can be viewed as a rotation term that leaves the worldline C unchanged and thus can be set $\Lambda = 0$ without a loss of generality (for more detail see appendix C.1). Equation (4.11) simply becomes:

$$d\widetilde{U} = \frac{q}{m} F. \tag{4.12}$$

With this in mind, we now introduce a split $F = \langle F \rangle + F_{\text{fast}}$, where we have separated the fast-oscillation averaged electromagnetic 2-form $\langle F \rangle$ and the contribution F_{fast} from the rapid oscillations of the electromagnetic field. A visualisation of this procedure is sketched in figure 4.1. From the previously stated properties of the averaging map, equation (4.12) can be decomposed as:

$$d\langle \widetilde{U} \rangle = \frac{q}{m} \langle F \rangle, \tag{4.13}$$

$$d\widetilde{U}_{\text{fast}} = \frac{q}{m} F_{\text{fast}}, \tag{4.14}$$

where $U_{\text{fast}} = U - \langle U \rangle$. Equation (4.8) then becomes:

$$\langle U \rangle \cdot \langle U \rangle + 2\langle U \rangle \cdot U_{\text{fast}} + U_{\text{fast}} \cdot U_{\text{fast}} = -1. \tag{4.15}$$

Applying the averaging operator to both sides of equation (4.15) we obtain:

$$\langle U \rangle \cdot \langle U \rangle + \langle U_{\text{fast}} \cdot U_{\text{fast}} \rangle = -1. \tag{4.16}$$

This motivates the introduction of a re-scaled vector field $\mathcal{U}$ of the form:

$$\mathcal{U} = \frac{\langle U \rangle}{\sqrt{-\langle U \rangle \cdot \langle U \rangle}}. \tag{4.17}$$

This then results in equation (4.13) becoming:

$$d\left(\sqrt{1 + \langle U_{\text{fast}}^2 \rangle} \widetilde{\mathcal{U}} \right) = \frac{q}{m} \langle F \rangle, \tag{4.18}$$

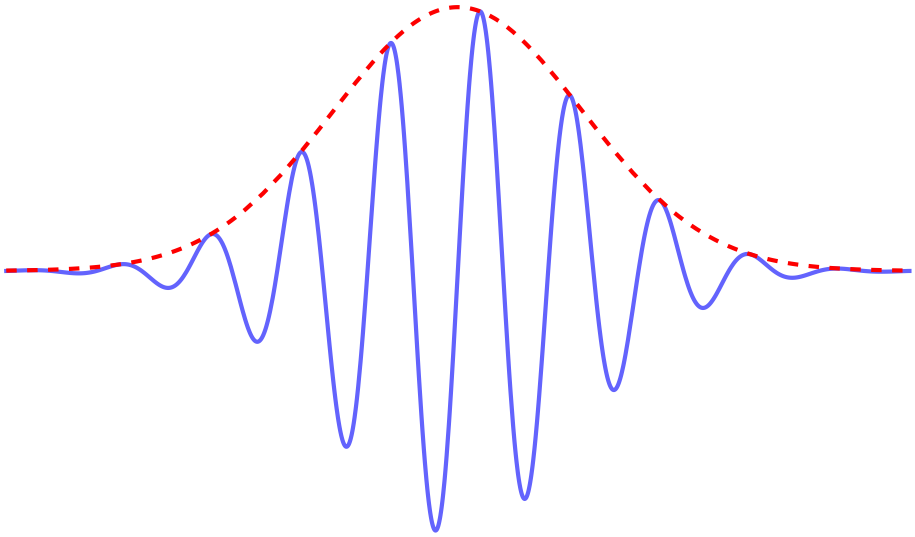

Figure 4.1: An illustration visualising the splitting of the averaged motion characterised by the envelope of the wave and the fast scale behaviour characterised by the rapid oscillations.

where $\langle U^2_{\text{fast}}\rangle = \langle U_{\text{fast}} \cdot U_{\text{fast}}\rangle$. Applying ι_u to both sides and expanding the exterior derivative term we obtain:

$$\iota_{\mathcal{U}} d\widetilde{\mathcal{U}} = -\Pi_{\mathcal{U}} d\ln\left(\sqrt{1+\langle U^2_{\text{fast}}\rangle}\right) + \frac{1}{\sqrt{1+\langle U^2_{\text{fast}}\rangle}}\frac{q}{m}\iota_{\mathcal{U}}\langle F\rangle. \tag{4.19}$$

Equation (4.19) can be evaluated along the integral curve $\mathcal{C}$ of the vector field $\mathcal{U}$ in order to describe the averaged motion of a particle:

$$m\nabla_{\dot{\mathcal{C}}}\widetilde{\dot{\mathcal{C}}} = -m\Pi_{\dot{\mathcal{C}}} d\ln\left(\sqrt{1+\langle U^2_{\text{fast}}\rangle}\right) + \frac{1}{\sqrt{1+\langle U^2_{\text{fast}}\rangle}} q\iota_{\dot{\mathcal{C}}}\langle F\rangle, \tag{4.20}$$

with

$$g(\dot{\mathcal{C}},\dot{\mathcal{C}}) = -1, \tag{4.21}$$

where $\dot{\mathcal{C}}$ is the 4-velocity of the averaged motion of a particle with worldline $\mathcal{C}$. The first term on the right-hand side of equation (4.20) is known as the ponderomotive force (alternatively the ponderomotive pressure gradient force due to the resemblance to a pressure gradient term, where $m\ln\left(\sqrt{1+\langle U^2_{\text{fast}}\rangle}\right)$ is the effective pressure). We note that in order to determine the averaged dynamics of a particle, we need to know the form of the averaged out fast dynamics $\langle U^2_{\text{fast}}\rangle$ and the averaged dynamics of the electro-magnetic field $\langle F\rangle$. So far we have been dealing with the motion of a single test particle in a background electromagnetic field, but it is very easily extended to include a background current 3-form $\mathcal{J}$. The averaging map can be applied to the sourced Maxwell's equations $d\star F = \mathcal{J}$ and $dF = 0$ to give:

$$d\star\langle F\rangle = \langle\mathcal{J}\rangle, \tag{4.22}$$

$$d\langle F\rangle = 0. \tag{4.23}$$

The fast scale dynamics of the background current are given by:

$$d \star d\widetilde{U}_{\text{fast}} = \frac{q}{m}\mathcal{J}_{\text{fast}}, \tag{4.24}$$

where $\mathcal{J}_{\text{fast}} = \mathcal{J} - \langle \mathcal{J} \rangle$. We note that for the case of ambient currents, the motion of a test particle is in principle specified by $\langle \mathcal{J} \rangle$ and $\mathcal{J}_{\text{fast}}$.

We note that the formalism discussed so far has been focusing on the motion of a single particle. In principle, this formalism can be extended to a multi-particle one, where each particle obeys its own set of equations of the form (4.20) and (4.21). It goes without saying that calculations using such an approach would quickly become intractable, and the more desirable approach would be to work with a charged continuum. Shifting from the single-particle description to the continuum case poses many problems and ambiguities that require further assumptions in order to make computations. As such, we shift to a perspective that considers an action principle with an application of the previously defined averaging map.

4.3 Action Approach to the Ponderomotive Force

As stated in the previous section, in this approach we will want to consider the ponderomotive formalism from the perspective of an action principle. We first begin by considering an action principle with just the electro-magnetic field terms, with the averaging map applied to the Lagrangian:

$$S = \int_{\mathcal{M}} \frac{1}{2}\langle F \wedge \star F \rangle = \int_{\mathcal{M}} \left(\frac{1}{2}\langle F \rangle \wedge \star \langle F \rangle + \frac{1}{2}\langle F_{\text{fast}} \wedge \star F_{\text{fast}} \rangle \right). \tag{4.25}$$

In order to compute the averaged dynamics, we need to specify the fast-scale dynamics due to F_{fast}. A very simple model for the fast scale dynamics is to prescribe plane wave motion in $\widetilde{U}_{\text{fast}}$ i.e.

$$\widetilde{U}_{\text{fast}} = \frac{q}{m}\,\text{Re}[\alpha e^{iW}] \tag{4.26}$$

where α is a 1-form and W is a 0-form such that e^{iW} is rapidly oscillating relative to the point-wise dependence of α. When evaluating $d\widetilde{U}_{\text{fast}}$, we drop the terms not containing dW, as the terms containing dW dominate. Therefore, from equation (4.14), we have:

$$\langle F_{\text{fast}} \wedge \star F_{\text{fast}} \rangle = \frac{1}{2} dW \wedge \bar{\alpha} \wedge (\star dW \wedge \alpha), \tag{4.27}$$

where $W = \langle W \rangle$ and $\alpha = \langle \alpha \rangle$ are assumed. For the rest of this section, we shall drop the averaging map brackets $\langle - \rangle$ as they will be implied. The purely electromagnetic part of the averaged action is then expressed as:

$$S = \int_{\mathcal{M}} \left(\frac{1}{2} F \wedge \star F + \frac{1}{4} dW \wedge \bar{\alpha} \wedge (\star dW \wedge \alpha) \right). \tag{4.28}$$

4.3.1 The Averaged Dynamics Coupled to Matter

We now want to consider a full action that describes a system of a laser pulse and a charged fluid. For this purpose, we propose an action of the form:

$$S = \int_{\mathcal{M}} \left(\lambda(n,\mu) \star 1 + qA \wedge (j - j_{\text{ext}}) + \frac{1}{2} F \wedge \star F + \frac{1}{4} dW \wedge \bar{\alpha} \wedge \star (dW \wedge \alpha) \right), \tag{4.29}$$

where $F = dA$, $\mu = \frac{\bar{\alpha} \cdot \alpha}{2}$ and $n = \sqrt{j \cdot j}$. We note that j and j_{ext} are number 3-currents, hence the minus sign in the second term in (4.29). The $\lambda(n,\mu)$ term corresponds to the effective equation of state for the charged fluid (we can obtain the pressure of the system via the expression $p = n\frac{\partial \lambda}{\partial n} - \lambda(n,\mu)$), which, alongside the external number current 3-form j_{ext}, will be taken as data. Note that the inclusion of μ in the equation of state is due to the fact that the averaging over the fast oscillations induces a contribution to the effective pressure in the system.

With an action specified, we can easily generate equations of motion for the system. Firstly, variations with respect to the map f result in the equation of motion:

$$\iota_V d \left(\frac{\partial \lambda}{\partial n} \widetilde{V} \right) = q \iota_V F, \tag{4.30}$$

where V is the time-like vector field for the velocity of the charged fluid defined by $V = \frac{1}{n} \widetilde{\star j}$. A variation with respect to A naturally leads to the sourced Maxwell equation:

$$d \star F = q(j_{\text{ext}} - j), \tag{4.31}$$

where we remind the reader that these are the averaged fields.
Now, let us consider the variation of the action with respect to W. The variation takes the form:

$$\delta_W S = \int_{\mathcal{M}} \frac{1}{4} [d\delta W \wedge \bar{\alpha} \wedge \star (dW \wedge \alpha) + dW \wedge \bar{\alpha} \wedge \star (d\delta W \wedge \alpha)]. \tag{4.32}$$

Assuming compact support of δW and integrating by parts gives:

$$\delta_W S = - \int_{\mathcal{M}} \frac{1}{4} \delta W d[\bar{\alpha} \wedge \star (dW \wedge \alpha) + \alpha \wedge \star (dW \wedge \bar{\alpha})]. \tag{4.33}$$

In order to satisfy the stationary condition for the action, the equation of motion for W is given by:

$$d[\bar{\alpha} \wedge \star (dW \wedge \alpha) + \alpha \wedge \star (dW \wedge \bar{\alpha})] = 0. \tag{4.34}$$

In turn, the variation with respect to $\bar{\alpha}$ takes the form:

$$\delta_{\bar{\alpha}} S = \int_{\mathcal{M}} \left(\frac{\partial \lambda}{\partial \mu} \frac{1}{2} \delta \bar{\alpha} \wedge \star \alpha - \frac{1}{4} \delta \bar{\alpha} \wedge dW \wedge \star (dW \wedge \alpha) \right), \tag{4.35}$$

where we have used $\delta_{\bar{\alpha}}\mu \star 1 = \frac{1}{2}\delta\bar{\alpha} \cdot \alpha \star 1 = \frac{1}{2}\delta\bar{\alpha} \wedge \star\alpha$, noting that $\cdot$ denotes the metric inner product. The stationary condition leads to the equation of motion:

$$dW \wedge \star(dW \wedge \alpha) = 2\frac{\partial\lambda}{\partial\mu} \star \alpha. \tag{4.36}$$

We can use equation (4.36) to immediately yield the condition:

$$dW \wedge \star\alpha = 0, \tag{4.37}$$

which follows simply from the application of an interior product $\iota_{\widetilde{\alpha}}$ to (4.36):

$$\begin{aligned} \iota_{\widetilde{\alpha}}(dW \wedge \star(dW \wedge \alpha)) &= \iota_{\widetilde{\alpha}}(2\frac{\partial\lambda}{\partial\mu} \star \alpha) \\ \iota_{\widetilde{\alpha}}dW \wedge \star(dW \wedge \alpha) - dW \wedge \iota_{\widetilde{\alpha}} \star (dW \wedge \alpha) &= 0 \\ (\alpha \cdot dW) \star (dW \wedge \alpha) - dW \wedge \iota_{\widetilde{\alpha}}\iota_{\widetilde{\alpha}} \star dW &= 0 \\ (\alpha \cdot dW) \star (dW \wedge \alpha) &= 0, \end{aligned} \tag{4.38}$$

and the fact that $dW \wedge \alpha$ is not identically zero. The last line of (4.38) only holds in general for the case of:

$$dW \cdot \alpha = 0, \tag{4.39}$$

which we note is equivalent to (4.37), due to the identity $\alpha \cdot \beta = \star^{-1}(\alpha \wedge \star\beta)$, for p-forms α and β. Using equation (4.39) and the identity:

$$\widetilde{X} \wedge \star\beta = (-1)^{p-1} \star (\iota_X \beta) \tag{4.40}$$

for a vector field X and p-form β, we can write equation (4.36) as:

$$dW \cdot dW = -2\frac{\partial\lambda}{\partial\mu}. \tag{4.41}$$

We note that the variation of the action from equation (4.29) with respect to α simply leads to the complex conjugate of equation (4.39), i.e.:

$$dW \cdot \bar{\alpha} = 0, \tag{4.42}$$

therefore we can write equation (4.34) as:

$$d(\mu \star dW) = 0. \tag{4.43}$$

Here we note that equation (4.43) doesn't depend explicitly on α, rather it depends on μ. This means that in order to generate the dynamics of V, F and W from the equations of motion, we only need to prescribe the form of $\bar{\alpha} \cdot \alpha$ and, except for (4.39), the actual direction of α is irrelevant.

Finally, we turn our attention to the function $\lambda(n,\mu)$, which is the equation of state constraint on the system. In order for our equations of motion to coincide with equation (4.18), we need to prescribe the form of $\lambda(n,\mu)$ such that $\frac{\partial\lambda}{\partial n} = \sqrt{m^2+q^2\mu}$ (this can be thought of as the electrons gaining effective mass that has a contribution from the ponderomotive pressure). The motivation for the prescription of this condition comes from comparing equations (4.18) and (4.30), and noting that:

$$\begin{aligned}\langle U_{\text{fast}}^2\rangle &= \langle \frac{q^2}{m^2}\frac{1}{4}\left(\alpha e^{iW}+\bar{\alpha}e^{-iW}\right)\cdot\left(\alpha e^{iW}+\bar{\alpha}e^{-iW}\right)\rangle \\ &= \frac{q^2}{m^2}\frac{1}{4}\langle \alpha\cdot\alpha e^{2iW}+2\alpha\cdot\bar{\alpha}+\bar{\alpha}\cdot\bar{\alpha}e^{-2iW}\rangle \\ &= \frac{1}{2}\frac{q^2}{m^2}\alpha\cdot\bar{\alpha},\end{aligned} \tag{4.44}$$

which in turn leads to:

$$m\sqrt{1+\langle U_{\text{fast}}^2\rangle} = m\sqrt{1+\frac{q^2}{m^2}\frac{1}{2}\alpha\cdot\bar{\alpha}} = \sqrt{m^2+q^2\mu}. \tag{4.45}$$

If we consider the case of a cold fluid, we want the pressure, given by $p = n\frac{\partial\lambda}{\partial n} - \lambda(n,\mu)$, to vanish; thus we can write λ down as:

$$\lambda = n\sqrt{m^2+q^2\mu}. \tag{4.46}$$

This, in turn, lets us write (4.41) as:

$$dW\cdot dW = -\frac{q^2 n}{\sqrt{m^2+q^2\mu}}. \tag{4.47}$$

We note that for the case of small values of $\frac{q^2\mu}{m^2}$ and $j = j_{\text{ext}}$, we have $dW\cdot dW \approx -\frac{q^2 n_{\text{ext}}}{m}$. It is clear that the right-hand side of (4.47) is the negative of the square of a plasma frequency. The time-like unit normalized vector field $\frac{\widetilde{dW}}{\sqrt{-dW\cdot dW}}$ is the 4-velocity of a collection of observers who see the electro-magnetic field F_{fast} oscillate at the plasma frequency of the electron fluid. A non-covariant form of this result, with some work from the reader, can be found in [78].

4.4 Ponderomotive Axion Dynamics

We now wish to apply our formalism to an axion-laser-plasma system. Returning to the underlying, unaveraged, variables:

$$\begin{aligned}S = \int_{\mathcal{M}} \Big(& mn\star 1 + qA\wedge(j-j_{\text{ext}}) + \frac{1}{2}F\wedge\star F + \frac{1}{2}d\Psi\wedge\star d\Psi \\ & + \frac{1}{2}m_\Psi^2\Psi^2\star 1 - \frac{1}{2}g_\Psi\Psi F\wedge F\Big),\end{aligned} \tag{4.48}$$

where Ψ is the pseudo-scalar field for the axion, m_Ψ is the axion mass and g_Ψ is the axion-photon coupling constant. We apply the averaging map to the Lagrangian to arrive at the ponderomotive

dynamics. We split the fast and averaged dynamics of the electro-magnetic and the axion fields:

$$\begin{aligned} A &= \langle A \rangle + A_{\text{fast}}, \\ \Psi &= \langle \Psi \rangle + \Psi_{\text{fast}}, \end{aligned} \tag{4.49}$$

where the electro-magnetic 2-form is given by $F = \langle F \rangle + F_{\text{fast}}$, which follows directly from $F = dA$. We prescribe the fast-scale dynamics of the electro-magnetic and axion fields as:

$$\Psi_{\text{fast}} = \text{Re}[\psi e^{iW}], \tag{4.50}$$

$$A_{\text{fast}} = \text{Re}[\alpha e^{iW}]. \tag{4.51}$$

We now consider the averaging map applied to each term in the Lagrangian in the action from equation (4.48). Firstly, the EM-Axion coupling term becomes:

$$\begin{aligned} \langle \Psi F \wedge F \rangle = &\langle (\langle \Psi \rangle + \frac{1}{2}\psi e^{iW} + \frac{1}{2}\bar{\psi} e^{-iW}) \\ &(\langle F \rangle + \frac{1}{2} i dW \wedge \alpha e^{iW} - \frac{1}{2} i dW \wedge \bar{\alpha} e^{-iW} + \dots) \\ &\wedge (\langle F \rangle + \frac{1}{2} i dW \wedge \alpha e^{iW} - \frac{1}{2} i dW \wedge \bar{\alpha} e^{-iW} + \dots) \rangle. \end{aligned} \tag{4.52}$$

Expanding out the terms we obtain:

$$\langle \Psi F \wedge F \rangle = \langle \Psi \rangle \langle F \rangle \wedge \langle F \rangle - \left(\frac{1}{2} i \psi dW \wedge \bar{\alpha} - \frac{1}{2} i \bar{\psi} dW \wedge \alpha \right) \wedge \langle F \rangle + \dots, \tag{4.53}$$

where the $\dots$ denote terms which contain $d\alpha$, $d\bar{\alpha}$ and $d\psi$ which will be dropped as the magnitudes of the components of $d\psi$ and $d\alpha$ are typically much less than the magnitudes of the components of dW. We also note that the term due to $\langle F_{\text{fast}} \wedge F_{\text{fast}} \rangle$ is negligible, as it contains products of small quantities F_{fast} as well as being of order g_Ψ in the already small axion photon coupling constant; thus this term is dropped. The kinetic axion term, in turn, yields:

$$\langle d\Psi \wedge \star d\Psi \rangle = d\langle \Psi \rangle \wedge \star d\langle \Psi \rangle + \frac{1}{2} |\psi|^2 dW \wedge \star dW + \dots, \tag{4.54}$$

and the axion mass term is simply:

$$\langle \frac{1}{2} m_\Psi^2 \Psi^2 \star 1 \rangle = \frac{1}{2} m_\Psi^2 \langle \Psi \rangle^2 \star 1 + \frac{1}{4} m_\Psi^2 |\psi|^2 \star 1. \tag{4.55}$$

Having derived the averaged terms in the Lagrangian, we are now in a position to propose an action S_P for the ponderomotive dynamics. Dropping the angled brackets for simplicity we have:

$$\begin{aligned} S_{\text{P}} = \int_{\mathcal{M}} \big(&\lambda(n,\mu) \star 1 + qA \wedge (j - j_{\text{ext}}) + \frac{1}{2} F \wedge \star F + \frac{1}{4} dW \wedge \bar{\alpha} \wedge \star (dW \wedge \alpha) \\ &+ \frac{1}{2} d\Psi \wedge \star d\Psi + \frac{1}{4} |\psi|^2 dW \wedge \star dW + \frac{1}{2} m_\Psi^2 \Psi^2 \star 1 + \frac{1}{4} m_\Psi^2 |\psi|^2 \star 1 \\ &- \frac{1}{2} g_\Psi \Psi F \wedge F - \frac{1}{4} g_\Psi dW \wedge (i\bar{\psi}\alpha - i\psi\bar{\alpha}) \wedge F \big), \end{aligned} \tag{4.56}$$

where $\mu = \frac{\bar{\alpha}\cdot\alpha}{2}$ and $\lambda = n\sqrt{m^2 + q^2\mu}$, just like in the previous section.

4.4.1 Ponderomotive Equations of Motion

Having introduced an action functional, we are now in a position to derive the equations of motion for the system.

Variation of the action in equation (4.56), with respect to α, results in:

$$\frac{q^2 n}{\sqrt{m^2 + q^2\mu}} \star \bar{\alpha} - dW \wedge \star(dW \wedge \bar{\alpha}) + g_\Psi i\bar{\psi} dW \wedge F = 0. \tag{4.57}$$

The ψ variation leads to:

$$dW \wedge \star dW\bar{\psi} + m_\Psi^2 \bar{\psi} \star 1 + g_\Psi i dW \wedge \bar{\alpha} \wedge F = 0. \tag{4.58}$$

The condition seen in equation (4.39) also holds for the current system. This can be arrived at by taking the wedge product between dW and equation (4.57), thus once again leading to:

$$dW \cdot \bar{\alpha} = 0. \tag{4.59}$$

Due to this condition and the identity (4.40), we can use (4.57) to express $\bar{\alpha}$ as:

$$\bar{\alpha} = -\frac{1}{dW \cdot dW + \frac{q^2 n}{\sqrt{m^2+q^2\mu}}} g_\Psi i\bar{\psi} \star (dW \wedge F). \tag{4.60}$$

We now substitute (4.60) into equation (4.58) to obtain:

$$(dW \cdot dW + m_\Psi^2)(dW \cdot dW + \frac{q^2 n}{\sqrt{m^2 + q^2\mu}}) + g_\Psi^2 (dW \wedge F) \cdot (dW \wedge F) = 0. \tag{4.61}$$

The coefficient ψ in the axion's fast term follows from equation (4.58) and $\star\star 1 = -1$. We obtain:

$$\psi = -\frac{i g_\Psi \star (dW \wedge \alpha \wedge F)}{dW \cdot dW + m_\Psi^2}. \tag{4.62}$$

Turning our attention to the equation of motion that is generated via the variation of the ponderomotive action with respect to W, we obtain:

$$d\left(\frac{1}{4}\bar{\alpha} \wedge \star(dW \wedge \alpha) + \frac{1}{4}\alpha \wedge \star(dW \wedge \bar{\alpha}) + \frac{1}{2}|\psi|^2 \star dW - \frac{1}{4} i g_\Psi (\bar{\psi}\alpha - \psi\bar{\alpha}) \wedge F\right) = 0. \tag{4.63}$$

4.4.2 Conservation Law

We can introduce a vector field $K = \frac{\widetilde{dW}}{||dW||}$. We will also assume that dW is time-like i.e. $dW \cdot dW < 0$. We also denote the metric norm of dW as :

$$||dW|| = \Omega, \tag{4.64}$$

where Ω can be interpreted as the angular frequency of the fast-scale oscillations of a laser pulse, for an observer with a 4-velocity K. We can use this to decompose the electro-magnetic 2-form F with respect to the vector field K:

$$F = -\widetilde{K} \wedge E - \#B, \tag{4.65}$$

where the Hodge map # acts as:

$$\#\beta = \star(\widetilde{K} \wedge \beta) \tag{4.66}$$

for p-forms β. Also note that $\iota_K B = 0$ and $\iota_K E = 0$. With that in mind, we can express:

$$\begin{aligned} dW \wedge F &= \Omega \widetilde{K} \wedge F \\ &= -\Omega \widetilde{K} \wedge \#B. \end{aligned} \tag{4.67}$$

This then lets us write:

$$\begin{aligned} dW \wedge F \wedge \star(dW \wedge F) &= \Omega^2 \widetilde{K} \wedge \#B \wedge \star(\widetilde{K} \wedge \#B) \\ &= \Omega^2 \widetilde{K} \wedge \#B \wedge \#\#B \\ &= \Omega^2 \widetilde{K} \wedge \#B \wedge B \\ &= \Omega^2 \widetilde{K} \wedge (B \cdot B \#1) \\ &= -\Omega^2 B \cdot B \star 1. \end{aligned} \tag{4.68}$$

We note that we used the definition of (4.66) in the second line of (4.68) and used the fact that $\#\#\beta = \beta$ for p-forms β that satisfy $\iota_K \beta = 0$. Equation (4.68) lets us express equation (4.61) as:

$$\left(\Omega^2 - m_\Psi^2\right)\left(\Omega^2 - \Omega_p^2\right) - g_\Psi^2 \Omega^2 B^2 = 0, \tag{4.69}$$

where $\Omega_p^2 = \frac{nq^2}{\sqrt{m^2+q^2\mu}}$ is the square of the effective plasma frequency. Equation (4.62) allows us to arrive at the final expression for the complex amplitude of the fast scale portion of the axion field:

$$\psi = \frac{-i g_\Psi \Omega \alpha \cdot B}{\Omega^2 - m_\Psi^2}. \tag{4.70}$$

(4.70) illustrates that a resonance occurs at $\Omega = m_\Psi$ and we shall investigate this case in subsection 4.4.3.

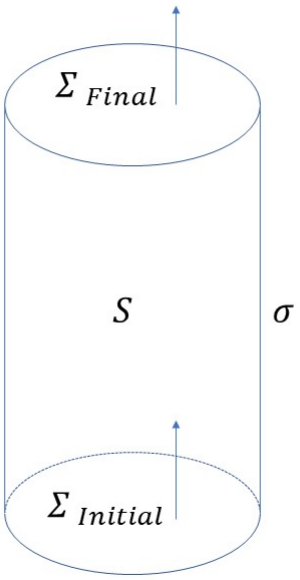

Figure 4.2: An illustration of the region S.

Having derived an explicit expression for the axion field, we see that (4.63) suggests the introduction of the current 3-form $\mathcal{J}$:

$$\mathcal{J} = \left(\frac{1}{2}\alpha \cdot \bar{\alpha} + \frac{1}{2}|\psi|^2\right) \star dW - \frac{1}{4} i g_\Psi \left(\bar{\psi}\alpha - \psi\bar{\alpha}\right) \wedge F. \tag{4.71}$$

Expression (4.71) allows us to restate (4.63) as a local conservation law:

$$d\mathcal{J} = 0. \tag{4.72}$$

We now introduce a four-dimensional region of space-time S, which is illustrated in Figure 4.2. We define S such that :

$$\begin{aligned} \Sigma^*_{\text{Initial}} \widetilde{K} &= 0, \\ \Sigma^*_{\text{Final}} \widetilde{K} &= 0. \end{aligned} \tag{4.73}$$

This choice can be interpreted as choosing S such that Σ_{Initial} and Σ_{Final} are surfaces of constant W. Integrating (4.72) over S yields:

$$\int_S d\mathcal{J} = \int_{\partial S} \mathcal{J} = 0, \tag{4.74}$$

where the second equality comes from Stokes's theorem. The integral $\int_{\partial S} \mathcal{J}$ can be split up into:

$$\int_{\partial S} \mathcal{J} = \int_{\Sigma_{\text{Initial}}} \mathcal{J} - \int_{\Sigma_{\text{Final}}} \mathcal{J} + \int_\sigma \mathcal{J} = 0. \tag{4.75}$$

If we consider the case in which the fields ψ and α vanish on σ, then (4.75) yields the condition:

$$\int_{\Sigma \text{ Initial}} \mathcal{J} = \int_{\Sigma_{\text{Final}}} \mathcal{J}. \tag{4.76}$$

We can reduce this condition by decomposing $\mathcal{J}$ with respect to K:

$$\mathcal{J} = \rho\#1 - \frac{1}{4} i g_\Psi \widetilde{K} \wedge \left(\psi\bar{\alpha} - \bar{\psi}\alpha\right) \wedge E, \tag{4.77}$$

where:

$$\begin{aligned} \rho &= \frac{1}{2}\left(\alpha \cdot \bar{\alpha} + \psi\bar{\psi}\right) ||dW|| + \frac{1}{4} i g_\Psi \left(\bar{\psi}\alpha \cdot B + \psi\bar{\alpha} \cdot B\right) \\ &= \frac{1}{2}\left(\alpha \cdot \bar{\alpha} + \frac{g_\Psi^2 m_\Psi^2 |\alpha \cdot B|^2}{(\Omega^2 - m_\Psi^2)^2}\right)\Omega, \end{aligned} \tag{4.78}$$

where we used equation (4.70) to eliminate ψ. The integral conservation condition (4.76) simply becomes:

$$\int_{\Sigma_{\text{Initial}}} \rho\#1 = \int_{\Sigma_{\text{Final}}} \rho\#1. \tag{4.79}$$

We shall use equation (4.79) in subsection 4.4.4 to derive a simple formula for the depletion of the fast-scale laser pulse due to an external magnetic field.

4.4.3 Axion Flux and the Resonant Case

Let us consider a case of an electromagnetic wave travelling in a plasma along the z axis with a phase velocity of v (note that $0 < v < 1$) in the lab frame. We introduce a co-ordinate co-frame $\{\gamma d\xi, \gamma d\zeta, dx, dy\}$, which is adapted to an observer travelling along with the electromagnetic wave with velocity v and γ is the usual Lorentz factor $\gamma = \frac{1}{\sqrt{1-v^2}}$. We can write $d\xi$ and $d\zeta$ in terms of Cartesian co-ordinates in the lab frame as:

$$\begin{aligned} d\zeta &= dz - vdt, \\ d\xi &= vdz - dt. \end{aligned} \tag{4.80}$$

In order to compute the fast scale axion flux we have to specify the form of dW, α and B. For the purposes of obtaining estimates on the axion flux one would expect in an experiment, we simply set all the relevant quantities to be constants. We have already defined the magnitude $||dW|| = \Omega$, so we only need to define the direction:

$$dW = \Omega\gamma d\xi. \tag{4.81}$$

For the purposes of specifying α, we will assume that the electromagnetic wave is linearly polarised along x. This allows us to simply write:

$$\alpha = a dx, \tag{4.82}$$

where a is the amplitude of the fast scale electromagnetic potential. Finally, we prescribe that the external magnetic field will be aligned with the polarisation of the electromagnetic wave, i.e.:

$$B = Bdx. \tag{4.83}$$

With these assumptions, the magnitude of the fast axion flux is given by:

$$|\psi| = \left| \frac{g_\psi \Omega B a}{m_\psi^2 - \Omega^2} \right|. \tag{4.84}$$

Assuming that we are in the resonant regime i.e. $\frac{q^2 n}{\sqrt{m^2+q^2\mu}} = m_\psi^2$ and the condition $|\alpha \cdot B| = |\alpha||B|$, we can use (4.61) and (4.62) to find the magnitude of ψ:

$$|\psi| = \frac{|\star(dW \wedge \alpha \wedge F)|}{||dW \wedge F||}. \tag{4.85}$$

where $||dW \wedge F|| = \sqrt{|\star^{-1}((dW \wedge F) \wedge \star(dW \wedge F))|}$. We can apply all of our previous prescriptions for dW, α and B to equation (4.85) to simply arrive at:

$$|\psi| = |a|. \tag{4.86}$$

Therefore, in the resonant case, the axion production depends only on the magnitude of the electromagnetic potential due to the laser.

4.4.4 Ponderomotive Current Analysis

Having derived an expression for a conserved current for the fast-scale fields in (4.79), we can conduct an analysis of its behaviour. The first issue to consider with this analysis is the alignment of the fast pulse oscillations and the external magnetic field. This is done by specifying the form of the metric inner product:

$$\begin{aligned} |\alpha \cdot B|^2 &= (\alpha \cdot B)(\bar{\alpha} \cdot B) \\ &= (\mathrm{Re}(\alpha \cdot B))^2 + (\mathrm{Im}(\alpha \cdot B))^2. \end{aligned} \tag{4.87}$$

We further note that we can express the real and imaginary parts of the metric inner product:

$$\mathrm{Re}(\alpha \cdot B) = |\mathrm{Re}(\alpha)||B| \cos(\theta_R), \tag{4.88}$$

$$\mathrm{Im}(\alpha \cdot B) = |\mathrm{Im}(\alpha)||B| \cos(\theta_I), \tag{4.89}$$

where θ_R and θ_I correspond to the angles between the magnetic field B and the real and imaginary parts of the pulse. This results in an expression for ρ:

$$\rho = \rho_I + \rho_R, \tag{4.90}$$

where:

$$\begin{aligned}\rho_R &= \frac{1}{2}\left(1+\frac{g_\Psi^2 m_\Psi^2 \cos^2(\theta_R)B^2}{(\Omega^2-m_\Psi^2)^2}\right)(\mathrm{Re}(\alpha))^2\Omega,\\ \rho_I &= \frac{1}{2}\left(1+\frac{g_\Psi^2 m_\Psi^2 \cos^2(\theta_I)B^2}{(\Omega^2-m_\Psi^2)^2}\right)(\mathrm{Im}(\alpha))^2\Omega.\end{aligned} \tag{4.91}$$

Let us now consider a scenario where there are two regions: I and II. In region I, there is no externally applied magnetic field B, and in the region II, the field is switched on. Assuming linear polarisation of the laser pulse, we can derive a simple formula for its depletion in an external magnetic field. Assuming that $\alpha \in \mathbb{R}$ and is aligned with B, due to the conservation law (4.79) we have:

$$\frac{\alpha_{II}}{\alpha_I} = \left(1+\frac{g_\Psi^2 m_\Psi^2 B^2}{(\Omega^2-m_\Psi^2)^2}\right)^{-\frac{1}{2}}, \tag{4.92}$$

where α_I and α_{II} refer to the value of α in regions I and II respectively.

Chapter 5

Quantum Axion Production

5.1 Introduction

In this chapter, we shall approach the problem of axion creation while considering quantum effects.

5.2 Perturbative Quantization and Toy Model

Let us begin by considering the action for axion-electrodynamics:

$$S[A,\psi] = \int \frac{1}{2}F \wedge \star F + \frac{1}{2}d\psi \wedge \star d\psi + \frac{1}{2}m_\psi^2\psi^2 \star 1 - \frac{1}{2}g_\psi \psi F \wedge F. \tag{5.1}$$

We then write down the fields as a sum of the classical field solutions and quantum fluctuations:

$$\begin{aligned} A &= A_0 + A_1, \\ \psi &= \psi_0 + \psi_1, \end{aligned} \tag{5.2}$$

where the 0 and 1 subscripts denote the classical solutions to the equations of motion and quantum fluctuations, respectively. The action can then be written as:

$$\begin{aligned} S = \int & \frac{1}{2}F_0 \wedge \star F_0 + F_0 \wedge \star F_1 + \frac{1}{2}F_1 \wedge \star F_1 \\ & + \frac{1}{2}d\psi_0 \wedge \star d\psi_0 + d\psi_0 \wedge \star d\psi_1 + \frac{1}{2}d\psi_1 \wedge \star d\psi_1 \\ & + \frac{1}{2}m_\psi^2\psi_0^2 \star 1 + m_\psi^2\psi_0\psi_1 + \frac{1}{2}m_\psi^2\psi_1^2 \star 1 \\ & - \frac{1}{2}g_\psi\psi_0 F_0 \wedge F_0 - \frac{1}{2}g_\psi\psi_1 F_0 \wedge F_0 - g_\psi\psi_0 F_0 \wedge F_1 \\ & - \frac{1}{2}g_\psi\psi_0 F_1 \wedge F_1 - g_\psi\psi_1 F_0 \wedge F_1 + \mathcal{O}(3^{\text{rd}}\text{order}), \end{aligned} \tag{5.3}$$

where $\mathcal{O}(3^{\text{rd}}\text{order})$ denotes terms of order 3 in the fluctuations that we shall disregard, as a consequence of the small value of g_ψ. We also lose all the boundary terms (due to physical consideration of the fields vanishing at infinity) and terms that are linear in the classical fields, as they will not

affect the dynamics due to cancelling with the classical equations of motion. The action can then be written as:

$$S = S_0 + S_2 + S_3 + \text{Boundary Terms}, \tag{5.4}$$

where S_0 is the action for the fields satisfying the classical equations of motion, S_2 is the action containing all the terms that are of second order in the quantum fluctuations and similarly S_3 contains all the terms of the third order in the fluctuations. As mentioned before, we drop the terms of order 3 and any boundary terms. The term that captures the quantum effects in our problem is S_2, which results in a linear description. For now, let us consider the case where axions are created from fully quantum effects (meaning that we set $\psi_0 = 0$), and we prescribe the form of the classical electromagnetic field (thus neglecting its dynamics). The action we shall consider is then:

$$S = -\int \frac{1}{2}F \wedge \star F + \frac{1}{2}d\psi \wedge \star d\psi + \frac{1}{2}m_\psi^2\psi^2 \star 1 - g_\psi \psi F \wedge F_0, \tag{5.5}$$

where we have dropped the 1 subscript from the fluctuation fields and added a minus sign in front for future convenience, as it will ensure that the Hamiltonian describing our system is positive. We can write (5.5) in a more standard form using vector calculus:

$$S[A,\phi,\psi] = \int dt \int d^3x \frac{1}{2}(\mathbf{E}^2 - \mathbf{B}^2) + \frac{1}{2}(\partial_t\psi)^2 - \frac{1}{2}(\nabla\psi)^2 - \frac{1}{2}m_\psi^2\psi^2 - g_\psi\psi(\mathbf{E}\cdot\mathbf{B}_0 + \mathbf{E}_0\cdot\mathbf{B}), \tag{5.6}$$

with $\mathbf{E} = -\nabla\phi - \partial_t\mathbf{A}$ and $\mathbf{B} = \nabla\times\mathbf{A}$, where ϕ is the scalar potential for the electric field and $\mathbf{A}$ is the vector potential for the magnetic field. For our purposes, we shall set $\mathbf{E}_0 = 0$ and assume that $\mathbf{B}_0$ is constant, as we are interested in the case of axion conversion in a constant external magnetic field[1]. We switch to a Hamiltonian formalism via the use of a Legendre transform:

$$H = \int d^3x \, (P\partial_t\psi + \mathbf{\Pi}\cdot\partial_t\mathbf{A}) - L, \tag{5.7}$$

where $P = \frac{\delta L}{\delta\dot{\psi}}$ and $\mathbf{\Pi} = \frac{\delta L}{\delta\dot{\mathbf{A}}}$ are the canonical momenta of the axion and the electromagnetic field respectively and the Lagrangian is naturally given by:

$$L = \int d^3x \, \frac{1}{2}(\mathbf{E}^2 - \mathbf{B}^2) + \frac{1}{2}(\partial_t\psi)^2 - \frac{1}{2}(\nabla\psi)^2 - \frac{1}{2}m_\psi^2\psi^2 - g_\psi\psi(\mathbf{E}\cdot\mathbf{B}_0). \tag{5.8}$$

We then shall also have to fix the gauge for the electromagnetic potential. We are looking to eliminate ϕ from the equations of motion, and as such we choose the Coulomb gauge i.e.:

$$\nabla\cdot\mathbf{A} = 0. \tag{5.9}$$

[1] In this subsection we are considering axion-photon conversion in an external magnetic field, and as such we set $\mathbf{E}_0 = 0$. In the next section, we will consider a case where both of the classical fields $\mathbf{E}_0$ and $\mathbf{B}_0$ will contribute (axion production due to a plasma wave and an external magnetic field), but we will not be considering the quantum nature of $\mathbf{E}$ and $\mathbf{B}$, due to the relevant field parameters being well within the classical regime.

Using integration by parts and the condition that all of our fields vanish at infinity, we find that the integral of $\partial_t \mathbf{A} \cdot \nabla\phi$ vanishes in the Coulomb gauge. We can then write the Lagrangian as:

$$\begin{aligned} L = \int d^3x \, & \frac{1}{2}(\nabla\phi)^2 + \frac{1}{2}(\partial_t \mathbf{A})^2 - \frac{1}{2}(\nabla \times \mathbf{A})^2 \\ & + \frac{1}{2}(\partial_t \psi)^2 - \frac{1}{2}(\nabla\psi)^2 + \frac{1}{2}m_\psi^2 \psi^2 \\ & + g_\psi \psi \nabla\phi \cdot \mathbf{B}_0 + g_\psi \psi \partial_t \mathbf{A} \cdot \mathbf{B}_0. \end{aligned} \tag{5.10}$$

Proceeding with the elimination of ϕ from the action, we consider the equation of motion for ϕ given by:

$$\frac{\delta S}{\delta \phi} = 0 \rightarrow \nabla^2 \phi = -g_\psi \nabla\psi \cdot \mathbf{B}_0, \tag{5.11}$$

where $\nabla \cdot \mathbf{B}_0 = 0$ has been used. Equation (5.11) can be solved formally as:

$$\phi = -g_\psi \nabla^{-2}(\mathbf{B}_0 \cdot \nabla\psi), \tag{5.12}$$

where ∇^{-2} is the formal operator inverse of ∇^2 (which is simply the integral operator $\int d^3y G(x,y)$, where $G(x,y)$ is the Greens function of ∇^2). Singling out the expressions in the Lagrangian that contain ϕ we have:

$$\int d^3x \frac{1}{2}(\nabla\phi)^2 + g_\psi \psi \nabla\phi \cdot \mathbf{B}_0. \tag{5.13}$$

We can integrate (5.13) by parts to obtain:

$$\begin{aligned} & \int d^3x \left(-\frac{1}{2}\phi\nabla^2\phi - \phi g_\psi \nabla\psi \cdot \mathbf{B}_0 \right) \\ & = \int \frac{1}{2}\phi\nabla^2\phi, \end{aligned} \tag{5.14}$$

where we used (5.11) to obtain the second line in (5.14). Finally, using (5.11) and (5.14), the Lagrangian for our system can be written as:

$$\begin{aligned} L = \int d^3x \, & \frac{1}{2}g_\psi^2 \nabla\psi \cdot \mathbf{B}_0 \nabla^{-2}(\nabla\psi \cdot \mathbf{B}_0) + \frac{1}{2}(\partial_t \mathbf{A})^2 - \frac{1}{2}(\nabla \times \mathbf{A})^2 \\ & + \frac{1}{2}(\partial_t \psi)^2 - \frac{1}{2}(\nabla\psi)^2 - \frac{1}{2}m_\psi^2 \psi^2 \\ & + g_\psi \psi \partial_t \mathbf{A} \cdot \mathbf{B}_0. \end{aligned} \tag{5.15}$$

Having arrived at this form of our Lagrangian, we can now perform the Legendre transform to obtain our Hamiltonian. The canonical momenta are then given:

$$\begin{aligned} \mathbf{\Pi} &= \frac{\delta L}{\delta \partial_t \mathbf{A}} = \partial_t \mathbf{A} + g_\psi \psi \mathbf{B}_0, \\ P &= \frac{\delta L}{\delta \partial_t \psi} = \partial_t \psi. \end{aligned} \tag{5.16}$$

Finally, we can write down the Hamiltonian:

$$\begin{aligned} H = \int d^3x \, & \frac{1}{2}P^2 + \frac{1}{2}(\mathbf{\Pi} - g_\psi \psi \mathbf{B}_0)^2 \\ & -\frac{1}{2}g_\psi^2 \nabla\psi \cdot \mathbf{B}_0 \nabla^{-2}(\nabla\psi \cdot \mathbf{B}_0) \\ & +\frac{1}{2}(\nabla \times \mathbf{A})^2 + \frac{1}{2}(\nabla\psi)^2 + \frac{1}{2}m_\psi^2\psi^2. \end{aligned} \tag{5.17}$$

We then drop the $\mathcal{O}(g_\psi^2)$ terms to obtain the final version of our Hamiltonian:

$$H = \int d^3x \, \frac{1}{2}P^2 + \frac{1}{2}\mathbf{\Pi}^2 + \frac{1}{2}(\nabla \times \mathbf{A})^2 + \frac{1}{2}(\nabla\psi)^2 + \frac{1}{2}m_\psi^2\psi^2 - g_\psi\psi\mathbf{\Pi}\cdot\mathbf{B}_0. \tag{5.18}$$

5.2.1 Quantization of the Hamiltonian

We can quantise the Hamiltonian given in (5.18) through the usual prescriptions of canonical quantisation[2]. We propose a quantum Hamiltonian:

$$\hat{H} = \int d^3x \, \frac{1}{2}\hat{P}^2 + \frac{1}{2}\hat{\mathbf{\Pi}}^2 + \frac{1}{2}(\nabla \times \hat{\mathbf{A}})^2 + \frac{1}{2}(\nabla\hat{\psi})^2 + \frac{1}{2}m_\psi^2\hat{\psi}^2 - g_\psi\hat{\psi}\hat{\mathbf{\Pi}}\cdot\mathbf{B}_0. \tag{5.19}$$

The Hamiltonian in equation (5.19) can be split up into a free and an interacting part i.e. $\hat{H} = \hat{H}_0 + \hat{H}_I$, where:

$$\hat{H}_0 = \int d^3x \, \frac{1}{2}\hat{P}^2 + \frac{1}{2}\hat{\mathbf{\Pi}}^2 + \frac{1}{2}(\nabla \times \hat{\mathbf{A}})^2 + \frac{1}{2}(\nabla\hat{\psi})^2 + \frac{1}{2}m_\psi^2\hat{\psi}^2, \tag{5.20}$$

and

$$\hat{H}_I = -\int d^3x \, g_\psi\hat{\psi}\hat{\mathbf{\Pi}}\cdot\mathbf{B}_0. \tag{5.21}$$

For mathematical convenience, it is helpful to consider our system to have a finite volume V. We can expand the free field operators as:

$$\begin{aligned} \hat{\psi}(\mathbf{x}) &= \sum_{\mathbf{k}} \frac{1}{\sqrt{2\omega_\psi V}}\left(\hat{b}_{\mathbf{k}}e^{i\mathbf{k}\cdot\mathbf{x}} + \hat{b}_{\mathbf{k}}^\dagger e^{-i\mathbf{k}\cdot\mathbf{x}}\right) \qquad \hat{\mathbf{A}}(\mathbf{x}) = \sum_{\mathbf{k}} \frac{1}{\sqrt{2\omega_A V}}\left(\hat{a}_{\mathbf{k}}e^{i\mathbf{k}\cdot\mathbf{x}} + \hat{a}_{\mathbf{k}}^\dagger e^{-i\mathbf{k}\cdot\mathbf{x}}\right) \\ \hat{P}(\mathbf{x}) &= -i\sum_{\mathbf{k}} \sqrt{\frac{\omega_\psi}{2V}}\left(\hat{b}_{\mathbf{k}}e^{i\mathbf{k}\cdot\mathbf{x}} - \hat{b}_{\mathbf{k}}^\dagger e^{-i\mathbf{k}\cdot\mathbf{x}}\right) \qquad \hat{\mathbf{\Pi}}(\mathbf{x}) = -i\sum_{\mathbf{k}} \sqrt{\frac{\omega_\psi}{2V}}\left(\hat{a}_{\mathbf{k}}e^{i\mathbf{k}\cdot\mathbf{x}} - \hat{a}_{\mathbf{k}}^\dagger e^{-i\mathbf{k}\cdot\mathbf{x}}\right), \end{aligned}$$

where $\omega_\psi = \sqrt{\mathbf{k}^2 + m_\psi^2}$ and $\omega_A = |\mathbf{k}|$. The commutation relations for the operators are given:

$$[\hat{b}_{\mathbf{k}}, \hat{b}_{\mathbf{k}'}^\dagger] = \delta_{\mathbf{k}\mathbf{k}'}, \tag{5.22}$$

$$[\hat{\mathbf{a}}_{\mathbf{k}}, \hat{\mathbf{a}}_{\mathbf{k}'}^\dagger] = \delta_{\mathbf{k}\mathbf{k}'}\mathbf{I}_\perp, \tag{5.23}$$

[2] We note that the principle of linearising the system and then quantising it is a standard method within condensed matter physics, known as Bogoliubov theory. This was first applied to a weakly interacting bose gas, and can be found in most textbooks on Bose-Einstein condensates such as [79]

where $\mathbf{I}_\perp$ is the projector into the $\mathbf{k}$-orthogonal plane.

We want to note that, for operators $\hat{f}(\mathbf{x})$ and $\hat{g}(\mathbf{x})$ defined over a region of volume V we have:

$$\int d^3x\, \hat{f}(\mathbf{x})\hat{g}(\mathbf{x}) = \frac{1}{V}\sum_{\mathbf{k}\mathbf{k}'}\int d^3x\, \hat{f}_k e^{i\mathbf{k}\cdot\mathbf{x}}\hat{g}_{k'}e^{i\mathbf{k}'\cdot\mathbf{x}} = \sum_{\mathbf{k}}\hat{f}_{\mathbf{k}}\hat{g}_{-\mathbf{k}} \tag{5.24}$$

where:

$$\hat{f}(\mathbf{x}) = \sum_{\mathbf{k}}\frac{1}{\sqrt{V}}\hat{f}_k e^{i\mathbf{k}\cdot\mathbf{x}}. \tag{5.25}$$

Using the relation given in (5.24) we can write down the full form of the Hamiltonian as:

$$\hat{H} = \sum_{\mathbf{k}}\omega_\psi(\hat{b}^\dagger_{\mathbf{k}}\hat{b}_{\mathbf{k}} + \frac{1}{2}) + \omega_A(\hat{\mathbf{a}}^\dagger_{\mathbf{k}}\cdot\hat{\mathbf{a}}_{\mathbf{k}} + 1) - ig_\psi\frac{1}{2}\sqrt{\frac{\omega_A}{\omega_\psi}}(\hat{b}_{\mathbf{k}} + \hat{b}^\dagger_{-\mathbf{k}})(\mathbf{a}^\dagger_{\mathbf{k}} - \mathbf{a}_{-\mathbf{k}})\cdot\mathbf{B}_0. \tag{5.26}$$

The Hamiltonian in equation (5.26) is quadratic and can be, in principle, exactly diagonalised. However, we will restrict ourselves to the subspaces of n and $n-1$ photon states and 0 and 1 axion states. This restriction simplifies the problem and allows us to capture the key features of axion-photon transitions, as will be shown in the subsequent subsection.

5.2.2 Toy Model of Axion Creation

As a first step in the quantum consideration of our problem, let us consider a simplified model, where we have a two-level axion system. We consider two states, a zero axion state $|0_\psi\rangle$ and a single axion state with momentum $\mathbf{q}$. The zero and one axion subspace lead to the following:

$$\begin{aligned}
\langle 0_\psi|\,\hat{H}\,|0_\psi\rangle &= \sum_{\mathbf{k}}\frac{1}{2}\omega_{\psi_{\mathbf{k}}} + \omega_{A_{\mathbf{k}}}(\hat{\mathbf{a}}^\dagger_{\mathbf{k}}\cdot\hat{\mathbf{a}}_{\mathbf{k}} + 1),\\
\langle \mathbf{q}_\psi|\,\hat{H}\,|0_\psi\rangle &= -ig_\psi\frac{1}{2}\sqrt{\frac{\omega_{A_{\mathbf{q}}}}{\omega_{\psi_{\mathbf{q}}}}}(\hat{\mathbf{a}}^\dagger_{-\mathbf{q}} - \hat{\mathbf{a}}_{\mathbf{q}})\cdot\mathbf{B}_0,\\
\langle 0_\psi|\,\hat{H}\,|\mathbf{q}_\psi\rangle &= -ig_\psi\frac{1}{2}\sqrt{\frac{\omega_{A_{\mathbf{q}}}}{\omega_{\psi_{\mathbf{q}}}}}(\hat{\mathbf{a}}^\dagger_{\mathbf{q}} - \hat{\mathbf{a}}_{-\mathbf{q}})\cdot\mathbf{B}_0,\\
\langle \mathbf{q}_\psi|\,\hat{H}\,|\mathbf{q}_\psi\rangle &= \omega_{\psi_{\mathbf{q}}} + \sum_{\mathbf{k}}\frac{1}{2}\omega_{\psi_{\mathbf{k}}} + \omega_{A_{\mathbf{k}}}(\hat{\mathbf{a}}^\dagger_{\mathbf{k}}\cdot\hat{\mathbf{a}}_{\mathbf{k}} + 1),
\end{aligned} \tag{5.27}$$

where $\omega_{\psi_q} = \sqrt{\mathbf{q}^2 + m_\psi^2}$ and $\omega_{A_q} = |\mathbf{q}|$. We introduce the operator:

$$\hat{a} = \frac{\hat{\mathbf{a}}_q\cdot\mathbf{B}_0}{B_0}, \tag{5.28}$$

where $B_0 = |\mathbf{B}_0|$. We now further restrict the scope of our model by only considering the photon states with momentum $\mathbf{q}$, which allows us to write down the Hamiltonian for our model as:

$$\begin{aligned}
\hat{\mathbb{H}} =&(-\frac{1}{2}\omega_\psi + \omega_A\hat{a}^\dagger\hat{a})\,|\downarrow\rangle\langle\downarrow| + ig_\psi\frac{1}{2}\sqrt{\frac{\omega_A}{\omega_\psi}}\hat{a}B_0\,|\downarrow\rangle\langle\uparrow|\\
&- ig_\psi\frac{1}{2}\sqrt{\frac{\omega_A}{\omega_\psi}}\hat{a}^\dagger B_0\,|\uparrow\rangle\langle\downarrow| + (\frac{1}{2}\omega_\psi + \omega_A\hat{a}^\dagger\hat{a})\,|\uparrow\rangle\langle\uparrow|\,,
\end{aligned} \tag{5.29}$$

where $\langle\uparrow| \equiv \langle \mathbf{q}_\psi|$, $\langle\downarrow| = \langle 0_\psi|$ and the quantities ω_ψ and ω_A are implicitly evaluated at $\mathbf{k} = \mathbf{q}$. It should be noted that (5.29) is equivalent to the Jaynes-Cummings model, a ubiquitous model within quantum optics[75]. Equation (5.29) can be written in matrix form as:

$$\hat{\mathbb{H}} = \omega_0 \hat{a}^\dagger \hat{a} \mathbb{I} + \frac{1}{2} \begin{pmatrix} \epsilon & ig\hat{a} \\ -ig\hat{a}^\dagger & -\epsilon \end{pmatrix}, \tag{5.30}$$

where $g = g_\psi \sqrt{\frac{\omega_A}{\omega_\psi}} B_0$, $\omega_0 = \omega_A$, $\epsilon = \omega_\psi$ and $\mathbb{I}$ is the 2×2 identity matrix. Let us now consider a solution to the Schrödinger equation, given the Hamiltonian given in (5.30), of the form:

$$|\psi\rangle = \alpha(t) \begin{pmatrix} |n-1\rangle \\ 0 \end{pmatrix} + \beta(t) \begin{pmatrix} 0 \\ |n\rangle \end{pmatrix}, \tag{5.31}$$

where $|\alpha|^2 + |\beta|^2 = 1$. Using a standard result from quantum mechanics, which can be found in many introductory textbooks such as [80], we can write down an expression for the coefficients α and β in the following form:

$$\begin{pmatrix} \alpha \\ \beta \end{pmatrix} = e^{-i\omega_0(n-\frac{1}{2})t} \left(e^{-i\frac{\Omega}{2}t} \begin{pmatrix} -i\cos\left(\frac{\theta}{2}\right) \\ \sin\left(\frac{\theta}{2}\right) \end{pmatrix} \sin\left(\frac{\theta}{2}\right) + e^{i\frac{\Omega}{2}t} \begin{pmatrix} i\sin\left(\frac{\theta}{2}\right) \\ \cos\left(\frac{\theta}{2}\right) \end{pmatrix} \cos\left(\frac{\theta}{2}\right) \right), \tag{5.32}$$

where $\Omega = \sqrt{(\epsilon - \omega_0)^2 + g^2 n}$, $\Omega\cos(\theta) = \epsilon - \omega_0$ and $\Omega\sin(\theta) = -g\sqrt{n}$. Finally, the transition probability for a transition from the n - photon / 0 - axion state to a $n-1$ - photon / 1 - axion state is given by:

$$\boxed{|\alpha|^2 = \frac{1}{2}(1 - \cos(\Omega t)) \frac{g^2 n}{(\epsilon - \omega_0)^2 + g^2 n}.} \tag{5.33}$$

Equation (5.33) is analogous to a calculation we shall perform in section 5 of this chapter. A comparison between this result and the result from section 5, will be discussed in the aforementioned section.

5.3 The Axion Driven by a Classical Source

In this section, we will set up the formalism needed to describe a quantum axion field driven by a classical field. This is relevant as it can be used to model axion creation via plasma interactions, without having to invoke quantum effects at the level of the plasma system. The Lagrangian describing the Axion-Electromagnetic system is given by:

$$\boxed{\mathcal{L} = \frac{1}{2}\partial_\mu\psi\partial^\mu\psi - \frac{1}{2}m_\psi^2\psi^2 - \frac{1}{4}F_{\mu\nu}F^{\mu\nu} - \frac{1}{4}g_\psi\psi F_{\mu\nu}\widetilde{F}^{\mu\nu},} \tag{5.34}$$

where ψ is the axion pseudo-scalar field, $F^{\mu\nu}$ is the electromagnetic tensor, $\widetilde{F}^{\mu\nu}$ is the dual electromagnetic tensor and g_ψ is the axion-photon coupling constant. The equation of motion for the

axion field is given by:

$$\boxed{\partial_t^2\psi - \nabla^2\psi + m_\psi^2\psi = -g_\psi \mathbf{E}\cdot\mathbf{B}.} \tag{5.35}$$

For the purposes of the calculation, we treat the electromagnetic field as a classical source for the axions, and only give the quantum treatment to the axion particles.

5.3.1 Classical Field Solution

Before we move on to the quantum theory of the problem, it would be instructive to consider the classical field theory first. A comprehensive treatment of the classical case can be found in [66], but here we will state some of the basic results. We start by considering a sourced Klein-Gordon equation:

$$\partial_t^2\psi - \nabla^2\psi + m_\psi^2\psi = \rho, \tag{5.36}$$

where $\rho \equiv \rho(\mathbf{x}, t)$ is a source term. Let us assume the initial conditions of the form:

$$\begin{aligned} \psi(\mathbf{x}, 0) &= 0, \\ \partial_t\psi(\mathbf{x}, 0) &= 0. \end{aligned} \tag{5.37}$$

Assuming that the field is "trapped" in a finite volume i.e. has compact support on a subset of $\mathbb{R}^3$, we can expand the axion field as a Fourier series:

$$\psi(\mathbf{x}, t) = \sum_{\mathbf{k}} \frac{1}{\sqrt{V}}\psi_{\mathbf{k}}(t)e^{i\mathbf{k}\cdot\mathbf{x}}. \tag{5.38}$$

This then lets us obtain a differential equation for the individual modes of the axion field:

$$\frac{d^2}{dt^2}\psi_{\mathbf{k}} + \omega_{\mathbf{k}}^2\psi_{\mathbf{k}} = \rho_{\mathbf{k}}, \tag{5.39}$$

which is solved by:

$$\psi_{\mathbf{k}}(t) = \int_{t_i}^{t} dt^{'} \frac{\sin\Big(\omega_{\mathbf{k}}(t - t^{'})\Big)}{\omega_{\mathbf{k}}}\rho_{\mathbf{k}}(t^{'}), \tag{5.40}$$

where $\omega_{\mathbf{k}} = \sqrt{m_\psi^2 + k^2}$. We are interested in the momentum flux of an axion field coming out of the plasma. To calculate this, we first consider the stress energy tensor for the free axion field, which is given by:

$$T_{\mu\nu} = \partial_\mu\psi\partial_\nu\psi - \frac{1}{2}(\eta^{\lambda\omega}\partial_\lambda\psi\partial_\omega\psi - m_\psi^2\psi^2)\eta_{\mu\nu}. \tag{5.41}$$

Now the momentum flux is given by T_{0j}, which evaluates to:

$$T_{0j} = \partial_t\psi\partial_j\psi. \tag{5.42}$$

The total momentum is then given by:

$$\mathbf{P} = \int d^3x \partial_t \psi \nabla \psi. \tag{5.43}$$

We can use the solution to the classical equation of motion from (5.40) to directly compute the total momentum:

$$\mathbf{P} = \sum_{\mathbf{k}} \mathbf{k} \frac{\mid \rho^*_{\mathbf{k}}(\omega_{\mathbf{k}}) \mid^2}{2\omega_{\mathbf{k}}}, \tag{5.44}$$

where the second tilde denotes a Fourier transform in time, i.e.:

$$f_{\mathbf{k}}(\omega_{\mathbf{k}}) = \int dt f_{\mathbf{k}}(t) e^{-i\omega_{\mathbf{k}} t}. \tag{5.45}$$

5.3.2 Coherent States of the Axion Field

5.3.2.1 The Hamiltonian

If we consider the EM-axion action, coupled to a generic source term ρ, we can construct a Hamiltonian for the system:

$$\hat{H} = \int d^3x : \frac{1}{2}\hat{\Pi}^2 + \frac{1}{2}(\nabla\hat{\psi})^2 + \frac{1}{2}m_\psi^2\hat{\psi}^2 + \hat{\psi}\rho :, \tag{5.46}$$

where :: denotes normal ordering and $\hat{\Pi}$ is the canonical momentum operator. The operators $\hat{\psi}(\mathbf{x}, t)$ and $\hat{\Pi}(\mathbf{x}, t)$ satisfy the equal time canonical commutation relations:

$$\begin{aligned} [\hat{\psi}(\mathbf{x}), \hat{\psi}(\mathbf{x}')] &= 0, \\ [\hat{\Pi}(\mathbf{x}), \hat{\Pi}(\mathbf{x}')] &= 0 \\ [\hat{\psi}(\mathbf{x}), \hat{\Pi}(\mathbf{x}')] &= i\delta(\mathbf{x} - \mathbf{x}') \end{aligned} \tag{5.47}$$

If we once again assume a finite volume then we can expand $\hat{\psi}$ and $\hat{\Pi}$ as a Fourier series:

$$\begin{aligned} \hat{\psi}(\mathbf{x}, t) &= \sum_{\mathbf{k}} \frac{1}{\sqrt{2\omega_k V}} (\hat{b}_{\mathbf{k}}(t) e^{i\mathbf{k}\cdot\mathbf{x}} + \hat{b}^\dagger_{\mathbf{k}}(t) e^{-i\mathbf{k}\cdot\mathbf{x}}), \\ \hat{\Pi}(\mathbf{x}, t) &= -i \sum_{\mathbf{k}} \sqrt{\frac{\omega_{\mathbf{k}}}{2V}} (\hat{b}_{\mathbf{k}}(t) e^{i\mathbf{k}\cdot\mathbf{x}} - \hat{b}^\dagger_{\mathbf{k}}(t) e^{-i\mathbf{k}\cdot\mathbf{x}}). \end{aligned} \tag{5.48}$$

The Hamiltonian is then expressed by:

$$\hat{H} = \sum_{\mathbf{k}} \left(\omega_{\mathbf{k}} \hat{b}^\dagger_{\mathbf{k}} \hat{b}_{\mathbf{k}} - \frac{1}{\sqrt{2\omega_{\mathbf{k}}}} (\hat{b}_{\mathbf{k}} + \hat{b}^\dagger_{-\mathbf{k}}) \rho^*_{\mathbf{k}} \right), \tag{5.49}$$

where $\rho(\mathbf{x}, t) = \sum_{\mathbf{k}} \frac{1}{\sqrt{V}} \rho_{\mathbf{k}} e^{i\mathbf{k}\cdot\mathbf{x}}$. Since ρ is real, we have $\rho^*_{\mathbf{k}} = \rho_{-\mathbf{k}}$, it then follows that the Hamiltonian can be re-written as:

$$\hat{H} = \sum_{\mathbf{k}} \left(\omega_{\mathbf{k}} \hat{b}^\dagger_{\mathbf{k}} \hat{b}_{\mathbf{k}} - \frac{1}{\sqrt{2\omega_{\mathbf{k}}}} (\hat{b}_{\mathbf{k}} \rho^*_{\mathbf{k}} + \hat{b}^\dagger_{\mathbf{k}} \rho_{\mathbf{k}}) \right). \tag{5.50}$$

5.3.2.2 Coherent State Path Integral

For the purposes of our calculation, we can consider the case of a quantum mechanical system of a forced harmonic oscillator. Within the field of quantum optics, it is a well-known result that a classical source driving the vacuum state of a harmonic oscillator generates a coherent state (this can be found in most quantum optics textbooks, such as [75]). In anticipation of this, we will use the coherent state path integral formalism in order to calculate the form of the coherent state generated by the classical source. This is equivalent to doing the calculation for a single mode of a quantum field theory; therefore, generalising this result will be quite straightforward.

Now, let us consider the transition function $0 \to n$ for a time interval $[t_i, t_f]$ for a system of a forced harmonic oscillator. It is well established that coherent states can be used to generate number states, and as such, we can write transition function as:

$$\langle n, t_f | 0, t_i \rangle = \frac{1}{\sqrt{n!}} \left(\frac{\partial}{\partial z_f^*} \right)^n \langle z_f^*, t_f \big| 0, t_i \rangle |_{z_f^*=0}, \tag{5.51}$$

where $\left\langle z_f^*, t \middle| z_i, t \right\rangle$ is the amplitude for the transition from the coherent state with index z_i at t_i to a coherent state with index z_f at t_f. This then gives us motivation to evaluate the coherent state path integral for our system

$$\langle z_f^*, t_f \big| 0, t_i \rangle = \int \mathcal{D}z \mathcal{D}z^* e^{iS[z,z^*]}. \tag{5.52}$$

For our case of the forced harmonic oscillator the transition function simply evaluates to:

$$\langle z_f^*, t_f \big| 0, t_i \rangle = e^{iS[z_c, z_c^*]}, \tag{5.53}$$

This result can be found in [81]. The action is of the form:

$$iS[z, z^*] = z^* z(t_f) - \int_{t_i}^{t_f} dt (z^* \dot{z} + iH(z^*, z)), \tag{5.54}$$

with the Hamiltonian of the form:

$$H = \omega z^* z - \frac{z^* \varrho}{\sqrt{2\omega}} - \frac{z \varrho^*}{\sqrt{2\omega}}. \tag{5.55}$$

In order to evaluate the classical action $S[z_c, z_c^*]$ we need to solve the Euler-Lagrange equations to find z_c , z_c^*. The E-L equations yield a pair of ODE's:

$$\begin{aligned} \dot{z}_c + i\omega z_c - \frac{i\varrho}{\sqrt{2\omega}} = 0, \\ \dot{z}_c^* - i\omega z_c^* + \frac{i\varrho^*}{\sqrt{2\omega}} = 0, \end{aligned} \tag{5.56}$$

The boundary conditions for (5.56) are simply $z_c(t_i) = z_i$ and $z_c(t_f) = z_f$. Equations (5.56), when solved, allow us to write down the classical action explicitly:

$$\begin{aligned} iS[z_c, z_c^*] &= z_f^* z_i e^{-i\omega(t_f - t_i)} \\ &+ i\int_{t_i}^{t_f} dt \frac{1}{\sqrt{2\omega}}(z_f^* \varrho(t) e^{-i\omega(t_f - t)} + z_i \varrho^*(t) e^{-i\omega(t - t_i)}) \\ &- \frac{1}{2\omega}\int_{t_i}^{t_f} dt \int_{t_i}^{t} dt^{'} \varrho(t^{'}) \varrho^*(t) e^{-i\omega(t - t^{'})}. \end{aligned} \tag{5.57}$$

With the classical action written out in explicit form, we can now evaluate the transition function:

$$\begin{aligned} \langle n, t_f | 0, t_i \rangle &= \frac{1}{\sqrt{n!}} \left(\frac{i}{\sqrt{2\omega}} \int_{t_i}^{t_f} dt e^{-i\omega(t_f - t)} \varrho(t) \right)^n \exp\left(-\frac{1}{2} \frac{\mid \varrho^*(\omega) \mid^2}{2\omega} \right) \exp(i\phi) \\ &= \frac{1}{\sqrt{n!}} \left(\frac{i}{\sqrt{2\omega}} e^{-i\omega t_f} \varrho^*(\omega)^* \right)^n \exp\left(-\frac{1}{2} \frac{\mid \varrho^*(\omega) \mid^2}{2\omega} \right) \exp(i\phi), \end{aligned} \tag{5.58}$$

where ϕ is a global phase factor, and is thus neglected. Additionally we note that: $\varrho^*(\omega)^* = \int_{t_i}^{t_f} dt e^{i\omega t} \varrho^*$.

We can use this result to find the coherent state that will be generated via the classical source, as mentioned in the beginning of the subsection. To do this, we note that we can expand the vacuum state at time t_i in the basis of $|n, t_f\rangle$. This is expressed as:

$$\begin{aligned} |0, t_i\rangle &= \sum_n |n, t_f\rangle \langle n, t_f | 0, t_i \rangle \\ &= \exp(i\phi) \exp\left(-\frac{1}{2} \frac{\mid \varrho^*(\omega) \mid^2}{2\omega} \right) \exp\left(\frac{i}{\sqrt{2\omega}} e^{-i\omega t_f} \varrho^*(\omega)^* \hat{a}^\dagger(t_f) \right) |0, t_f\rangle. \end{aligned} \tag{5.59}$$

Applying an annihilation operator at time t_f to (5.59) gives:

$$\hat{a}(t_f) |0, t_i\rangle = \frac{i}{\sqrt{2\omega}} e^{-i\omega t_f} \varrho^*(\omega)^* |0, t_i\rangle, \tag{5.60}$$

which shows us that the time-evolved state is a coherent state. Coherent states are the eigenstates of the annihilation operator.

With the result for the quantum mechanical case obtained, we can "translate" our result into the language of an axion field driven by a classical source. We identify the driving term ϱ as:

$$\varrho = \rho_{\mathbf{k}}(t) = \frac{1}{\sqrt{V}} \int d^3x \rho(\mathbf{x}, t) e^{-i\mathbf{k}\cdot\mathbf{x}}. \tag{5.61}$$

This means that :

$$\begin{aligned} \varrho^* &= \rho_{\mathbf{k}}^*(\omega) \\ \mid \varrho^* \mid &= \mid \rho_{\mathbf{k}}^*(\omega) \mid. \end{aligned} \tag{5.62}$$

Therefore the action of the annihilation operator $\hat{a}_{\mathbf{k}}(t_f)$ on the initial axion vacuum state $|0, t_i\rangle$ leads to a coherent state of the form:

$$\boxed{\hat{a}_{\mathbf{k}}(t_f)\,|0,t_i\rangle = \frac{i}{\sqrt{2\omega}} e^{-i\omega t_f}\rho^*_{\mathbf{k}}(\omega)^*\,|0,t_i\rangle\,.} \tag{5.63}$$

5.4 The ALP Flux

The physical quantity that we are interested in calculating is the particle flux of the ALPs. Performing such a calculation will allow us to compare our estimates to those of solar axions, thus showing the viability of a terrestrial laboratory approach. The stress-energy tensor contains information about the energy and momentum flux of the axion field. To consider the stress energy tensor in a Quantum Field Theory context, we need to impose some form of ordering on the operator. The simplest choice for it is to use normal ordering i.e. $: \hat{T}^{\mu\nu} :$. We can define a "total energy" tensor $\mathcal{E}^{\mu\nu}$ for the purposes of trying to analyse the total energy-momentum of the ALP field we could expect in a laser-plasma experiment. We define $\mathcal{E}^{\mu\nu}$ to be:

$$\boxed{\mathcal{E}^{\mu\nu} = \lim_{T\to\infty}\frac{1}{T}\int_t^{t+T} dt' \int d^3x\,\langle 0,t_i| : \hat{T}^{\mu\nu}(\mathbf{x},t') : |0,t_i\rangle\,,} \tag{5.64}$$

where $t > t_f$ with t_f being the time at which ρ vanishes. The time integral is introduced to remove oscillatory terms in the space-space components. A more thorough explanation is included in Appendix D.3. We can evaluate (5.64) for our set up, to give us:

$$\mathcal{E}^{\mu\nu} = \sum_{\mathbf{k}} \frac{k^\mu k^\nu}{\omega_{\mathbf{k}}}\frac{1}{2\omega_{\mathbf{k}}}\mid \rho^*_{\mathbf{k}}(\omega_{\mathbf{k}})\mid^2, \tag{5.65}$$

where $k^\mu = (\omega_{\mathbf{k}}, \mathbf{k})$ and $\omega_{\mathbf{k}} = \sqrt{m^2 + \mathbf{k}^2}$.

5.4.1 The Infinite Volume Limit and Moments

In order to evaluate $\mathcal{E}^{\mu\nu}$, we will have to take the limit as $V \to \infty$, so that we can evaluate an integral rather than an infinite series. We invoke relation (5.24):

$$\int d^3x \hat{f}(\mathbf{x})\hat{g}(\mathbf{x}) = \sum_{\mathbf{k}} \hat{f}_{\mathbf{k}}\hat{g}_{-\mathbf{k}} = \sum_{\mathbf{k}} \frac{1}{V}\sqrt{V}\hat{f}_{\mathbf{k}}\sqrt{V}\hat{g}_{-\mathbf{k}}. \tag{5.66}$$

The transition to the infinite volume ($V \to \infty$) then involves us making the substitutions:

$$\sum_{\mathbf{k}} \frac{1}{V} \to \int đ^3k, \tag{5.67}$$

$$\sqrt{V}\hat{f}_{\mathbf{k}} \to \hat{f}(\mathbf{k}), \tag{5.68}$$

where $\not{d}^n k = \frac{d^n k}{(2\pi)^n}$. Equation (5.65) in the infinite volume limit then becomes:

$$\mathcal{E}^{\mu\nu} = \int \not{d}^3 k \frac{k^\mu k^\nu}{\omega_k} \frac{1}{2\omega_k} \mid \rho^*(\omega_k) \mid^2, \tag{5.69}$$

which is one of our main results. Since the frequency term $\omega_{\mathbf{k}}$ only depends on the magnitude of the vector $k = |\mathbf{k}|$, we will denote it as ω_k from now on. We quickly note that we can now express the term inside the modulus bracket as:

$$\rho^*(\omega_k, \mathbf{k}) = \int_{t_i}^{t_f} dt \int d^3x \rho(\mathbf{x}, t) e^{i(\mathbf{k}\cdot\mathbf{x} - \omega_k t)}. \tag{5.70}$$

The structure of $\mathcal{E}^{\mu\nu}$ can be interpreted as a second-order moment integral, which motivates us to define a more general object, an n^{th} order moment integral.

$$\boxed{\mathcal{E}^{\mu\ldots\nu} = \int \not{d}^3 k \frac{k^\mu \ldots k^\nu}{\omega_k} \frac{1}{2\omega_k} \left| \int_{t_i}^{t_f} dt \int d^3x \rho(\mathbf{x}, t) e^{i(\mathbf{k}\cdot\mathbf{x} - \omega_k t)} \right|^2} \tag{5.71}$$

$\mathcal{E}^{\mu\nu}$ can be interpreted as containing information about the energy and momentum of the axion field and the first order moment $\mathcal{E}^\mu$ can then be interpreted as a particle number 4-vector.

5.4.2 Computation

In order to compute $\mathcal{E}^{\mu\nu}$ and $\mathcal{E}^\mu$ we will need to specify the form our source will take. We will prescribe the form of the source term from the analysis of plasma waves.

5.4.2.1 Plasma Wave Dynamics

For the purposes of this calculation, we will be following the prescriptions given in [82] and [66]. In the description of the plasma, we neglect the dynamics of the ions and assume that the electron fluid is pressureless (cold plasma approximation). The electron fluid satisfies:

$$\partial_t \mathbf{p} + (\mathbf{u} \cdot \nabla)\mathbf{p} = -e(\mathbf{E} + \mathbf{u} \times \mathbf{B}), \tag{5.72}$$

where e is the elementary charge, $\mathbf{u}$ is the electron fluid 3-velocity and $\mathbf{p}$ is the electron fluid 3-momentum given by:

$$\mathbf{p} = \frac{m_e \mathbf{u}}{\sqrt{1 - \mathbf{u}^2}}, \tag{5.73}$$

where m_e is the electron mass. We also note that the charge density of the ions ρ_0 is uniform in this treatment; thus we can write down the expressions for charge density ρ and electron currents $\mathbf{J}$:

$$\rho = \rho_0 + \rho_e, \qquad \mathbf{J} = \rho_e \mathbf{u}, \tag{5.74}$$

where ρ_e is the charge density of the plasma electrons. The focus of this specific calculation lies within the analysis of a nonlinear electron density wave in a magnetized plasma driving the creation

of ALPs. In this setup, the density wave travels parallel to an externally applied uniform magnetic field with field strength B. In order to make this calculation tractable we will restrict ourselves to the case where all of the fields depend on only one co-ordinate $\zeta = z - vt$, where ζ is the phase of the plasma wave and v is the associated phase velocity satisfying $0 < v < 1$. Furthermore we express the electron fluid momentum $p(\zeta)$ in terms in terms of a dimensionless function $\xi(\zeta)$ as:

$$p = m_e\gamma(v\xi - \sqrt{\xi^2 - 1}) \tag{5.75}$$

where γ is the Lorentz factor $\gamma = \frac{1}{\sqrt{1-v^2}}$. We note that $m_e\xi$ corresponds to the energy of the plasma electrons in the inertial frame which is moving with velocity v along the z coordinate. This naturally introduces the condition $\xi > 1$. Given $p(\xi)$, we can use (5.73) to express the z component of the electron fluid 3-velocity $\mathbf{u}_z = u$ as:

$$u = \frac{v\xi - \sqrt{\xi^2 - 1}}{\xi - v\sqrt{\xi^2 - 1}}. \tag{5.76}$$

Using (5.76) we can write (5.72) as:

$$E = -\frac{m_e}{\gamma e}\xi'. \tag{5.77}$$

We now introduce an expression for the EM-Plasma-Axion system:

$$\left[\frac{1}{2}E^2 - \frac{1}{2}(\frac{\psi'^2}{\gamma^2} - m_\psi^2\psi^2) - \frac{m_e\gamma\rho_0}{e}(v\sqrt{\xi^2 - 1} - \xi)\right]' = 0, \tag{5.78}$$

which is the first integral of the system which we will derive in Appendix D.1. In order to obtain a relation for the non-linear plasma wave, we neglect the effect of the axions by ignoring $\mathcal{O}(g_\psi^2)$ terms. Using the fact that B is constant and equations (5.77) and (5.78), we obtain an ODE that captures the dynamics of the non-linear plasma wave:

$$\frac{d\xi}{d\zeta} = \sqrt{2\gamma^3}\omega_p\sqrt{v\sqrt{\xi^2 - 1} - \xi + 1}. \tag{5.79}$$

Equation (5.79) is formally solved in terms of the phase $\zeta(\xi)$ by:

$$\zeta(\xi) = \frac{1}{\sqrt{2\gamma^3}\omega_p}\int_1^\xi \frac{1}{(v\sqrt{\chi^2 - 1} - \chi + 1)^{\frac{1}{2}}}d\chi, \tag{5.80}$$

where we have chosen $\zeta(1) = 0$. In the ultra-relativistic limit (see Appendix D.2), i.e. $\gamma \gg 1$, we find the solution:

$$\zeta(\xi) = \sqrt{\frac{\gamma}{2}}\frac{4}{\omega_p}\left(1 - \sqrt{1 - \frac{\xi}{2\gamma^2}}\right). \tag{5.81}$$

From inspecting equation (5.79) at the turning point $\frac{d\xi}{d\zeta} = 0$, we can immediately find that the minimum and maximum values of ξ are $\xi_{\min} = 1$ and $\xi_{\max} = \gamma^2(1 + v^2)$ respectively. Using this,

we can find the period length l:

$$l = 2\zeta|_1^{\gamma^2(1+v^2)} \approx \frac{4\sqrt{2\gamma}}{\omega_p}. \tag{5.82}$$

We can now invert equation (5.81) to arrive at an expression for ξ in terms of ζ:

$$\xi(\zeta) \approx 8\gamma^2 \frac{\zeta}{l}(1 - \frac{\zeta}{l}) \text{ for } 0 \leq \zeta \leq l. \tag{5.83}$$

Later on in this calculation, we will want to use a Fourier series representation of $\xi(\zeta)$. In anticipation of that task we can find the coefficients of the Fourier expansions as such:

$$\xi_n = \frac{1}{l}\int_0^l e^{-i\frac{2\pi n\zeta}{l}}\xi(\zeta)d\zeta \approx \begin{cases} \frac{4\gamma^2}{3} & \text{for } n = 0 \\ -\frac{4\gamma^2}{\pi^2 n^2} & \text{for } n \neq 0 \end{cases}. \tag{5.84}$$

5.4.2.2 Structure of the Source function

Finally, we shall prescribe the form of the source function. To capture the scenario of axions leaving the plasma, we introduce a temporal cut-off in the source via a step function:

$$\rho(\mathbf{x}, t) = \Theta(-t) g_\psi \mathbf{E} \cdot \mathbf{B}, \tag{5.85}$$

where $\Theta(-t)$ is the step function. In the previous section, we have specified that $\mathbf{B}$ is constant and applied along the z direction, i.e. $\mathbf{B} = B\hat{\mathbf{z}}$. We also have determined in the previous section that one can express $\mathbf{E} = E(\zeta)\hat{\mathbf{z}}$, which leads to an expression for the source term (visualised in Figure 5.1) of the form:

$$\rho(\mathbf{x}, t) = g_\psi B \Theta(-t) E(\zeta). \tag{5.86}$$

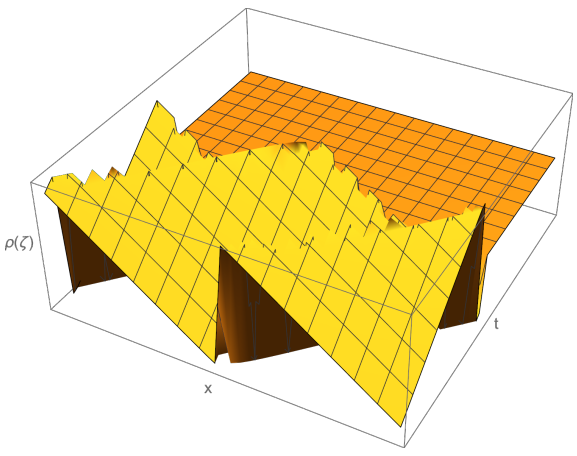

Figure 5.1: An illustration of the plot of equation. (5.86)

5.4.2.3 Calculating $\mathcal{T}^{00}$.

We need to evaluate the integral:

$$\int_{t_i}^{t_f} dt \int d^3x \rho(\mathbf{x}, t) e^{i(\mathbf{k}\cdot\mathbf{x} - \omega_k t)}, \tag{5.87}$$

where we now also want to take $t_i \to -\infty$ and $t_f \to \infty$. This then allows us to write the integral as:

$$\int d^4x \rho(\mathbf{x}, t) e^{i(\mathbf{k}\cdot\mathbf{x} - \omega_k t)}. \tag{5.88}$$

Applying all the results from the previous section, we can use (5.85) and the result:

$$\int dt \Theta(t) e^{-i\omega t} = \pi\delta(\omega) + \frac{i}{\omega}, \tag{5.89}$$

to write (5.88) as:

$$g_\psi B \int d^4x \Theta(-t) E(\zeta) e^{i(\mathbf{k}\cdot\mathbf{x} - \omega_k t)} = g_\psi B \bar{\delta}^{(2)}(\mathbf{k}_\perp) E(k_\parallel)^* \frac{i}{\omega_k - k_\parallel v}, \tag{5.90}$$

where $\bar{\delta}^n = (2\pi)^n \delta^n$. We used the fact that $\omega_k - k_\parallel v > 0$, which eliminates the delta function term in the Fourier transform of $\Theta(t)$. We now take the modulus square of the right-hand side of equation (5.90):

$$\left| g_\psi B \bar{\delta}^{(2)}(\mathbf{k}_\perp) E(k_\parallel)^* \frac{i}{\omega_k - k_\parallel v} \right|^2 = g_\psi^2 B^2 A \bar{\delta}^{(2)}(\mathbf{k}_\perp) \mid E(k_\parallel) \mid^2 \frac{1}{(\omega_k - k_\parallel v)^2}, \tag{5.91}$$

where we set $A = \bar{\delta}^{(2)}(0)$ as a formally infinite area factor which follows from $\bar{\delta}^{(2)}(\mathbf{k}_\perp) = \int dx dy \, e^{-i\mathbf{k}_\perp \cdot \mathbf{x}_\perp}$, with $\mathbf{x}_\perp = (x, y)$. We will circumvent the issue of this type of infinity by "dividing out" any infinite factors that come from the fact that we are working with an infinite volume. The expression for $\mathcal{E}^{\mu\nu}$ is then given as:

$$\mathcal{E}^{\mu\nu} = \int \bar{d}^3k \frac{k^\mu k^\nu}{\omega_k} \frac{1}{2\omega_k} A g_\psi^2 B^2 \bar{\delta}^{(2)}(\mathbf{k}_\perp) \mid E(k_\parallel) \mid^2 \frac{1}{(\omega_k - k_\parallel v)^2}, \tag{5.92}$$

where $E(k_\parallel) = \int_{-\infty}^{+\infty} d\zeta E(\zeta) e^{-ik_\parallel \zeta}$. We now look at individual components of $\mathcal{E}^{\mu\nu}$ in order to look at the total energy and the momentum flux of the axion field.

Firstly, we look at the $\mathcal{E}^{00}$ component. The integral will have the form of:

$$\mathcal{E}^{00} = \frac{1}{2} A \int \bar{d}^3k g_\psi^2 B^2 \bar{\delta}^{(2)}(\mathbf{k}_\perp) \mid E(k_\parallel) \mid^2 \frac{1}{(\omega_k - k_\parallel v)^2}, \tag{5.93}$$

We can immediately integrate out the delta function to give us:

$$\mathcal{E}^{00} = \frac{1}{2} A g_\psi^2 B^2 \int \bar{d}k_\parallel \mid E(k_\parallel) \mid^2 \frac{1}{(\omega_k - k_\parallel v)^2}, \tag{5.94}$$

where $\omega_k = \sqrt{k_\parallel^2 + m_\psi^2}$ because the delta function sets $\mathbf{k}_\perp = 0$. To progress with our calculation, we need to express $E(\zeta)$ using Fourier series :

$$E(\zeta) = \sum_n E_n e^{i\frac{2\pi n}{l}\zeta}, \tag{5.95}$$

where l denotes the period of the saw-tooth wave. With that in mind $E(k_\parallel)$ is expressed:

$$\begin{aligned} E(k_\parallel) &= \int d\zeta E(\zeta) e^{-ik\zeta} \\ &= \int d\zeta \sum_n E_n e^{i\frac{2\pi n}{l}\zeta} e^{-ik\zeta} \\ &= \sum_n E_n \int d\zeta e^{i(\frac{2\pi n}{l} - k_\parallel)\zeta} \\ &= \sum_n E_n \eth\left(k_\parallel - \frac{2\pi n}{l}\right). \end{aligned} \tag{5.96}$$

Taking the modulus squared of $E(k_\parallel)$ gives:

$$\mid E(k_\parallel) \mid^2 = \sum_n \sum_{n'} E_n E_{n'}^* \eth\left(k_\parallel - \frac{2\pi n}{l}\right) \eth\left(k_\parallel - \frac{2\pi n^{'}}{l}\right). \tag{5.97}$$

Hence,

$$\int đk_\parallel \frac{\left|E(k_\parallel)\right|^2}{(\omega_k - k_\parallel v)^2} = \sum_n \sum_{n'} \frac{E_n E_{n'}^*}{(\omega_k - k_\parallel v)^2} \eth\left(\frac{2\pi n^{'}}{l} - \frac{2\pi n}{l}\right). \tag{5.98}$$

The delta function has imposed the relation $k_\parallel = \frac{2\pi n}{l}$. Substituting (5.98) into equation (5.94) we arrive at an expression for $\mathcal{E}^{00}$:

$$\mathcal{E}^{00} = V\frac{1}{2} g_\psi^2 B^2 \sum_n \mid E_n \mid^2 \frac{1}{(\omega_k - k_\parallel v)^2}, \tag{5.99}$$

because $\eth(\frac{2\pi(n'-n)}{l}) = L\delta_{nn'}$ where $L = \frac{V}{A} = \eth(0)$ is the (formally infinite) length of the domain. We recall that equation (5.77) gives an expression for the electric field in terms of ξ i.e. $E = -\frac{m_e}{\gamma e}\xi'$. With that in mind, we can relate E_n with ξ_n:

$$E_n = -\frac{2i\pi n m_e}{\gamma e l}\xi_n. \tag{5.100}$$

We can combine equations (5.99), (5.84) and (5.82) to express $\mathcal{E}^{00}$ as:

$$\mathcal{E}^{00} = V\sum_{n\neq 0} \frac{g_\psi^2 B^2 m_e^2 \omega_p^2 \gamma}{e^2\pi^2} \frac{1}{n^2} \frac{1}{\left(\sqrt{\frac{\omega_p^2\pi^2}{8\gamma}n^2 + m_\psi^2} - v\frac{\omega_p \pi}{\sqrt{8\gamma}}n\right)^2}. \tag{5.101}$$

Considering that the term outside of the summation in the expression for $\mathcal{E}^{00}$ is formally infinite, we want to introduce a finite object. We do this by dividing out the formally infinite volume term

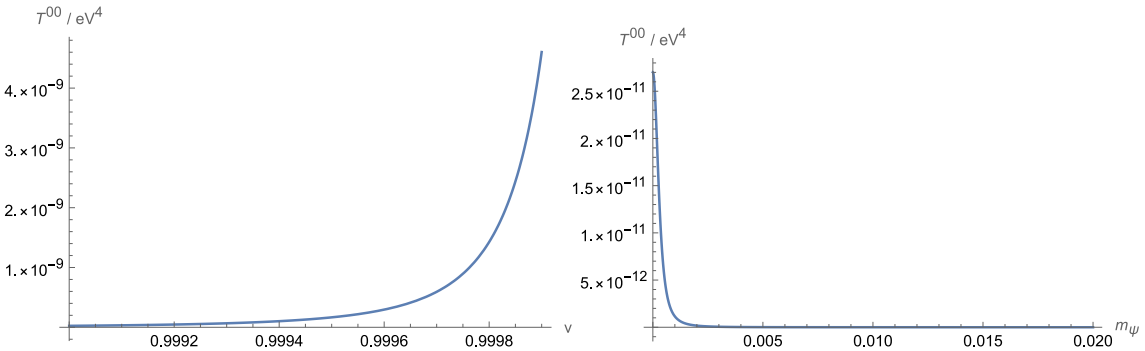

(a) $\mathcal{T}^{00}$ vs v (b) $\mathcal{T}^{00}$ vs m_ψ

Figure 5.2: Plots of the $\mathcal{T}^{00}$ component against the wake velocity and axion mass. The relevant physical parameters are $g_\psi = 0.66 \times 10^{-19}\text{eV}$, $B = 7 \times 10^3\text{eV}^2$ ($B \approx 35T$), $\omega_p = 4.12 \times 10^{-2}\text{eV}$. The choice $m_\psi = 10^{-4}\text{eV}$ is made in plot (a), whilst $v = 0.995$ is made in plot (b).

V to arrive at an expression for the stress-energy tensor:

$$\mathcal{T}^{\mu\nu} = \frac{\mathcal{E}^{\mu\nu}}{V}. \tag{5.102}$$

We can now write down a cleaned-up expression:

$$\mathcal{T}^{00} = C \sum_{n\neq 0} \frac{1}{n^2 \left(\sqrt{A^2n^2 + m_\psi^2} - vAn\right)^2}, \tag{5.103}$$

where $C = \frac{g_\psi^2 B^2 m_e^2 \omega_p^2 \gamma}{e^2\pi^2}$ and $A = \frac{\omega_p \pi}{\sqrt{8\gamma}}$. This can be further split up into:

$$\mathcal{T}^{00} = C \sum_{n=1}^{\infty} \left(a_n + b_n\right), \tag{5.104}$$

where:

$$\begin{aligned} a_n &= \frac{1}{n^2 \left(\sqrt{A^2n^2 + m_\psi^2} - vAn\right)^2}, \\ b_n &= \frac{1}{n^2 \left(\sqrt{A^2n^2 + m_\psi^2} + vAn\right)^2}. \end{aligned} \tag{5.105}$$

Equation (5.104) is plotted in Figure 5.2. Finally, we note that one can easily find a general expression for an n^{th} order tensor as:

$$\boxed{\mathcal{T}^{\mu\ldots\nu} = \frac{\mathcal{E}^{\mu\ldots\nu}}{V} = \frac{1}{2} g_\psi^2 B^2 \sum_n \mid E_n \mid^2 \frac{k^\mu \ldots k^\nu}{\omega_k^2} \frac{1}{(\omega_k - k_\parallel v)^2}.} \tag{5.106}$$

5.4.2.4 Calculating $\mathcal{T}^{03}$

Having calculated $\mathcal{E}^{00}$, which can be thought of as corresponding to the energy density of the axion field, we now want to focus on the momentum density in the propagation direction i.e. $\mathcal{E}^{03}$. It is

given by:

$$\mathcal{E}^{03} = V\frac{1}{2}g_\psi^2 B^2 \sum_n \mid E_n \mid^2 \frac{k_\parallel}{\omega_k}\frac{1}{(\omega_k - k_\parallel v)^2}, \tag{5.107}$$

this can be re-written as:

$$\mathcal{E}^{03} = V g_\psi^2 B^2 \sum_n \mid E_n \mid^2 \frac{k_\parallel^2 v}{(\omega_k^2 - k_\parallel^2 v^2)^2}. \tag{5.108}$$

which then allows to compute $\mathcal{T}^{03}$:

$$\mathcal{T}^{03} = A\sum_{n\neq 0}\frac{1}{(n^2+s^2)^2}, \tag{5.109}$$

where $A = \frac{16 g_\psi^2 B^2 m_e^2 v\gamma^6}{\pi^4 e^2}$ and $s = \frac{m_\psi 2\sqrt{2}\gamma^{\frac{3}{2}}}{\pi\omega_p}$. We can express the infinite sum in (5.109) as:

$$\sum_{n\neq 0}\frac{1}{(n^2+s^2)^2} = \frac{\pi(\pi\coth^2(\pi s)s - \pi s + \coth(\pi s))}{2s^3} - \frac{1}{s^4}, \tag{5.110}$$

which in turn leads to the final expression:

$$\mathcal{T}^{03} = \frac{16 g_\psi^2 B^2 m_e^2 v\gamma^6}{\pi^4 e^2}\left(\frac{\pi(\pi\coth^2(\pi s)s - \pi s + \coth(\pi s))}{2s^3} - \frac{1}{s^4}\right). \tag{5.111}$$

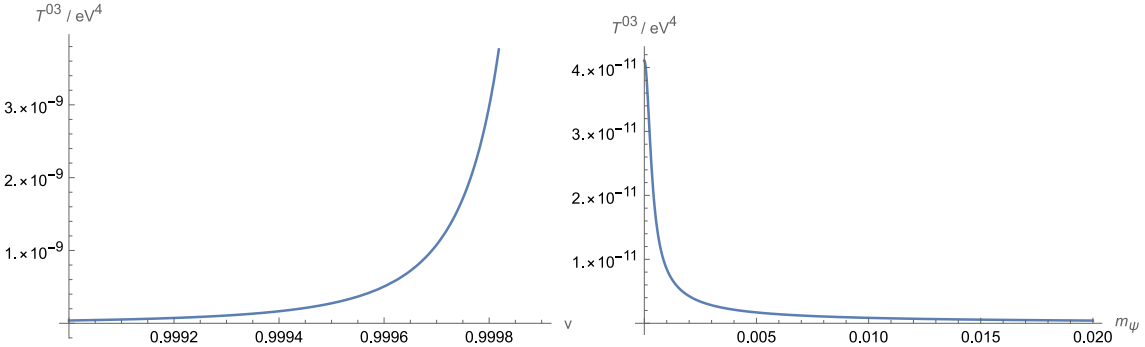

(a) $\mathcal{T}^{03}$ vs v (b) $\mathcal{T}^{03}$ vs m_ψ

Figure 5.3: Plots of the $\mathcal{T}^{03}$ component against the wake velocity and axion mass. The relevant physical parameters are $g_\psi = 0.66 \times 10^{-19}$eV, $B = 7 \times 10^3$eV^2 ($B \approx 35T$), $\omega_p = 4.12 \times 10^{-2}$eV. The choice $m_\psi = 10^{-4}$eV is made in plot (a), whilst $v = 0.995$ is made in plot (b).

Equation (5.111) is plotted in Figure 5.3. This result is analogous to the axion momentum flux calculated in [59].

5.4.2.5 Calculating $\mathcal{T}^0$

The $\mathcal{E}^0$ is given by:

$$\mathcal{E}^0 = \int \bar{d}^3 k \frac{k^0}{2\omega_k}\frac{1}{\omega_k}\left|\int d^4x \rho(x,t) e^{i(\mathbf{k}\cdot\mathbf{x}-\omega t)}\right|^2. \tag{5.112}$$

This leads to a number density of the form:

$$\mathcal{T}^0 = g_\psi^2 B^2 \sum_n |E_n|^2 \frac{1}{2\omega_k(\omega_k - k_\parallel v)^2} \tag{5.113}$$

which in the ultra-relativistic limit is given by:

$$\mathcal{T}^0 = \frac{8^{\frac{3}{2}} g_\psi^2 B^2 \gamma^{\frac{5}{2}} m_e^2}{e^2\pi^5\omega_p} \sum_{n\neq 0} \frac{1}{n^2} \frac{1}{(n^2+s^2)^{\frac{3}{2}} - 2nv(n^2+s^2) + n^2v^2(n^2+s^2)^{\frac{1}{2}}}, \tag{5.114}$$

where $s = \frac{2\sqrt{2\gamma}m_\psi}{\pi\omega_p}$. We can split up the terms inside the sum to give:

$$\mathcal{T}^0 = \frac{8^{\frac{3}{2}} g_\psi^2 B^2 \gamma^{\frac{5}{2}} m_e^2}{e^2\pi^5\omega_p} \sum_{n=1}^{\infty} (\alpha_n + \beta_n)\,. \tag{5.115}$$

Where:

$$\begin{aligned} \alpha_n &= \frac{1}{n^2} \frac{1}{(n^2+s^2)^{\frac{3}{2}} - 2nv(n^2+s^2) + n^2v^2(n^2+s^2)^{\frac{1}{2}}}, \\ \beta_n &= \frac{1}{n^2} \frac{1}{(n^2+s^2)^{\frac{3}{2}} + 2nv(n^2+s^2) + n^2v^2(n^2+s^2)^{\frac{1}{2}}}. \end{aligned} \tag{5.116}$$

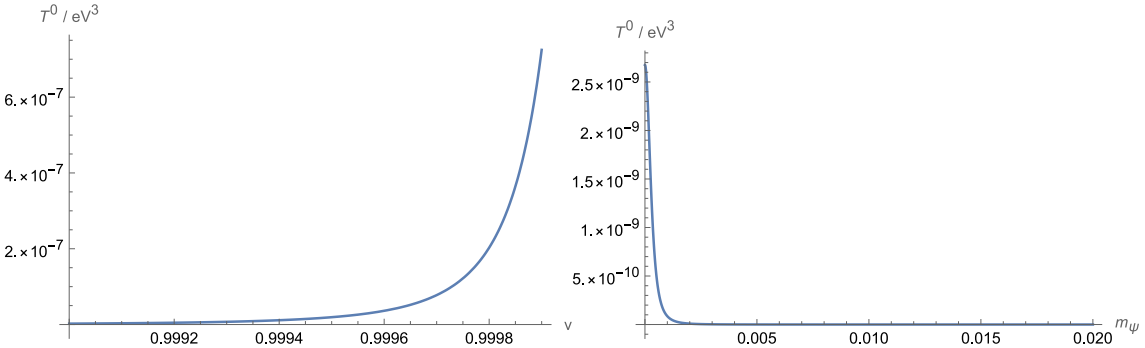

(a) $\mathcal{T}^0$ vs v (b) $\mathcal{T}^0$ vs m_ψ

Figure 5.4: Plots of the $\mathcal{T}^0$ component against the wake velocity and axion mass. The relevant physical parameters are $g_\psi = 0.66 \times 10^{-19}$eV, $B = 7 \times 10^3$eV^2 ($B \approx 35T$), $\omega_p = 4.12 \times 10^{-2}$eV. The choice $m_\psi = 10^{-4}$eV is made in plot (a), whilst $v = 0.995$ is made in plot (b).

Equation (5.114) is plotted in Figure 5.4. In the zero mass limit $\mathcal{T}^0$ becomes:

$$\mathcal{T}^0 = \frac{2^{\frac{11}{2}} \gamma^{\frac{13}{2}} g_\psi^2 B^2 m_e^2 (1+v^2)}{e^2\pi^5\omega_p} \zeta(5), \tag{5.117}$$

where $\zeta(5)$ is the Riemann zeta function evaluated at 5. In the ultra-relativistic limit this gives:

$$\mathcal{T}^0 = \frac{(2\gamma)^{\frac{13}{2}} g_\psi^2 B^2 m_e^2}{e^2\pi^5\omega_p} \zeta(5). \tag{5.118}$$

5.4.2.6 Calculating $\mathcal{T}^3$

The $\mathcal{E}^3$ term is given by:

$$\mathcal{E}^3 = \int đ^3k \frac{k^3}{2\omega_k^2} \left| \int d^4x \rho(\mathbf{x}, t) e^{i(\mathbf{k}\cdot\mathbf{x} - \omega_k t)} \right|^2. \tag{5.119}$$

Invoking the same procedure as in the previous calculation, we factor out the formally infinite factor A and we obtain:

$$\mathcal{E}^3 = \frac{1}{2} A g_\psi^2 B^2 \int đk_\parallel \frac{k_\parallel}{\omega_k^2} \frac{1}{(\omega_k - k_\parallel v)^2} \left| E(k_\parallel) \right|^2. \tag{5.120}$$

Expanding the source term with a Fourier series yields a result that can be written as:

$$\mathcal{E}^3 = V g_\psi^2 B^2 \sum_n |E_n|^2 \frac{k_\parallel^2 v}{\omega_k(\omega_k^2 - k_\parallel^2 v^2)^2}. \tag{5.121}$$

Expressing (5.121) as a component of $\mathcal{T}^\mu$:

$$\mathcal{T}^3 = g_\psi^2 B^2 \sum_n |E_n|^2 \frac{k_\parallel^2 v}{\omega_k(\omega_k^2 - k_\parallel^2 v^2)^2}. \tag{5.122}$$

We can approximate (5.122) in the ultra-relativistic limit to be:

$$\mathcal{T}^3 = \frac{(2\gamma)^{\frac{13}{2}} g_\psi^2 B^2 m_e^2 v}{e^2 \pi^5 \omega_p} \sum_{n=1}^{\infty} \frac{1}{(n^2 + \frac{8\gamma m_\psi^2}{\omega_p^2 \pi^2})^{\frac{1}{2}} (n^2 + \frac{8\gamma^3 m_\psi^2}{\omega_p^2 \pi^2})^2}. \tag{5.123}$$

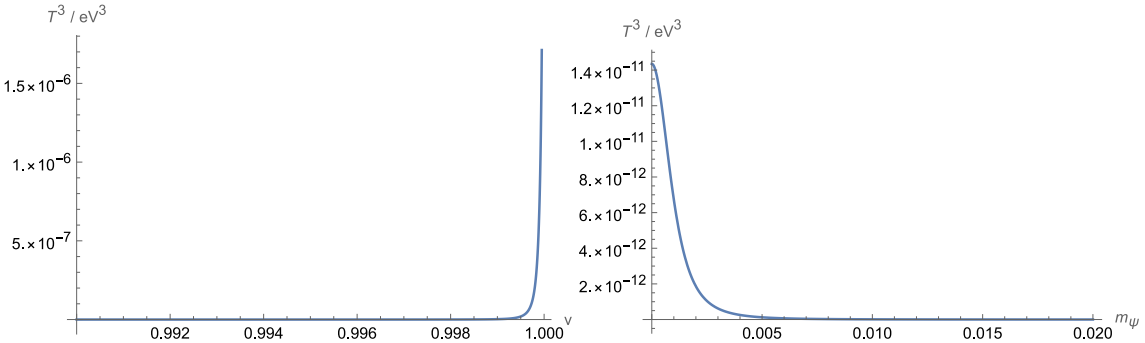

(a) $\mathcal{T}^3$ vs v (b) $\mathcal{T}^3$ vs m_ψ

Figure 5.5: Plots of the $\mathcal{T}^3$ component against the wake velocity and axion mass. The relevant physical parameters are $g_\psi = 0.66 \times 10^{-19}$eV, $B = 7 \times 10^3$eV^2 ($B \approx 35T$), $\omega_p = 4.12 \times 10^{-2}$eV. The choice $m_\psi = 10^{-4}$eV is made in plot (a), whilst $v = 0.995$ is made in plot (b).

Equation (5.123) is plotted in Figure 5.5. In the limit $m_\psi \to 0$ we have:

$$\mathcal{T}^3 = \frac{(2\gamma)^{\frac{13}{2}} g_\psi^2 B^2 m_e^2 v}{e^2 \pi^5 \omega_p} \zeta(5), \tag{5.124}$$

where $\zeta(5) \approx 1$ is the Riemann zeta function evaluated at $z = 5$. We note that this is exactly the

same expression as $\mathcal{T}^0_{m_\psi \to 0}$ in the ultra-relativistic limit.

5.4.3 Classical vs Quantum Results

In this section, we will compare the classical axion flux results that were obtained in [66] and the quantum results we obtained in the previous sections. We can immediately identify that the momentum flux of the axion field P_ψ obtained in [66] is equal to expression $\mathcal{T}^{03}$. This, of course, makes a great deal of sense, as the quantum axion field is driven by a classical source (in our case, a plasma wave) which leaves it in a coherent state. In order to obtain a number flux density N_ψ from the classical expression, the axion energy in [66] was divided out i.e.:

$$N_\psi = \frac{P_\psi}{\gamma m_\psi}. \tag{5.125}$$

In our formalism, we identify the axion number flux density with $\mathcal{T}^3$. In Figure 5.6 we see a comparison of the classical and quantum results. We note that we have switched to the use of metric units for ease of comparison to another result. We see that the quantum calculation shows that the axion number flux actually grows faster with the speed of the wake than the classical theory would predict; additionally, we do not run into the problem of the divergence in the zero axion mass limit for the number flux, which arises in the classical calculation.

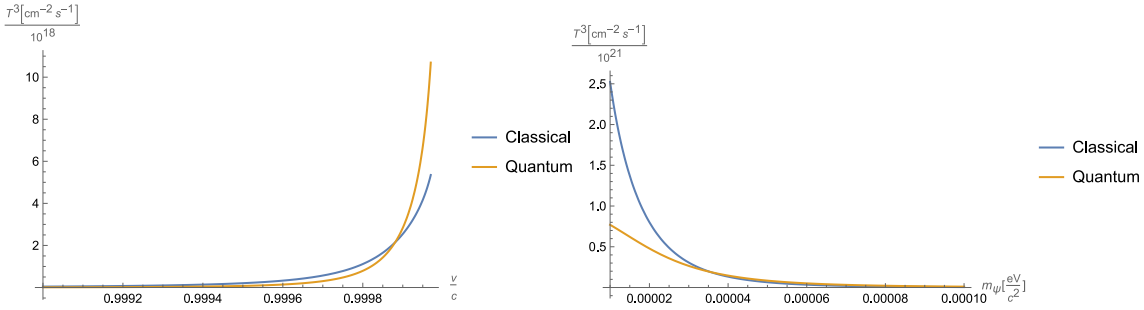

(a) $\mathcal{T}^3$ vs v (b) $\mathcal{T}^3$ vs m_ψ

Figure 5.6: Plots of the classical axion number flux density N_ψ and $\mathcal{T}^3$ against the wake velocity and axion mass. The relevant physical parameters are $g_\psi = 0.66 \times 10^{-19}\mathrm{eV}$, $B = 7 \times 10^3 \mathrm{eV}^2$ ($B \approx 35T$), $\omega_p = 4.12 \times 10^{-2}\mathrm{eV}$ and $v = 0.99995$ for the constant v plot and $m_\psi = 10^{-4}\mathrm{eV}$.

This work improves on the previous classical result obtained in [66] as our result has a finite value in the zero mass limit for the axion. The expected axion flux of solar axions, considering an axion mass in the range $m_\psi \lesssim 10^{-4}\mathrm{eV}c^{-2}$, the axion photon coupling of $g_\psi = 0.66 \times 10^{-19}\mathrm{eV}$ and some representative physical parameters for a LWFA set up being $B = 7 \times 10^3\mathrm{eV}^2$ ($B \approx 35T$), $\omega_p = 4.12 \times 10^{-2}\mathrm{eV}$, and $v = 0.99995$, is estimated to be $N_{Solar\psi} \approx 1.73 \times 10^{11}\mathrm{cm}^{-2}\mathrm{s}^{-1}$ [83], while our estimates predict a number flux of $N_{\mathrm{LWFA}\psi} \approx 6.74 \times 10^{18}\mathrm{cm}^{-2}\mathrm{s}^{-1}$ ($N_{\mathrm{LWFA}m_\psi=0} \approx 1.7 \times 10^{20}\mathrm{cm}^{-2}\mathrm{s}^{-1}$ in the massless case). Naturally, the real flux density would be smaller due to 3D effects in the plasma, but we can estimate that the flux density would be roughly 25% of our predicted value in the 3D bubble regime [59]. Additionally, the flux density will also decrease as the axions leave the barrier due to beam dispersion.

5.5 Axion-Photon Oscillations

In this section, we discuss the case of axions transitioning into photons in a strong magnetic field, as motivated by the LSWT experiment discussed in subsection 1.3.3.

5.5.1 Photon Conversion

In this calculation, we want to focus on the region of the LSTW experiment outside the barrier. The interaction Hamiltonian for the axion-photon system is given by:

$$\hat{H}_I = -ig_\psi \frac{1}{2} \int đ^3k \sqrt{\frac{\omega_{A_\mathbf{k}}}{\omega_{\psi_\mathbf{k}}}} \left(\hat{b}_\mathbf{k} + \hat{b}^\dagger_{-\mathbf{k}}\right) \left(\underline{\hat{a}}^\dagger_\mathbf{k} - \underline{\hat{a}}_{-\mathbf{k}}\right) \cdot \underline{\mathbb{B}}, \tag{5.126}$$

where $\omega_{A_\mathbf{k}}$ is the photon frequency given by $\omega_{A_\mathbf{k}} = |\mathbf{k}|$, $\omega_{\psi_\mathbf{k}}$ is the axion frequency given by $\omega_{\psi_\mathbf{k}} = \sqrt{\mathbf{k}^2 + m_\psi^2}$, $\underline{\mathbb{B}}$ denotes a strong external magnetic field which corresponds to B_2 in figure 1.2 and g_ψ denotes the axion photon coupling. Additionally, we also used an underline as an alternative vector notation for the operators $\underline{\hat{a}}_\mathbf{k}$, $\underline{\hat{a}}^\dagger_\mathbf{k}$ and the magnetic field $\underline{\mathbb{B}}$. We are interested in the case of the transition amplitude:

$$P_{\psi\to\gamma} = \left|\langle n_\psi, 1|z, 0\rangle_I\right|^2, \tag{5.127}$$

where the bra state is a number state of 1 photon with momentum $\mathbf{k}$ and n_ψ axions with momentum $\mathbf{k}$ and the ket state is a coherent state of axions with parameter z and a photon vacuum state. The transition amplitude is given by:

$$\langle n_\psi, 1|z, 0\rangle_I = \langle n_\psi, 1| \hat{T}[e^{-i\int_{t_i}^{t_f} dt \hat{H}_I}] |z, 0\rangle . \tag{5.128}$$

To first order in the Dyson series, this can be expanded as:

$$\langle n_\psi, 1| \left(1 - i\int_{t_i}^{t_f} \hat{H}_I dt\right) |z, 0\rangle . \tag{5.129}$$

We now note that the non-interacting Hamiltonian is given by:

$$\hat{H}_0 = \int đ^3k \ \left(\omega_{\psi_\mathbf{k}} \hat{b}^\dagger_\mathbf{k} \hat{b}_\mathbf{k} + \omega_{A_\mathbf{k}} \underline{\hat{a}}^\dagger_\mathbf{k} \cdot \underline{\hat{a}}_\mathbf{k}\right). \tag{5.130}$$

We can use the Heisenberg equation to find the time dependence of the creation and annihilation operators i.e.:

$$i\dot{\hat{b}}_\mathbf{k} = \left[\hat{b}_\mathbf{k}, \hat{H}_0\right] = \omega_{\psi_\mathbf{k}} \hat{b}_\mathbf{k}. \tag{5.131}$$

This can be immediately solved by:

$$\hat{b}_\mathbf{k}(t) = e^{-i\omega_{\psi_\mathbf{k}}(t-t_i)} \hat{b}_\mathbf{k}(t_i). \tag{5.132}$$

With this in mind, we can begin the calculation. The first perturbative term, corresponding to no interaction is simply:

$$\langle n_\psi, 1|z, 0\rangle = 0. \tag{5.133}$$

The first-order interaction term is:

$$P_1 = -i \langle n_\psi, 1| \int_{t_i}^{t_f} \hat{H}_I dt \, |z, 0\rangle \, . \tag{5.134}$$

To evaluate this term, we want to find an explicit expression for $\int_{t_i}^{t_f} \hat{H}_I dt$. We choose $\underline{\mathbb{B}}$ such that:

$$\underline{\hat{a}}_{\mathbf{k}} \cdot \underline{\mathbb{B}} = \hat{a}_{1\mathbf{k}} \mathbb{B}, \tag{5.135}$$

where 1 denotes the polarisation of the photon field. For simplicity, we drop the 1 in the subscript $\hat{a}_{1\mathbf{k}} \equiv \hat{a}_{\mathbf{k}}$. With that in mind, we have:

$$\begin{aligned}
\int_{t_i}^{t_f} \hat{H}_I dt = -\frac{1}{2} i g_\psi \mathbb{B} \int đ^3k \sqrt{\frac{\omega_{A_\mathbf{k}}}{\omega_{\psi_\mathbf{k}}}} \Bigg(& -\frac{\hat{b}_\mathbf{k} \hat{a}_\mathbf{k}^\dagger e^{-i(\omega_{\psi_\mathbf{k}} - \omega_{A_\mathbf{k}})(t_f - t_i)}}{i(\omega_{\psi_\mathbf{k}} - \omega_{A_\mathbf{k}})} + \frac{\hat{b}_\mathbf{k} \hat{a}_\mathbf{k}^\dagger}{i(\omega_{\psi_\mathbf{k}} - \omega_{A_\mathbf{k}})} \\
& + \frac{\hat{b}_\mathbf{k} \hat{a}_{-\mathbf{k}} e^{-i(\omega_{\psi_\mathbf{k}} + \omega_{A_{-\mathbf{k}}})(t_f - t_i)}}{i(\omega_{\psi_\mathbf{k}} + \omega_{A_{-\mathbf{k}}})} - \frac{\hat{b}_\mathbf{k} \hat{a}_{-\mathbf{k}}}{i(\omega_{\psi_\mathbf{k}} + \omega_{A_{-\mathbf{k}}})} \\
& + \frac{\hat{b}_{-\mathbf{k}}^\dagger \hat{a}_\mathbf{k}^\dagger e^{i(\omega_{\psi_{-\mathbf{k}}} + \omega_{A_\mathbf{k}})(t_f - t_i)}}{i(\omega_{\psi_{-\mathbf{k}}} + \omega_{A_\mathbf{k}})} - \frac{\hat{b}_{-\mathbf{k}}^\dagger \hat{a}_\mathbf{k}^\dagger}{i(\omega_{\psi_{-\mathbf{k}}} + \omega_{A_\mathbf{k}})} \\
& - \frac{\hat{b}_{-\mathbf{k}}^\dagger \hat{a}_{-\mathbf{k}} e^{i(\omega_{\psi_{-\mathbf{k}}} - \omega_{A_{-\mathbf{k}}})(t_f - t_i)}}{i(\omega_{\psi_{-\mathbf{k}}} - \omega_{A_{-\mathbf{k}}})} + \frac{\hat{b}_{-\mathbf{k}}^\dagger \hat{a}_{-\mathbf{k}}}{i(\omega_{\psi_{-\mathbf{k}}} - \omega_{A_{-\mathbf{k}}})} \Bigg),
\end{aligned} \tag{5.136}$$

where the operators are evaluated at t_i in the result of the integral of t. The previous result simplifies to:

$$\begin{aligned}
\int_{t_i}^{t_f} \hat{H}_I dt = -\frac{1}{2} i g_\psi \mathbb{B} \int đ^3k \sqrt{\frac{\omega_{A_\mathbf{k}}}{\omega_{\psi_\mathbf{k}}}} (& \frac{1 - e^{-i(\omega_{\psi_\mathbf{k}} - \omega_{A_\mathbf{k}})(t_f - t_i)}}{i(\omega_{\psi_\mathbf{k}} - \omega_{A_\mathbf{k}})} \hat{b}_\mathbf{k} \hat{a}_\mathbf{k}^\dagger \\
& - \frac{1 - e^{-i(\omega_{\psi_\mathbf{k}} + \omega_{A_{-\mathbf{k}}})(t_f - t_i)}}{i(\omega_{\psi_\mathbf{k}} + \omega_{A_{-\mathbf{k}}})} \hat{b}_\mathbf{k} \hat{a}_{-\mathbf{k}} \\
& - \frac{1 - e^{i(\omega_{\psi_{-\mathbf{k}}} + \omega_{A_\mathbf{k}})(t_f - t_i)}}{i(\omega_{\psi_{-\mathbf{k}}} + \omega_{A_\mathbf{k}})} \hat{b}_{-\mathbf{k}}^\dagger \hat{a}_\mathbf{k}^\dagger \\
& + \frac{1 - e^{i(\omega_{\psi_{-\mathbf{k}}} - \omega_{A_{-\mathbf{k}}})(t_f - t_i)}}{i(\omega_{\psi_{-\mathbf{k}}} - \omega_{A_{-\mathbf{k}}})} \hat{b}_{-\mathbf{k}}^\dagger \hat{a}_{-\mathbf{k}}).
\end{aligned} \tag{5.137}$$

We note that the only term in (5.137) that does not vanish is the term containing the operator $\hat{b}_\mathbf{k} \hat{a}_\mathbf{k}^\dagger$. The transition amplitude is thus:

$$P_{\psi \to \gamma}(\mathbf{k}) = \left| \frac{1}{2} g_\psi \mathbb{B} \sqrt{\frac{\omega_{A_\mathbf{k}}}{\omega_{\psi_\mathbf{k}}}} \frac{1 - e^{-i(\omega_{\psi_\mathbf{k}} - \omega_{A_\mathbf{k}})(t_f - t_i)}}{(\omega_{\psi_\mathbf{k}} - \omega_{A_\mathbf{k}})} \frac{z_\mathbf{k}^{n_\psi + 1}}{\sqrt{(n_\psi + 1)!}} e^{-\frac{1}{2} \int đ^3k' |z_{\mathbf{k}'}|^2} \right|^2 . \tag{5.138}$$

Which can be simplified to:

$$\boxed{P_{\psi\to\gamma}(\mathbf{k}) = \frac{1}{2}g_\psi^2 B^2 \frac{\omega_{A_\mathbf{k}}}{\omega_{\psi_\mathbf{k}}} \frac{1-\cos\left((\omega_\psi-\omega_A)T\right)}{(\omega_\psi-\omega_A)^2} \frac{|z_\mathbf{k}|^{2(n_\psi+1)}}{(n_\psi+1)!} e^{-\int d^3k'|z_{\mathbf{k}'}|^2},} \tag{5.139}$$

where $T = t_f - t_i$. The coherent state index z comes from the driving term for the axion field. We have derived the form of it in equation (5.63) and the absolute value of it is given by :

$$|z_\mathbf{k}| = \frac{1}{\sqrt{2\omega_{\psi_\mathbf{k}}}}\left|\int_{-\infty}^{+\infty} d^4x \rho(x,t) e^{ik\cdot x - i\omega t}\right|. \tag{5.140}$$

In order to compute the axion-photon transition rate we have to introduce more cut-offs to the source, as the form of the source that was used in the previous section would lead to badly divergent solutions, due to the infinity arising through the source having an infinite cross section. We can propose a source function $\rho(\mathbf{x},t)$ of the form:

$$\rho(\mathbf{x},t) = g_\psi B\Theta(-t) e^{-\frac{(x^2+y^2)}{\Lambda^2}} E(\zeta), \tag{5.141}$$

where Λ sets the scale of the source's cross-section. The absolute value of the coherent state index is then given:

$$|z_k| = g_\psi B\sqrt{\frac{\Lambda^2\pi^2}{2\omega_{\psi_\mathbf{k}}}} \frac{e^{-\frac{\Lambda^2\mathbf{k}_\perp^2}{4}}}{\omega_{\psi_\mathbf{k}} - k_\parallel v}\left|E(k_\parallel)\right|. \tag{5.142}$$

5.5.1.1 Comparison with the Toy Model

As mentioned at the end of Section 5.2, one can draw an analogy between the result in equation (5.33) and the result in equation (5.139). The transition rate for a single photon transitioning into an axion under the influence of an external magnetic field in the toy model is given by:

$$P^{\text{Toy}}_{\psi\to\gamma} = \frac{1}{2}g_\psi^2 B^2 \frac{\omega_{A_\mathbf{k}}}{\omega_{\psi_\mathbf{k}}} \frac{1-\cos\left(\sqrt{(\omega_{\psi_\mathbf{k}}-\omega_{A_\mathbf{k}})^2 + g_\psi^2 B^2 \frac{\omega_{A_\mathbf{k}}}{\omega_{\psi_\mathbf{k}}}}T\right)}{(\omega_{\psi_\mathbf{k}}-\omega_{A_\mathbf{k}})^2 + g_\psi^2 B^2 \frac{\omega_{A_\mathbf{k}}}{\omega_{\psi_\mathbf{k}}}}. \tag{5.143}$$

If we neglect the $\mathcal{O}(g_\psi^2)$ terms within the expression, we obtain:

$$P^{\text{Toy}}_{\psi\to\gamma} = \frac{1}{2}g_\psi^2 B^2 \frac{\omega_{A_\mathbf{k}}}{\omega_{\psi_\mathbf{k}}} \frac{1-\cos\left((\omega_{\psi_\mathbf{k}}-\omega_{A_\mathbf{k}})T\right)}{(\omega_{\psi_\mathbf{k}}-\omega_{A_\mathbf{k}})^2}. \tag{5.144}$$

This then leads us to see that the coherent state case simply modifies the previous result:

$$P_{\gamma\to\psi} = P^{\text{Toy}}_{\psi\to\gamma} \frac{|z_\mathbf{k}|^{2(n_\psi+1)}}{(n_\psi+1)!} e^{-\int d^3k'|z_{\mathbf{k}'}|^2}. \tag{5.145}$$

As a final point of note, we can see that the $|z_\mathbf{k}|$ term in equation (5.145) should suppress transitions to high n_ψ number states, due to its dependence on g_ψ.

Chapter 6

Conclusions

The purpose of this PhD project was the exploration of axion production in laser-plasma systems from a theoretical perspective.

6.1 Overview of the Results

In Chapter 2, we formulated a scalar field approach to the theory of plasma waves. Subsequently, through the use of simplifying assumptions, we were able to describe 1+1-dimensional laser-plasma systems in a novel way. This then allowed us to derive a condition for the dimensionless laser amplitude required to drive the maximum plasma wakefield only in terms of the wake velocity.
Chapter 3 focused on the case of axion production from a classical field perspective. We derived some basic results of axion-photon conversion from the classical equations in terms of two-level and three-level systems. Furthermore, we derived a condition for axion resonance inside a laser travelling through a plasma, which relates a given axion mass to the laser-plasma parameters needed to achieve said resonance.
In Chapter 4, we looked at the case of axion production through the lens of the ponderomotive approach. We introduced a heuristic approach to ponderomotive dynamics, from which we were able to propose an effective action for the system. Having an action allowed us to derive equations of motion, a conservation law (which then allowed for a formula for laser depletion due to axions) and a dispersion relation.
Finally, in Chapter 5, we looked at the case of axion production with considerations for the quantum nature of the axion. In this chapter, we first investigated a toy model of a photon-axion system coupled to an external magnetic field and calculated a transition rate from a given n-photon state to a 1-axion/$n-1$-photon state. Following this, we considered the case of a quantum axion field driven by a plasma wave with an applied external magnetic field. This investigation led to a definition of an n^{th} order tensor which contained information about the axion field produced from the plasma wave and the magnetic field. The case of interest was the first order, which gave us an expression for the number flux of the axion field produced in the plasma. We then were able

to compare the axion flux predicted from previous calculations and found that our result didn't diverge in the zero axion mass limit, unlike the results of the approach in [59]. It was also found that the expected axion flux from our calculations could, at the very least, match the hypothetical flux of solar axions. This result is a good motivation for the use of laser-plasma experiments in axion searches. The final thing that was investigated was the axion-photon transition rate in a hypothetical LSTW experiment, given a plasma source. A transition function was found, and a comparison with the toy model showed that it simply modified the toy model result with a multiplicative factor.

6.2 Final Thoughts and Further Exploration

This project explored a variety of approaches to the theory of axion production in laser-plasma experiments. It should be said that this exploration is by no means exhaustive, as there is a wide range of effects and considerations that were left out of our approach. As such we shall state some theoretical points our analysis was missing:

- *More Classical Considerations*: Throughout this thesis our treatment of the laser-plasma system has involved a lot of assumptions to facilitate analytical calculations. In order to probe the behaviour of the system with more detail, intensive computational approaches would be needed. In this way, one could account for the effect of the plasma on the laser pulse and the dynamics of the axions within the plasma. Such an attempt was featured in [84]. Another aspect that could certainly be expanded upon is the low dimensionality of the systems studied. One can extrapolate the behaviour of a low-dimensional LWFA to what one could expect in the full 3D case via scaling arguments [85], but in order to approach accurate results full multidimensional simulations are required.

- *More Quantum Considerations*: Due to the classical nature of a lot of plasma systems, it is not unreasonable to treat the problem of axion production mostly from a classical perspective. Despite this, axions are inherently quantum, and in a strong field QED regime, it is certainly possible that quantum effects of the laser and the plasma could potentially play a role in axion production (some work on how quantum effects modify the problem can for example be seen in [86], [87]).

To conclude, we hope that the work of this thesis will serve as motivation for further exploration of laser-plasma based searches for axions.

Appendix A

Theory of Relativistic Plasma Waves

A.1 The Lie Derivative And The Levi-Civita Connection

Introduce an operator $\mathcal{A}_X$ defined as:

$$\mathcal{A}_X \equiv \nabla_X - \mathcal{L}_X, \tag{A.1}$$

where X is an arbitrary vector field, ∇_X is the Levi-Civita connection and $\mathcal{L}_X$ is the Lie derivative, both with respect to X. Immediately we see that for an arbitrary 0-form f, i.e. scalar field, $\mathcal{A}_X$ always satisfies:

$$\mathcal{A}_X f = 0. \tag{A.2}$$

For the case of a vector field Y, $\mathcal{A}_X$ acts upon it as:

$$\mathcal{A}_X Y = \nabla_Y X, \tag{A.3}$$

where we have used the torsion-free property of the Levi-Civita connection ($\nabla_X Y - \nabla_Y X - [X, Y] = 0$). Now let us consider the case of the operator $\mathcal{A}_X$ acting on the inner product of vectors Y and Z induced by the metric i.e. :

$$\begin{aligned} \mathcal{A}_X[g(Y,Z)] &= 0 \\ &= \mathcal{A}_X g(Y,Z) + g(\mathcal{A}_X Y, Z) + g(Y, \mathcal{A}_X Z) \\ &= -\mathcal{L}_X g(Y,Z) + g(\nabla_Y X, Z) + g(Y, \nabla_Z X), \end{aligned} \tag{A.4}$$

Since the Levi-Civita connection is metric compatible, i.e. ($\nabla_X g = 0$), it follows:

$$\mathcal{L}_X g(Y,Z) = g(\nabla_Y X, Z) + g(Y, \nabla_Z X). \tag{A.5}$$

We now want to consider the case for which $Y = X = V$, where V is a time-like normalized vector field. Equation (A.5) then becomes:

$$\mathcal{L}_V g(V, Z) = g(\nabla_V V, Z) + g(V, \nabla_Z V). \tag{A.6}$$

We note that $g(V, \nabla_Z V) = 0$ because V is normalised and $\nabla_Z g(V, V) = 0$ using metric compatibility. Equation (A.6) then leads to:

$$\mathcal{L}_V g(V, Z) = g(\nabla_V V, Z). \tag{A.7}$$

Finally, we can re-write (A.7) as:

$$\mathcal{L}_V \widetilde{V}(Z) = \nabla_V \widetilde{V}(Z), \tag{A.8}$$

for an arbitrary vector field Z, and hence, $\mathcal{L}_V \widetilde{V} = \nabla_V \widetilde{V}$. The application of Cartan's identity, $\mathcal{L}_V \widetilde{V} = \iota_V d\widetilde{V} + d\iota_V \widetilde{V}$, and the fact $g(V, V)$ is constant gives:

$$\iota_V d\widetilde{V} = \nabla_V \widetilde{V}. \tag{A.9}$$

A.2 Interior operator relation

Suppose we have a 1-form β, where β is an element of the span of dt and dz. We also require that:

$$\beta(V_\parallel) \neq 0. \tag{A.10}$$

If we consider the equation:

$$\iota_{V_\parallel} d\widetilde{V}_\parallel = \frac{q}{m} \iota_{V_\parallel} (E \#_\parallel 1), \tag{A.11}$$

we can then apply the wedge product between it and β.

$$\beta \wedge \iota_{V_\parallel} (d\widetilde{V}_\parallel - \frac{q}{m} E \#_\parallel 1) = 0 \tag{A.12}$$

Let us denote $d\widetilde{V}_\parallel - \frac{q}{m} E \#_\parallel 1 = \Gamma$. Using the interior operator properties we get:

$$\begin{aligned} \beta \wedge \iota_{V_\parallel} \Gamma &= -\iota_{V_\parallel} (\beta \wedge \Gamma) + \iota_{V_\parallel} \beta \wedge \Gamma \\ &= \beta(V_\parallel) \Gamma \\ &= 0. \end{aligned} \tag{A.13}$$

We used the fact that $\iota_{V_\parallel} (\beta \wedge \Gamma)$ is identically zero because the wedge product of Γ and β results in a 3-form on a 2-dimensional subspace. Finally, (A.13) and (A.10) yield $\Gamma = 0$, which can be written:

$$d\widetilde{V}_\parallel = \frac{q}{m} E \#_\parallel 1. \tag{A.14}$$

A.3 The Double Hodge Operator Property

In this appendix, we will review a basic property of the Hodge star operator (for a beginner-friendly introduction to the broader formalism of geometrical methods in physics, see [88]). A pseudo-Riemannian metric on an n-dimensional manifold can always be written in terms of an orthonormal frame e^μ as:

$$g = \eta_{\mu\nu} e^\mu \otimes e^\nu, \tag{A.15}$$

where $\eta_{\mu\nu}$ are components of a matrix η and are given by:

$$\eta_{\mu\nu} = \begin{cases} +1 & \text{for } \mu = \nu \in 1, \dots, k \\ -1 & \text{for } \mu = \nu \in k+1, \dots, n \\ 0 & \text{for } \mu \neq \nu. \end{cases} \tag{A.16}$$

Now let $\alpha \in \Gamma\Lambda^p\mathcal{M}$, then the following holds true:

$$\star\star\alpha = (\det\eta)(-1)^{p(n-p)}\alpha. \tag{A.17}$$

This relation can be readily proved via induction. Firstly, we consider the action of the double Hodge star on a 0-form. Without the loss of generality, we can consider the action of $\star\star 1$:

$$\begin{aligned} \star\star 1 &= \star(e^1 \wedge \cdots \wedge e^n) \\ &= \iota_{\widetilde{e^n}} \dots \iota_{\widetilde{e^1}} \star 1 \\ &= g^{-1}(e^1, e^1) \dots g^{-1}(e^n, e^n) \\ &= \det\eta, \end{aligned} \tag{A.18}$$

since $\star\star\alpha = \alpha\star\star 1$ when $\alpha \in \Gamma\Lambda^0\mathcal{M}$. Before we proceed and prove the statement for forms of all orders, let us prove an identity that shall be useful in the proof:

$$\star\iota_V\alpha = (-1)^{p+1}\widetilde{V} \wedge \star\alpha, \tag{A.19}$$

where V is some vector field (i.e. $V \in \Gamma T\mathcal{M}$). We begin to prove this identity by considering the following expression:

$$\iota_X(\widetilde{V} \wedge \star\alpha) = \iota_X\widetilde{V} \star \alpha - \widetilde{V} \wedge \iota_X \star \alpha, \tag{A.20}$$

where $X \in \Gamma T\mathcal{M}$. However, it is also true that:

$$\begin{aligned} \iota_X\widetilde{V} \star \alpha &= \star(\iota_X\widetilde{V}\alpha) \\ &= \star(\iota_V\widetilde{X}\alpha) \\ &= \star(\iota_V(\widetilde{X} \wedge \alpha) + \widetilde{X} \wedge \iota_V\alpha), \end{aligned} \tag{A.21}$$

and

$$\widetilde{V} \wedge \iota_X \star \alpha = \widetilde{V} \wedge \star(\alpha \wedge \widetilde{X}). \tag{A.22}$$

By combining (A.21) and (A.22), equation (A.20) can then be written as:

$$\iota_X(\widetilde{V} \wedge \star\alpha) = \star(\iota_V(\widetilde{X} \wedge \alpha) + \widetilde{X} \wedge \iota_V\alpha) - \widetilde{V} \wedge \star(\alpha \wedge \widetilde{X}). \tag{A.23}$$

Furthermore:

$$\star(\widetilde{X} \wedge \iota_V\alpha) = (-1)^{p-1} \star (\iota_V\alpha \wedge \widetilde{X}) = (-1)^{p-1}\iota_X \star \iota_V\alpha. \tag{A.24}$$

This then leads us to the expression:

$$\iota_X(\widetilde{V} \wedge \star\alpha - (-1)^{p-1} \star \iota_V\alpha) = (-1)^p \star \iota_V(\alpha \wedge \widetilde{X}) - \widetilde{V} \wedge \star(\alpha \wedge \widetilde{X}). \tag{A.25}$$

Hence, if (A.19) is true (which can also be written as $\widetilde{V} \wedge \star\alpha = (-1)^{p-1} \star \iota_V\alpha$), then the following also holds true:

$$\widetilde{V} \wedge \star(\alpha \wedge \widetilde{X}) = (-1)^p \star \iota_V(\alpha \wedge \widetilde{X}). \tag{A.26}$$

For the case of $\alpha \in \Gamma\Lambda^1\mathcal{M}$ we have:

$$\begin{aligned} \widetilde{V} \wedge \star\alpha &= \widetilde{V} \wedge \iota_{\widetilde{\alpha}} \star 1 \\ &= -\iota_{\widetilde{\alpha}}(\widetilde{V} \wedge \star 1) + \iota_{\widetilde{\alpha}}\widetilde{V} \star 1 \\ &= \iota_V\alpha \star 1 \\ &= (-1)^0 \star \iota_V\alpha. \end{aligned} \tag{A.27}$$

If one takes $\widetilde{X} = dx^i$ (such that $\alpha \wedge dx^i \neq 0$) in (A.26), then invoking linearity and (A.27), one can see that higher order forms can be built up, thus proving the identity inductively.

Finally, we prove the double Hodge star property by first considering $\alpha \in \Gamma\Lambda^1\mathcal{M}$. We can then use (A.19) to write:

$$\begin{aligned} \star\star\alpha &= \star\iota_{\widetilde{\alpha}} \star 1 \\ &= (-1)^{n+1}\alpha \wedge \star\star 1 \\ &= (-1)^{n+1} \det(\eta)\alpha \\ &= (-1)^{n-1} \det(\eta)\alpha. \end{aligned} \tag{A.28}$$

This shows that the statement holds for the case of a 1-form. We now want to show that this holds for a p-form in order to prove the statement inductively. Without loss of generality, we now consider a p-form given by $\alpha \wedge \beta$, where α is a $(p-1)$-form and $\beta = dx^i$ (such that $\alpha \wedge dx^i \neq 0$).

The double action of the Hodge Star operator then gives:

$$\begin{aligned}
\star\star\,(\alpha\wedge\beta) &= \star\iota_{\widetilde{\beta}}\star\,\alpha \\
&= (-1)^{n-p+2}\beta\wedge\star\star\,\alpha \\
&= (-1)^{n-p+2}(-1)^{(p-1)(n-p+1)}\det(\eta)\beta\wedge\alpha \\
&= (-1)^{p(n-p+1)+1}\det(\eta)\beta\wedge\alpha \\
&= (-1)^{p(n-p)}\det(\eta)\alpha\wedge\beta.
\end{aligned} \tag{A.29}$$

Having shown this for the case of $\beta = dx^p$, one can easily see that this holds for the general case $\beta = \beta_1 dx^1 + \cdots + \beta_p dx^p$ via linearity. This then completes the proof.

Appendix B

Classical Axion Production

B.1 Schrödinger Equation for a Two-Level System and Rabi Oscillations

For ease of reading, we will include a step-by-step derivation of the Rabi frequency. Consider a Schrödinger equation of the form:

$$i\dot{\Phi} = \begin{bmatrix} \alpha & \beta e^{i\omega t} \\ \beta^* e^{-i\omega t} & -\alpha \end{bmatrix} \Phi, \tag{B.1}$$

where α and ω are real. Now introduce:

$$\Phi = \begin{bmatrix} e^{i\frac{\omega}{2}t} & 0 \\ 0 & e^{-i\frac{\omega}{2}t} \end{bmatrix} \psi. \tag{B.2}$$

The left-hand side of the Schrödinger equation then becomes:

$$i\dot{\Phi} = \begin{bmatrix} -\frac{\omega}{2}e^{i\frac{\omega}{2}t} & 0 \\ 0 & \frac{\omega}{2}e^{-i\frac{\omega}{2}t} \end{bmatrix} \psi + \begin{bmatrix} e^{i\frac{\omega}{2}t} & 0 \\ 0 & e^{-i\frac{\omega}{2}t} \end{bmatrix} i\dot{\psi} \tag{B.3}$$

and the right-hand side:

$$\begin{bmatrix} \alpha & \beta e^{i\omega t} \\ \beta^* e^{-i\omega t} & -\alpha \end{bmatrix} \Phi = \begin{bmatrix} \alpha & \beta e^{i\omega t} \\ \beta^* e^{-i\omega t} & -\alpha \end{bmatrix} \begin{bmatrix} e^{i\frac{\omega}{2}t} & 0 \\ 0 & e^{-i\frac{\omega}{2}t} \end{bmatrix} \psi. \tag{B.4}$$

The Schrödinger equation can be re-written as:

$$\begin{aligned} i\dot{\psi} &= -\begin{bmatrix} e^{-i\frac{\omega}{2}t} & 0 \\ 0 & e^{i\frac{\omega}{2}t} \end{bmatrix} \begin{bmatrix} -\frac{\omega}{2}e^{i\frac{\omega}{2}t} & 0 \\ 0 & \frac{\omega}{2}e^{-i\frac{\omega}{2}t} \end{bmatrix} \psi \\ &+ \begin{bmatrix} e^{-i\frac{\omega}{2}t} & 0 \\ 0 & e^{i\frac{\omega}{2}t} \end{bmatrix} \begin{bmatrix} \alpha & \beta e^{i\omega t} \\ \beta^* e^{-i\omega t} & -\alpha \end{bmatrix} \begin{bmatrix} e^{i\frac{\omega}{2}t} & 0 \\ 0 & e^{-i\frac{\omega}{2}t} \end{bmatrix} \psi \\ &= \begin{bmatrix} \frac{\omega}{2} & 0 \\ 0 & -\frac{\omega}{2} \end{bmatrix} \psi + \begin{bmatrix} \alpha & \beta \\ \beta^* & -\alpha \end{bmatrix} \psi. \end{aligned} \tag{B.5}$$

From this, it follows that there are exact solutions to equation (B.5) of the form:

$$i\dot{\psi} = \Omega\psi, \tag{B.6}$$

where Ω is an eigenvalue of the matrix:

$$\begin{bmatrix} \frac{\omega}{2} + \alpha & \beta \\ \beta^* & -(\frac{\omega}{2} + \alpha) \end{bmatrix}. \tag{B.7}$$

Ω is given by:

$$\Omega = \pm\sqrt{(\frac{\omega}{2} + \alpha)^2 + |\beta|^2}. \tag{B.8}$$

We find the eigenvectors corresponding to the two Ω naturally satisfy the relation:

$$\begin{bmatrix} \frac{\omega}{2} + \alpha - \Omega & \beta \\ \beta^* & -(\frac{\omega}{2} + \alpha) - \Omega \end{bmatrix} \begin{bmatrix} a \\ b \end{bmatrix} = 0. \tag{B.9}$$

Thus we obtain a relation between a and b:

$$b = -\frac{\frac{\omega}{2} + \alpha - \Omega}{\beta} a. \tag{B.10}$$

ψ is then given by:

$$\psi = e^{-i\Omega t} \begin{bmatrix} 1 \\ -\frac{\frac{\omega}{2}+\alpha-\Omega}{\beta} \end{bmatrix} \hat{a} + e^{i\Omega t} \begin{bmatrix} 1 \\ -\frac{\frac{\omega}{2}+\alpha+\Omega}{\beta} \end{bmatrix} \hat{b}. \tag{B.11}$$

Choosing the initial condition:

$$\psi(t=0) = \begin{bmatrix} 1 \\ 0 \end{bmatrix}, \tag{B.12}$$

leads to the following solutions for $\hat{a}$ and $\hat{b}$:

$$\begin{aligned} \hat{a} &= \frac{1}{2\Omega}(\Omega + \frac{\omega}{2} + \alpha), \\ \hat{b} &= \frac{1}{2\Omega}(\Omega - \frac{\omega}{2} - \alpha). \end{aligned} \tag{B.13}$$

Hence if we introduce $\psi = \begin{bmatrix} \psi_\uparrow \\ \psi_\downarrow \end{bmatrix}$, then we find that:

$$\psi_\downarrow = -\frac{i}{\Omega}\beta^* \sin(\Omega t), \tag{B.14}$$

and the magnitude squared $|\psi_\downarrow|^2$ is:

$$|\psi_\downarrow|^2 = \frac{1}{\Omega^2}|\beta|^2 \sin^2(\Omega t). \tag{B.15}$$

With this, we will note a few points:

- Note that the maximum conversion occurs at $\frac{\omega}{2} + \alpha = 0$, i.e. $\Omega = |\beta|$.
- The state Φ is normalized, so $\Phi^{\mathrm{T}}\Phi = 1$, i.e. $|\psi_\uparrow|^2 + |\psi_\downarrow|^2 = 1$.
- $\psi_\uparrow$ is given by $\psi_\uparrow = \cos(\Omega t) - \frac{1}{\Omega}(\frac{\omega}{2} + \alpha) i \sin(\Omega t)$.
- $\phi = \begin{bmatrix} \Phi_\uparrow \\ \Phi_\downarrow \end{bmatrix}$, where $\Phi_\uparrow = e^{i\frac{\omega}{2}t}\psi_\uparrow$ and $\Phi_\downarrow = e^{-i\frac{\omega}{2}t}\psi_\downarrow$.

B.2 Justification of $\psi' \approx -\frac{1}{2}$

Let us consider the $1+1$ D coupled system of the electron fluid and the laser pulse:

$$\left(\sqrt{1+a^2} \frac{1+\psi^{'} - v^2\psi^{'}}{\sqrt{(1+\psi^{'})^2 - v^2\psi^{'2}}} \right)^{'} = \omega_p^2 \psi, \tag{B.16}$$

$$a'' + \omega_0^2 a = \gamma^2 \omega_p^2 \frac{\sqrt{(1+\psi')^2 - v^2\psi'^2}}{\sqrt{1+a^2}} a. \tag{B.17}$$

We can solve this system numerically given some initial conditions. We assume that for the electron fluid $\psi(10) = 0$ and $\psi'(10) = 0$, which corresponds to the electrons at the front of the laser pulse being stationary, while the initial conditions for the laser pulse are $a(10) = 1$ and $a'(10) = 0$. Additionally, we want to make the choice $\omega_0^2 = 0.8\frac{\omega_p^2\gamma^2}{\sqrt{1+a(10)^2}}$ for the frequency. This is motivated by considering the plot of the term: $f = \gamma^2\omega_p^2 \frac{\sqrt{(1+\psi')^2 - v^2\psi'^2}}{\sqrt{1+a^2}} \frac{1}{\omega_0^2}$.

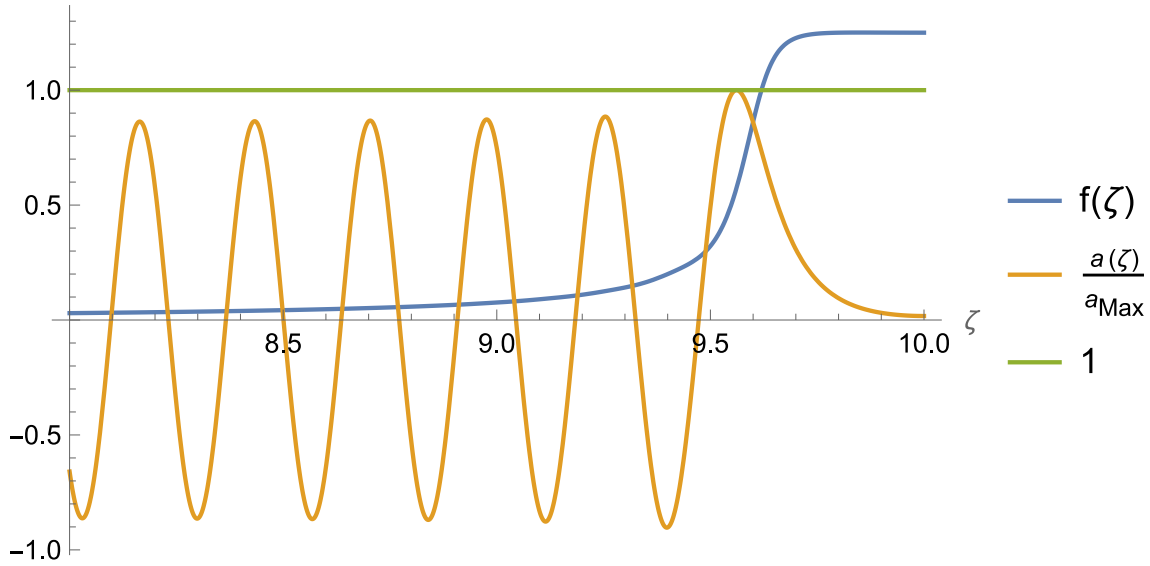

Figure B.1: A plot illustrating the transition from exponential to oscillatory behaviour of the laser pulse a. The value of a was normalised for readability.

We can see from Figure B.1 that whenever $f > 1$ we see exponential behaviour in the laser pulse, and oscillatory behaviour for $f < 1$. Thus our choice of ω_0^2 ensures we see a shock at the front of the pulse and remain in tandem with our previous analysis.

Figure B.2 shows the plots of the numerical solutions to equations (B.16) and (B.17). We are interested in the value of $\psi'(\zeta)$ in the region far from the initial shock at $\zeta = 10$. In the far-from-shock region we see that $\psi'(\zeta)$ is oscillating around the value of ≈ -0.495, thus it is not unreasonable to assume $\psi'(\zeta) \approx -\frac{1}{2}$ in a high γ regime.

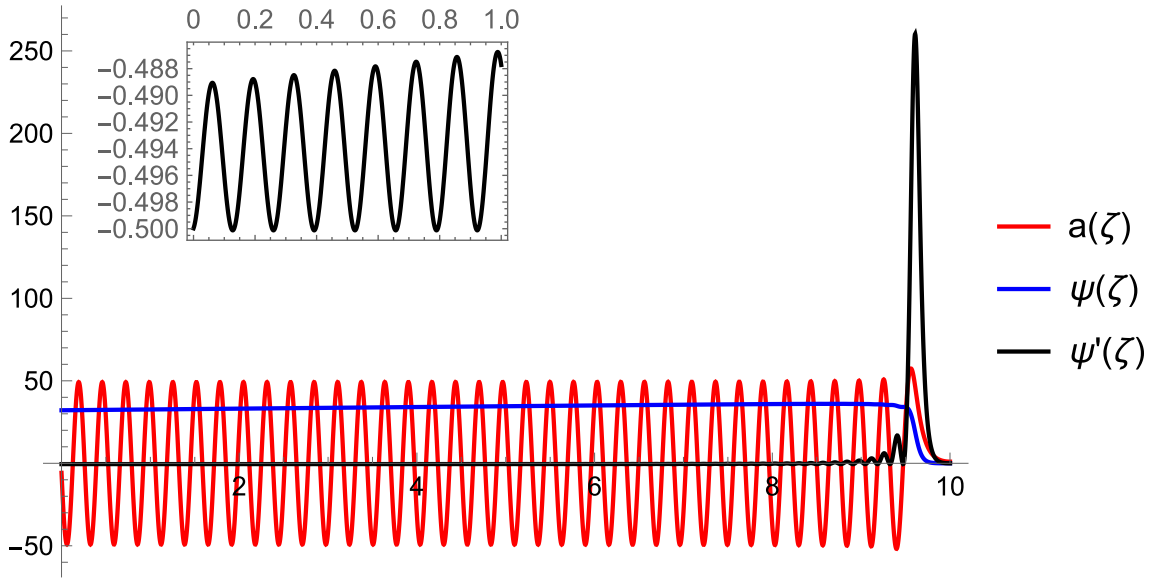

Figure B.2: A plot showing the numerical solutions of equations (B.16) and (B.17). The numerical parameters given for the calculation are $\gamma \approx 100$, $a(10) = 1$, $\omega_p = 1$ and $\omega_0 \approx 23$.

Appendix C

Ponderomotive Axion Production

C.1 The Interpretation of Λ and the Fermi-Walker Connection

In order to see how we can interpret the 2-form Λ, we will consider an object called the Fermi-Walker connection. Let us consider a worldline $C : \tau \to x^\mu = C^\mu(\tau)$. The Fermi Walker connection can be written as:

$$\nabla^F_{\dot{C}} Z = \nabla_{\dot{C}} Z - \widetilde{\mathcal{A}}(Z)\dot{C} + \widetilde{\dot{C}}(Z)\mathcal{A}, \tag{C.1}$$

where Z is a vector field, $\nabla_{\dot{C}}$ is the Levi-Civita connection and $\mathcal{A} = \nabla_{\dot{C}}\dot{C}$. We note that the Fermi-Walker connection is metric compatible i.e. $\nabla^F_{\dot{C}} g = 0$. Additionally, we can introduce projection operators $\Pi_{\dot{C}}$ and $P_{\dot{C}}$ such that:

$$\begin{aligned} \Pi_{\dot{C}} Z &= Z + \widetilde{\dot{C}}(Z)\dot{C}, \\ P_{\dot{C}} Z &= -\widetilde{\dot{C}}(Z)\dot{C}, \end{aligned} \tag{C.2}$$

which we can use to simply write:

$$\nabla^F_{\dot{C}} Z = \Pi_{\dot{C}} \nabla_{\dot{C}} \Pi_{\dot{C}} Z + P_{\dot{C}} \nabla_{\dot{C}} P_{\dot{C}} Z. \tag{C.3}$$

With this in mind, we can easily generalize the Fermi-Walker connection to be taken with respect to a vector field V i.e. $\nabla^F_V Z = \Pi_V \nabla_V \Pi_V Z + P_V \nabla_V P_V Z$. We now introduce a co-ordinate frame $\{V, Y_1, Y_2, Y_3\}$ (i.e. $[V, Y_j] = 0$ for $j = 1, 2, 3$).

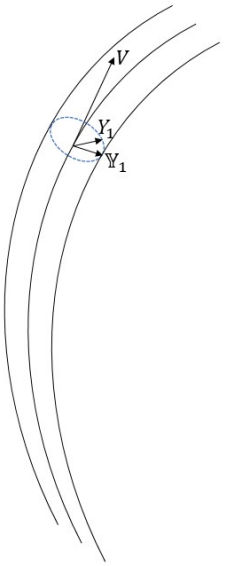

Figure C.1: An illustration of the co-ordinate frame.

Furthermore, we also want to denote the V orthogonal projection of Y_j as:

$$\mathbb{Y}_j = \Pi_V Y_j. \tag{C.4}$$

Now, we can write the action of the Fermi-Walker connection on $\mathbb{Y}_j$ as a linear combination:

$$\nabla_V^F \mathbb{Y}_j = Q_j{}^k \mathbb{Y}_k. \tag{C.5}$$

The rank 2 tensor Q is key in interpreting Λ, as its anti-symmetric part corresponds to particle rotation around an observer. We can express Q as:

$$Q = Q_{jk} E^j \otimes E^k \tag{C.6}$$

where $\{E^j\}_{j=1,2,3}$ is a set of co-vectors such that:

$$\begin{aligned} E^j(\mathbb{Y}_k) &= \delta^j_k \\ E^j(V) &= 0. \end{aligned} \tag{C.7}$$

With this in mind, we can write:

$$\begin{aligned} Q &= E^j \otimes Q_j{}^k \widetilde{\mathbb{Y}}_k \\ &= E^j \otimes \nabla_V^F \widetilde{\mathbb{Y}}_j. \end{aligned} \tag{C.8}$$

Using the fact that the Levi-Civita connection is torsionless, the relation $E^j(V) = 0$ and assuming

that V is unit normalized time-like vector field $g(V,V) = -1$, we can write:

$$\nabla^F_V \mathbb{Y}_j = \nabla_{\mathbb{Y}_j} V. \tag{C.9}$$

Finally, we can express Q as:

$$\begin{aligned} Q &= E^j \otimes \widetilde{\nabla_{\mathbb{Y}_j} V} \\ &= \Pi_V \left(-\widetilde{V} \otimes \nabla_V \widetilde{V} + E^j \otimes \nabla_{\mathbb{Y}_j} \widetilde{V} \right) \\ &= \Pi_V (e^a \otimes \nabla_{X_a} \widetilde{V}), \end{aligned} \tag{C.10}$$

where $\{X_a\}$ is any frame and $\{e^a\}$ is its natural co-frame. We can split Q into its symmetric and anti-symmetric parts:

$$\begin{aligned} Q &= Q_S + Q_{AS} \\ &= \Pi_V \frac{1}{2} (e^a \otimes \nabla_{X_a} \widetilde{V} - \nabla_{X_a} \widetilde{V} \otimes e^a) + \Pi_V \frac{1}{2} (e^a \otimes \nabla_{X_a} \widetilde{V} + \nabla_{X_a} \widetilde{V} \otimes e^a) \\ &= \frac{1}{2} \Pi_V \mathcal{L}_V \Pi_V g + \Pi_V d\widetilde{V}. \end{aligned} \tag{C.11}$$

As mentioned before, the anti-symmetric part of Q corresponds to the rotation of the particles relative to a family of observers travelling along the integral curves of V. If we consider the pre-contracted version of the Lorentz equation in (4.12) and take the U orthogonal projection:

$$\Pi_U d\widetilde{U} = \Pi_U \frac{q}{m} F. \tag{C.12}$$

The addition of a 2-form Λ as seen in equation (4.11) will only result in an additional rotation of the particles in the system around the worldline C and thus can be chosen as zero, as an initial condition.

Appendix D

Quantum Axion Production

D.1 First Integral

In this appendix the method of deriving equation (5.78) will be discussed. In reference [82] this is done via the calculation of the stress-energy 3-form, however, a more simple approach is to simply derive it from the combined Laser-Plasma-Axion equations of motion. The equations describing the electromagnetic field in our system are the macroscopic Maxwell equations:

$$\begin{aligned} \nabla \cdot \mathbf{D} &= \rho, \qquad & \nabla \times \mathbf{H} &= \mathbf{J} + \partial_t \mathbf{D}, \\ \nabla \cdot \mathbf{B} &= 0, \qquad & \nabla \times \mathbf{E} &= -\partial_t \mathbf{B}, \end{aligned} \tag{D.1}$$

where $\mathbf{D}$ is the displacement field and $\mathbf{H}$ is the magnetising field. In the presence of axions, these fields are given by:

$$\mathbf{D} = \mathbf{E} - g_\psi \psi \mathbf{B}, \tag{D.2}$$

$$\mathbf{H} = \mathbf{B} + g_\psi \psi \mathbf{E}. \tag{D.3}$$

If we apply the assumption that $\mathbf{B}$ is constant along z i.e. $\mathbf{B} = (0, 0, B)$ and that all other fields are of the form $\mathbf{f} = (0, 0, f(\zeta))$, the Maxwell equations for $\mathbf{D}$ become:

$$D' = \rho_0 + \rho_e, \quad D' = \frac{u}{v}\rho_e. \tag{D.4}$$

The macroscopic constitutive relation for $\mathbf{D}$ becomes:

$$D = E - g_\psi \psi B. \tag{D.5}$$

The axion field equation (5.35) becomes:

$$\frac{1}{\gamma^2}\psi'' - m_\psi^2 \psi = g_\psi E B. \tag{D.6}$$

Combining equations (D.5), (D.4),(D.6), (5.76) and (5.77) we obtain:

$$EE^{'} - \frac{\psi^{'}\psi^{''}}{\gamma^2} + m_{\psi}^2\psi^{'}\psi - \frac{m_e\gamma\rho_0}{e}\left(\frac{v\xi}{\sqrt{\xi^2-1}} - 1\right)\xi^{'} = 0. \tag{D.7}$$

From inspection, we can see that (D.7) can be written as:

$$\left[\frac{1}{2}E^2 - \frac{1}{2}(\frac{\psi'^2}{\gamma^2} - m_{\psi}^2\psi^2) - \frac{m_e\gamma\rho_0}{e}(v\sqrt{\xi^2-1} - \xi)\right]^{'} = 0. \tag{D.8}$$

D.2 Ultra-Relativistic Approximation

In this appendix, we will discuss the ultra-relativistic approximation of the expression:

$$\zeta(\xi) = \frac{1}{\sqrt{2\gamma^3}\omega_p}\int_1^{\xi}\frac{1}{(v\sqrt{\chi^2-1} - \chi + 1)^{\frac{1}{2}}}d\chi. \tag{D.9}$$

This method was included in the references [82] and [66]. We begin by introducing the variables $\bar{\xi} = \frac{\xi}{\gamma^2}$ and $\bar{\chi} = \frac{\chi}{\gamma^2}$. The integral can then be written as:

$$\zeta(\bar{\xi}) = \frac{1}{\sqrt{2\gamma}\omega_p}\int_{\gamma^{-2}}^{\bar{\xi}}\left[\sqrt{\left(1-\frac{1}{\gamma^2}\right)\left(\bar{\chi}^2 - \frac{1}{\gamma^4}\right)} - \bar{\chi} + \frac{1}{\gamma^2}\right]^{-\frac{1}{2}}d\bar{\chi}. \tag{D.10}$$

If we consider the integrand in (D.10) and neglect terms of order $\mathcal{O}(\frac{1}{\gamma^4})$ and higher we arrive at an approximation:

$$\sqrt{\left(1-\frac{1}{\gamma^2}\right)\left(\bar{\chi}^2 - \frac{1}{\gamma^4}\right)} - \bar{\chi} + \frac{1}{\gamma^2} \approx \frac{1}{\gamma^2}\left(1 - \frac{\bar{\chi}}{2}\right), \tag{D.11}$$

where also have used $\sqrt{1-\frac{1}{\gamma^2}} \approx 1 - \frac{1}{2\gamma^2}$. With this in mind, the integral is approximately:

$$\begin{aligned}\zeta(\bar{\xi}) &\approx \sqrt{\frac{\gamma}{2}}\frac{1}{\omega_p}\int_0^{\bar{\xi}}\frac{1}{\sqrt{1-\frac{\bar{\chi}}{2}}}d\bar{\chi} \\ &= \sqrt{\frac{\gamma}{2}}\frac{4}{\omega_p}\left(1 - \sqrt{1-\frac{\xi}{2\gamma^2}}\right).\end{aligned} \tag{D.12}$$

D.3 The Need For Time Averaging in $\mathcal{E}^{\mu\nu}$

In this appendix, we shall discuss the need to introduce time averaging in equation (5.64). We begin by re-stating the form of the stress-energy tensor for a free axion field:

$$T_{\mu\nu} = \partial_{\mu}\psi\partial_{\nu}\psi - \frac{1}{2}(\eta^{\lambda\omega}\partial_{\lambda}\psi\partial_{\omega}\psi - m_{\psi}^2\psi^2)\eta_{\mu\nu}. \tag{D.13}$$

If we identify that the canonical momentum of the axion field is given by:

$$P = \partial_t\psi, \tag{D.14}$$

then we can write down the different components of the stress-energy tensor:

$$\begin{aligned} T^{00} &= \frac{1}{2}(P^2 + (\nabla\psi)^2 + m_\psi^2\psi^2), \\ T^{0a} &= P\partial^a\psi, \\ T^{ab} &= \partial^a\psi\partial^b\psi - \frac{1}{2}(P^2 - (\nabla\psi)^2 - m_\psi^2\psi^2)\eta^{ab}, \end{aligned} \tag{D.15}$$

where a and b denote the spatial indices i.e. $a,\ b \in \{1,2,3\}$ and $\partial^a = \eta^{a\nu}\partial_\nu$. Quantizing the free axion field, we can write down the axion field operator and its corresponding canonical momentum field operator as:

$$\begin{aligned} \hat{\psi}(\mathbf{x},t) &= \sum_{\mathbf{k}} \frac{1}{\sqrt{2\omega_{\mathbf{k}}V}} \left(\hat{b}_{\mathbf{k}}(t)e^{i\mathbf{k}\cdot\mathbf{x}} + \hat{b}^\dagger_{\mathbf{k}}(t)e^{-i\mathbf{k}\cdot\mathbf{x}}\right), \\ \hat{P}(\mathbf{x},t) &= -i\sum_{\mathbf{k}} \sqrt{\frac{\omega_{\mathbf{k}}}{2V}} \left(\hat{b}_{\mathbf{k}}(t)e^{i\mathbf{k}\cdot\mathbf{x}} - \hat{b}^\dagger_{\mathbf{k}}(t)e^{-i\mathbf{k}\cdot\mathbf{x}}\right). \end{aligned} \tag{D.16}$$

We note that in the case of the free field, the time evolution of the ladder operators is given by $\hat{b}_{\mathbf{k}}(t) = \hat{b}_{\mathbf{k}}(t_i)e^{-i\omega_{\mathbf{k}}(t-t_i)}$ and $\hat{b}^\dagger_{\mathbf{k}}(t) = \hat{b}^\dagger_{\mathbf{k}}(t_i)e^{i\omega_{\mathbf{k}}(t-t_i)}$. In the case of the driven axion field, the time-dependent operator can be found from the Heisenberg equation of motion and is given by:

$$\hat{b}_{\mathbf{k}}(t) = \hat{b}_{\mathbf{k}}(t_i)e^{-i\omega_k(t-t_i)} + \frac{i}{\sqrt{2\omega_{\mathbf{k}}}}e^{-i\omega_{\mathbf{k}}t}\int_{t_i}^{t}\rho_{\mathbf{k}}e^{i\omega_{\mathbf{k}}t'}dt', \tag{D.17}$$

and the conjugate:

$$\hat{b}^\dagger_{\mathbf{k}}(t) = \hat{b}^\dagger_{\mathbf{k}}(t_i)e^{i\omega_k(t-t_i)} - \frac{i}{\sqrt{2\omega_{\mathbf{k}}}}e^{i\omega_{\mathbf{k}}t}\int_{t_i}^{t}\rho^*_{\mathbf{k}}e^{-i\omega_{\mathbf{k}}t'}dt'. \tag{D.18}$$

With that in mind, we can write down the expressions for the integral of the components of the quantised stress-energy tensor:

$$\int d^3x : \hat{T}^{00} := \sum_{\mathbf{k}} \frac{\omega_{\mathbf{k}}}{2}\hat{b}^\dagger_{\mathbf{k}}\hat{b}_{\mathbf{k}}. \tag{D.19}$$

The integral of the matrix element of the 00 component of the normal ordered stress-energy tensor is then given by:

$$\int d^3x \,\langle 0,t_i| : \hat{T}^{00}(t_f,\mathbf{x}) : |0,t_i\rangle = \sum_{\mathbf{k}} \frac{1}{2} \mid \rho^*_{\mathbf{k}}(\omega_{\mathbf{k}}) \mid^2 . \tag{D.20}$$

Similarly, the integral of the matrix element of the $0a$ component of the normal ordered stress-energy tensor:

$$\int d^3x \,\langle 0,t_i| : \hat{T}^{0a}(t_f,\mathbf{x}) : |0,t_i\rangle = \sum_{\mathbf{k}} \frac{k^a}{2\omega_{\mathbf{k}}} \mid \rho^*_{\mathbf{k}}(\omega_{\mathbf{k}}) \mid^2 . \tag{D.21}$$

A problem arises, however, whenever one considers the space-space components. The operator $\int d^3x : \hat{T}^{ab} :$ is given by:

$$\int d^3x : \hat{T}^{ab} := \sum_{\mathbf{k}} \frac{\omega_{\mathbf{k}}}{2}(\hat{b}_{\mathbf{k}}\hat{b}_{-\mathbf{k}} + \hat{b}^\dagger_{-\mathbf{k}}\hat{b}^\dagger_{\mathbf{k}})\eta^{ab} + \frac{k^a k^b}{2\omega_{\mathbf{k}}}(2\hat{b}^\dagger_{\mathbf{k}}\hat{b}_{\mathbf{k}} + \hat{b}_{\mathbf{k}}\hat{b}_{-\mathbf{k}} + \hat{b}^\dagger_{-\mathbf{k}}\hat{b}^\dagger_{\mathbf{k}}). \tag{D.22}$$

The matrix element of this operator is then given by:

$$\int d^3x \, \langle 0, t_i| : \hat{T}^{ab}(\mathbf{x}, t) : |0, t_i\rangle =$$
$$\sum_{\mathbf{k}} -\frac{\omega_{\mathbf{k}}}{2}\left(\frac{e^{-2i\omega_{\mathbf{k}}t}}{2\omega_{\mathbf{k}}}\int_{t_i}^{t}\int_{t_i}^{t}\rho_{\mathbf{k}}^{'}\rho_{-\mathbf{k}}^{''}e^{i\omega_{\mathbf{k}}(t'+t'')}dt'dt'' + \frac{e^{2i\omega_{\mathbf{k}}t}}{2\omega_{\mathbf{k}}}\int_{t_i}^{t}\int_{t_i}^{t}\rho_{-\mathbf{k}}^{*'}\rho_{\mathbf{k}}^{*''}e^{-i\omega_{\mathbf{k}}(t'+t'')}dt'dt''\right)\eta^{ab}$$
$$+\frac{k^a k^b}{2\omega_{\mathbf{k}}}\left(\frac{1}{\omega_{\mathbf{k}}}\int_{t_i}^{t}\int_{t_i}^{t}\rho_{\mathbf{k}}^{*'}\rho_{\mathbf{k}}^{''}e^{-i\omega_{\mathbf{k}}(t'-t'')}dt'dt'' - \frac{e^{-2i\omega_{\mathbf{k}}t}}{2\omega_{\mathbf{k}}}\int_{t_i}^{t}\int_{t_i}^{t}\rho_{\mathbf{k}}^{'}\rho_{-\mathbf{k}}^{''}e^{i\omega_{\mathbf{k}}(t'+t'')}dt'dt''\right.$$
$$\left.-\frac{e^{2i\omega_{\mathbf{k}}t}}{2\omega_{\mathbf{k}}}\int_{t_i}^{t}\int_{t_i}^{t}\rho_{-\mathbf{k}}^{*'}\rho_{\mathbf{k}}^{*''}e^{-i\omega_{\mathbf{k}}(t'+t'')}dt'dt''\right), \tag{D.23}$$

for a driven axion field and $t > t_i$, where $\rho_{\mathbf{k}}^{'} \equiv \rho_{\mathbf{k}}(t')$ and $\rho_{\mathbf{k}}^{''} \equiv \rho_{\mathbf{k}}(t'')$. As can be seen in equation (D.23), there are four terms containing oscillating factors of the form $e^{-2i\omega_{\mathbf{k}}t}$ and $e^{2i\omega_{\mathbf{k}}t}$. This time dependence is problematic, as it means that equation (5.65) does not match with (D.23). Introducing a time averaging in the definition given in (5.64) makes all the sinusoidal terms go to zero i.e.

$$\lim_{T\to\infty}\frac{1}{T}\int_{t}^{t+T}dt'\int d^3x \, \langle 0, t_i| : \hat{T}^{ab}(\mathbf{x}, t') : |0, t_i\rangle = \sum_{\mathbf{k}}\frac{k^a k^b}{\omega_{\mathbf{k}}}\frac{1}{2\omega_{\mathbf{k}}} \mid \rho_{\mathbf{k}}^{*}(\omega_{\mathbf{k}}) \mid^2 . \tag{D.24}$$

Bibliography

[1] Friedrich Wilhelm Bessel. "On the variations of the proper motions of Procyon and Sirius". In: *Monthly Notices of the Royal Astronomical Society, Vol. 6, p. 136-141* 6 (1844), pp. 136–141.

[2] Camille Flammarion. "The companion of Sirius". In: *Astronomical register, vol. 15, pp. 186-189* 15 (1877), pp. 186–189.

[3] J. M. Schaeberle. "Discovery of the companion to Procyon". In: *Publications of the Astronomical Society of the Pacific* 8.53 (Dec. 1896), 314a. DOI: 10.1086/121125. URL: https://dx.doi.org/10.1086/121125.

[4] S Shankaranarayanan and Joseph P Johnson. "Modified theories of gravity: Why, how and what?" In: *General Relativity and Gravitation* 54.5 (2022), p. 44.

[5] B. Kelvin. "Baltimore lectures on molecular dynamics and the wave theory of light". In: (1904).

[6] Henri Poincaré. "The Milky Way and the Theory of Gases". In: *Popular Astronomy* 14 (1906).

[7] Gianfranco Bertone and Dan Hooper. "History of dark matter". In: *Reviews of Modern Physics* 90.4 (2018), p. 045002.

[8] J. C. Kapteyn. "First Attempt at a Theory of the Arrangement and Motion of the Sidereal System". In: *Astrophys. J.* 55 (1922), pp. 302–328. DOI: 10.1086/142670.

[9] Jan H Oort. "The force exerted by the stellar system in the direction perpendicular to the galactic plane and some related problems". In: *Bulletin of the Astronomical Institutes of the Netherlands, Vol. 6, p. 249* 6 (1932), p. 249.

[10] Fritz Zwicky. "Republication of: The redshift of extragalactic nebulae". In: *General Relativity and Gravitation* 41.1 (2009), pp. 207–224.

[11] Edwin Hubble and Milton L Humason. "The velocity-distance relation among extra-galactic nebulae". In: *Astrophysical Journal, vol. 74, p. 43* 74 (1931), p. 43.

[12] Horace W Babcock. "The rotation of the Andromeda Nebula". In: *Lick Observatory bulletin; no. 498; Lick Observatory bulletins; no. 498., Berkeley: University of California Press,[1939], p. 41-51,[2] leaves of plates; 31 cm.* 19 (1939), pp. 41–51.

[13] Kenneth C Freeman. "On the disks of spiral and S0 galaxies". In: *Astrophysical Journal, vol. 160, p. 811* 160 (1970), p. 811.

[14] MS Roberts and AH Rots. "Comparison of rotation curves of different galaxy types". In: *Astronomy and Astrophysics, Vol. 26, p. 483-485 (1973)* 26 (1973), pp. 483–485.

[15] Jaan Einasto, Ants Kaasik, and Enn Saar. "Dynamic evidence on massive coronas of galaxies". In: *Nature* 250.5464 (1974), pp. 309–310.

[16] Jeremiah P Ostriker, Philip JE Peebles, and Amos Yahil. "The size and mass of galaxies, and the mass of the universe". In: *Astrophysical Journal, vol. 193, Oct. 1, 1974, pt. 2, p. L1-L4.* 193 (1974), pp. L1–L4.

[17] SM Faber and JS Gallagher. "Masses and mass-to-light ratios of galaxies". In: *Ann. Rev. Astron. Astrophys* 979.l7 (1979), pp. I35–87.

[18] Jaan Einasto. "Dark matter". In: *arXiv preprint arXiv:0901.0632* (2009).

[19] Alexandre Arbey and Farvah Mahmoudi. "Dark matter and the early Universe: a review". In: *Progress in Particle and Nuclear Physics* 119 (2021), p. 103865.

[20] Gerard 't Hooft. "Symmetry breaking through Bell-Jackiw anomalies". In: *Physical Review Letters* 37.1 (1976), pp. 8–11.

[21] Gerard 't Hooft. "Computation of the quantum effects due to a four-dimensional pseudoparticle". In: *Physical Review D* 14.12 (1976), pp. 3432–3450.

[22] Gerard 't Hooft. "How instantons solve the U(1) problem". In: *Physics Reports* 142.6 (1986), pp. 357–387.

[23] RJ Crewther et al. "Chiral estimate of the electric dipole moment of the neutron in quantum chromodynamics". In: *Physics Letters B* 88.1-2 (1979), pp. 123–127.

[24] "Chiral estimate of the electric dipole moment of the neutron in quantum chromodynamics: R.J. Crewther, P. Di Vecchia. G. Veneziano and E. Witten Phys. Lett. 88B (1979) 123." In: *Physics Letters B* 91.3 (1980), p. 487. ISSN: 0370-2693. DOI: https://doi.org/10.1016/0370-2693(80)91025-4. URL: https://www.sciencedirect.com/science/article/pii/0370269380910254.

[25] Varouzhan Baluni. "CP-nonconserving effects in quantum chromodynamics". In: *Phys. Rev. D* 19 (7 Apr. 1979), pp. 2227–2230. DOI: 10.1103/PhysRevD.19.2227. URL: https://link.aps.org/doi/10.1103/PhysRevD.19.2227.

[26] Maxim Pospelov and Adam Ritz. "Theta vacua, QCD sum rules, and the neutron electric dipole moment". In: *Nuclear Physics B* 573.1-2 (2000), pp. 177–200.

[27] Roberto D Peccei. "The Strong CP problem and axions". In: *Axions: Theory, Cosmology, and Experimental Searches*. Springer, 2008, pp. 3–17.

[28] Roberto D Peccei and Helen R Quinn. "Constraints imposed by CP conservation in the presence of pseudoparticles". In: *Physical Review D* 16.6 (1977), p. 1791.

[29] Steven Weinberg. "Time's (Almost) Reversible Arrow". In: *Quanta Magazine* (2016). URL: https://www.quantamagazine.org/how-axions-may-explain-times-arrow-20160107/.

[30] Steven Weinberg. "A new light boson?" In: *Physical Review Letters* 40.4 (1978), p. 223.

[31] William A Bardeen, S-HH Tye, and JAM Vermaseren. "Phenomenology of the new light Higgs boson search". In: *Physics Letters B* 76.5 (1978), pp. 580–584.

[32] Masahiro Kawasaki, Eisuke Sonomoto, and Tsutomu T Yanagida. "Cosmologically allowed regions for the axion decay constant Fa". In: *Physics Letters B* 782 (2018), pp. 181–184.

[33] Jihn E Kim. "Weak-interaction singlet and strong CP invariance". In: *Physical Review Letters* 43.2 (1979), p. 103.

[34] Mikhail A Shifman, AI Vainshtein, and Valentin I Zakharov. "Can confinement ensure natural CP invariance of strong interactions?" In: *Nuclear Physics B* 166.3 (1980), pp. 493–506.

[35] Michael Dine, Willy Fischler, and Mark Srednicki. "A simple solution to the strong CP problem with a harmless axion". In: *Physics letters B* 104.3 (1981), pp. 199–202.

[36] Pierre Sikivie. "Invisible axion search methods". In: *Reviews of Modern Physics* 93.1 (2021), p. 015004.

[37] David JE Marsh. "Axion cosmology". In: *Physics Reports* 643 (2016), pp. 1–79.

[38] Ian P Stern, ADMX, and ADMX-HF collaborations. "Axion dark matter searches". In: *AIP Conference Proceedings*. Vol. 1604. 1. American Institute of Physics. 2014, pp. 456–461.

[39] C Bartram et al. "Search for invisible axion dark matter in the 3.3–4.2 μ eV mass range". In: *Physical review letters* 127.26 (2021), p. 261803.

[40] M Arik et al. "Search for Sub-eV Mass Solar Axions by the CERN Axion Solar Telescope with He 3 Buffer Gas". In: *Physical Review Letters* 107.26 (2011), p. 261302.

[41] CAST Collaboration. "New CAST limit on the axion–photon interaction". In: *Nature Physics* 13.6 (2017), pp. 584–590.

[42] Emilio Zavattini et al. "Experimental observation of optical rotation generated in vacuum by a magnetic field". In: *Physical Review Letters* 96.11 (2006), p. 110406.

[43] Andreas Ringwald. "Axion interpretation of the PVLAS data?" In: *Journal of Physics: Conference Series*. Vol. 39. 1. IOP Publishing. 2006, p. 197.

[44] Yu N Gnedin, M Yu Piotrovich, and TM Natsvlishvili. "PVLAS experiment: some astrophysical consequences". In: *Monthly Notices of the Royal Astronomical Society* 374.1 (2007), pp. 276–281.

[45] E Zavattini et al. "New PVLAS results and limits on magnetically induced optical rotation and ellipticity in vacuum". In: *Physical Review D—Particles, Fields, Gravitation, and Cosmology* 77.3 (2008), p. 032006.

[46] H Primakoff. "Photo-production of neutral mesons in nuclear electric fields and the mean life of the neutral meson". In: *Physical Review* 81.5 (1951), p. 899.

[47] Quan-feng Wu and Xun-Jie Xu. “A comprehensive calculation of the Primakoff process andthe solar axion flux”. In: *Journal of Cosmology and Astroparticle Physics* 2024.07 (2024), p. 013.

[48] C Joshi. “Plasma-based accelerators: then and now”. In: *Plasma Physics and Controlled Fusion* 61.10 (2019), p. 104001.

[49] Toshiki Tajima and John M Dawson. “Laser electron accelerator”. In: *Physical review letters* 43.4 (1979), p. 267.

[50] Robert Bingham and R Trines. “Introduction to plasma accelerators: the basics”. In: *arXiv preprint arXiv:1705.10535* (2017).

[51] Daniel Papp et al. “Laser wakefield acceleration with high-power, few-cycle mid-IR lasers”. In: *Nuclear Instruments and Methods in Physics Research Section A: Accelerators, Spectrometers, Detectors and Associated Equipment* 909 (2018). 3rd European Advanced Accelerator Concepts workshop (EAAC2017), pp. 145–148. ISSN: 0168-9002. DOI: https://doi.org/10.1016/j.nima.2018.01.050. URL: https://www.sciencedirect.com/science/article/pii/S0168900218300676.

[52] Eric Esarey, Carl B Schroeder, and Wim P Leemans. “Physics of laser-driven plasma-based electron accelerators”. In: *Reviews of modern physics* 81.3 (2009), pp. 1229–1285.

[53] G. W. Kentwell. “An average Lagrangian formulation of ponderomotive forces in Vlasov plasmas”. In: *Journal of Plasma Physics* 34.2 (1985), pp. 289–298. DOI: 10.1017/S0022377800002853.

[54] D. Bauer, P. Mulser, and W. -H. Steeb. “Relativistic Ponderomotive Force, Uphill Acceleration, and Transition to Chaos”. In: *Phys. Rev. Lett.* 75 (25 Dec. 1995), pp. 4622–4625. DOI: 10.1103/PhysRevLett.75.4622.

[55] DA Burton et al. “Observations on the ponderomotive force”. In: *Relativistic Plasma Waves and Particle Beams as Coherent and Incoherent Radiation Sources II*. Vol. 10234. SPIE. 2017, pp. 17–22.

[56] DR Bituk and MV Fedorov. “Relativistic ponderomotive forces”. In: *Journal of Experimental and Theoretical Physics* 89 (1999), pp. 640–646.

[57] Javier Redondo and Andreas Ringwald. “Light shining through walls”. In: *Contemporary Physics* 52.3 (2011), pp. 211–236.

[58] R Ballou et al. “New exclusion limits on scalar and pseudoscalar axionlike particles from light shining through a wall”. In: *Physical Review D* 92.9 (2015), p. 092002.

[59] David A Burton and Adam Noble. “Plasma-based wakefield accelerators as sources of axion-like particles”. In: *New Journal of Physics* 20.3 (2018), p. 033022.

[60] Mark Aleksiejuk and David A Burton. “A scalar field theory of 1+ 1-dimensional laser wakefield accelerators”. In: *Journal of Physics A: Mathematical and Theoretical* 57.35 (2024), p. 355701.

[61] SV Bulanov et al. “On some theoretical problems of laser wake-field accelerators”. In: *Journal of Plasma Physics* 82.3 (2016), p. 905820308.

[62] KA Beyer et al. “Light-shining-through-wall axion detection experiments with a stimulating laser”. In: *Physical Review D* 105.3 (2022), p. 035031.

[63] Babette Döbrich and Holger Gies. “Axion-like-particle search with high-intensity lasers”. In: *Journal of High Energy Physics* 2010.10 (2010), pp. 1–27.

[64] JT Mendonça, JD Rodrigues, and H Terças. “Axion production in unstable magnetized plasmas”. In: *Physical Review D* 101.5 (2020), p. 051701.

[65] JT Mendonça, H Terças, and JD Rodrigues. “Axion excitation by intense laser fields in a plasma”. In: *Physica Scripta* 95.4 (2020), p. 045601.

[66] David A Burton and Adam Noble. “Plasma-based wakefield accelerators as sources of axion-like particles”. In: *New Journal of Physics* 20.3 (Mar. 2018), p. 033022. DOI: 10.1088/1367-2630/aab475. URL: https://dx.doi.org/10.1088/1367-2630/aab475.

[67] J-L Vay et al. “Modeling of advanced accelerator concepts”. In: *Journal of Instrumentation* 16.10 (2021), T10003.

[68] Gérard A Maugin. *Material inhomogeneities in elasticity*. CRC Press, 2020.

[69] Jerzy Kijowski and Giulio Magli. “Unconstrained variational principle and canonical structure for relativistic elasticity”. In: *Reports on Mathematical Physics* 39.1 (1997), pp. 99–112. ISSN: 0034-4877. DOI: https://doi.org/10.1016/S0034-4877(97)81475-9.

[70] Jerzy Kijowski and Giulio Magli. “Unconstrained Hamiltonian formulation of general relativity with thermo-elastic sources”. In: *Classical and Quantum Gravity* 15.12 (1998), p. 3891.

[71] David A Burton et al. “Exploring Born–Infeld electrodynamics using plasmas”. In: *Journal of Physics A: Mathematical and Theoretical* 44.9 (2011), p. 095501.

[72] R.V. Polovin A.I. Akhiezer. “Theory of Wave Motion of an Electron Plasma”. In: *Journal of Experimental and Theoretical Physics* 30 (1956), p. 915.

[73] Martin King et al. “Perspectives on laser-plasma physics in the relativistic transparency regime”. In: *The European Physical Journal A* 59.6 (2023), p. 132.

[74] S. V. Bulanov et al. “On some theoretical problems of laser wake-field accelerators”. In: *Journal of Plasma Physics* 82.3 (2016), p. 905820308. DOI: 10.1017/S0022377816000623.

[75] Christopher C Gerry and Peter L Knight. *Introductory quantum optics*. Cambridge university press, 2023.

[76] Nikolai Mitrofanovich Krylov and Nikolai Nikolaevich Bogoliubov. *Introduction to non-linear mechanics*. 11. Princeton university press, 1950.

[77] D Bauer, P Mulser, and W-H Steeb. “Relativistic ponderomotive force, uphill acceleration, and transition to chaos”. In: *Physical review letters* 75.25 (1995), p. 4622.

[78] Robert Alan Cairns, A Reitsma, and R Bingham. "Envelope equations and conservation laws describing wakefield generation and electron acceleration". In: *Physics of Plasmas* 11.2 (2004), pp. 766–770.

[79] Lev Pitaevskii and Sandro Stringari. *Bose-Einstein condensation and superfluidity*. Vol. 164. Oxford University Press, 2016.

[80] Claude Cohen-Tannoudji, Bernard Diu, and Franck Laloë. *Claude Cohen-Tannoudji; Bernard Diu; Franck Laloë: Quantenmechanik. Band 1*. Vol. 1. Walter de Gruyter, 2013.

[81] Christian Grosche and Frank Steiner. *Handbook of Feynman path integrals*. Vol. 145. Springer, 1998.

[82] D A Burton, A Noble, and T J Walton. "Axionic suppression of plasma wakefield acceleration". In: *Journal of Physics A: Mathematical and Theoretical* 49.38 (Aug. 2016), p. 385501. DOI: 10.1088/1751-8113/49/38/385501. URL: https://dx.doi.org/10.1088/1751-8113/49/38/385501.

[83] S Andriamonje et al and (CAST Collaboration). "An improved limit on the axion–photon coupling from the CAST experiment". In: *Journal of Cosmology and Astroparticle Physics* 2007.04 (Apr. 2007), p. 010. DOI: 10.1088/1475-7516/2007/04/010. URL: https://dx.doi.org/10.1088/1475-7516/2007/04/010.

[84] Xiangyan An et al. "Modeling of axion and electromagnetic fields interaction in particle-in-cell simulations". In: *Matter and Radiation at Extremes* 9.6 (2024).

[85] I Kostyukov, A Pukhov, and S Kiselev. "Phenomenological theory of laser-plasma interaction in "bubble" regime". In: *Physics of Plasmas* 11.11 (2004), pp. 5256–5264.

[86] Selym Villalba-Chávez, Anatoly E Shabad, and Carsten Müller. "Axion electrodynamics in strong magnetic backgrounds". In: *Journal of Physics: Conference Series*. Vol. 2249. 1. IOP Publishing. 2022, p. 012021.

[87] Selym Villalba-Chávez. "Laser-driven search of axion-like particles including vacuum polarization effects". In: *Nuclear Physics B* 881 (2014), pp. 391–413.

[88] David A Burton and Adam Noble. *A Geometrical Approach to Physics*. CRC Press, 2024.